Expression and Functional Studies of a Recombinant Surfactant Protein B

by © Jonathan Moulton

a Thesis submitted to the School of Graduate Studies

in partial fulfillment of the requirements for the degree of

Master of Science

Department of Biochemistry

Memorial University of Newfoundland

August 2013

St. John's

Newfoundland and Labrador

Abstract

Of the components of the respiratory system, one of the most crucial is the pulmonary surfactant. This mixture of phospholipids, cholesterol, and proteins act to reduce surface tension inside the lungs as well as fight infection. The surfactant associated proteins vary in their structure and function but the most important is surfactant protein B (SP-B) which is essential to life. Despite its importance, it has not yet been structurally characterized and as a result, its function still remains a mystery. Part of the problem is the difficulty in acquiring enough of the protein to work with. To attempt to solve this problem, a method has been developed to recombinantly express a variant of human SP-B in *Escherichia coli* in relative abundance. Also, a series of functional tests on the recombinant SP-B were completed to determine if it is a viable alternative to native SP-B for use in the laboratory and possible clinical applications. The functional tests included membrane leakage and lipid mixing assays, as well as captive bubble surfactometer studies. These experiments revealed that the recombinant SP-B displayed normal SP-B activity albeit not as effective as native SP-B.

Acknowledgements

Dr. Valerie Booth

Dr. Robert Brown

Donna Jackman

Nathan Agnew

Dr. Michael Morrow

Dr. Michael Hayley

Craig Skinner

Department of Biochemistry

Memorial University of Newfoundland

St. John's, Newfoundland

Bárbara Olmeda

Depto. Bioquímica y Biología Molecular I

Universidad Compultense de Madrid

Madrid, Spain

Canadian Institute of Health Research (CIHR)

Table of Contents

List of Tables

List of Figures

List of Abbreviations

ANTS	8-aminonaphthalene-l,3,6-trisulfonic acid
ARDS	acute respiratory distress syndrome
BLES	bovine lipid extracted surfactant
CAPS	N-cyclohexyl-3-aminopropanesulfonic acid
CBB	Coomassie Brilliant Blue
CBS	captive bubble surfactometer
CD	circular dichromism
CHAPS	3-[(3-Cholamidopropyl)dimethylammonio]-1-propanesulfonate
DNA	deoxyribonucleic acid
DPPC	dipalmitoylphosphatidylcholine
DPX	p-xylene-bis-N-pyrimidinum bromide
DTT	dithiothreitol
EDTA	disodium ethylenediamine tetraacetate
FRET	fluorescence resonance energy transfer
FTIR	Fourier transfer infrared spectroscopy
GST	glutathione S-transferase
HPLC	high performance liquid chromatography
IA	initial absorption
IMAC	immobilized metal ion affinity chromatography
IPTG	isopropyl-β-D-1-thiogalactopyranoside
LB	lamellar bodies

LS	lauroyl sarcosine
LUV	large unilamellar vesicle
MBP	maltose binding protein
MLV	multilamellar vesicle
NBD	7-nitro-4-benzofurazanyl
NMR	nuclear magnetic resonance
NOESY	nuclear Overhauser effect spectroscopy
nSP-B	native surfactant protein B
OD	optical density
PAGE	polyacrylamide get electrophoresis
PC	phosphatidylcholine
PDB	protein data bank
PE	phosphatidylethanolamine
PEA	post expansion absorption
PG	phosphatidylglycerol
PI	phosphatidylinositol
PMSF	phenylmethylsulfonyl fluoride
POPC	1-palmitoyl-2-oleoyl-*sn*-glycero-3-phosphocholine
POPG	1-palmitoyl-2-oleoyl-*sn*-glycero-3-phosphoglycerol
PS	phosphatidylserine
PVDF	polyvinylidene fluoride
RDS	respiratory distress syndrome
rSP-B	recombinant surfactant protein B

SDS	sodium dodecyl sulfate
SM	sphingomyelin
SN	staphyloccal nuclease
SP-A	surfactant protein A
SP-B	surfactant protein B
SP-C	surfactant protein C
SP-D	surfactant protein D
TBS	tris buffered saline
TE	tris ethanol
TEMED	tetramethylethylenediamine
TEV	tobacco etch virus
TM	tubular myelin
TOCSY	three dimensional total correlation spectroscopy
TTBS	tween tris buffered saline

1. Introduction

1.1 Respiratory System / Gas Exchange

Oxygen (O_2) is an essential component of many cellular processes. Most organisms including humans have to take in oxygen from the environment to meet this requirement. There also has to be a way of expelling carbon dioxide (CO_2), which is a common byproduct of metabolism. Both of these essential tasks take place in the respiratory system. Humans as well as other mammals have a respiratory system that centers on the lungs.

The lungs are very important organs in the mammalian respiratory system. They are so important, two out of the four chambers of the heart are dedicated to pumping blood to and from the lungs. As the deoxygenated blood moves into the lungs, it passes through progressively smaller blood vessels. Eventually they reach capillaries that are so thin that only one red blood cell can pass through at a time. The walls of these capillaries consist of an endothelium which is only one cell thick. These features provide a very efficient way for the gases to be exchanged between the blood and the environment.

Once in the lungs, inhaled air passes through increasingly smaller passages culminating in small sac-like structures known as alveoli (Figure 1). This inhalation is brought about by the expansion of the chest cavity by several muscles but mostly the diaphragm and muscles surrounding the ribcage. The obverse of this is exhalation and involves similar muscle groups contracting the chest cavity. This creates a positive internal pressure in the lungs which forces the air out.

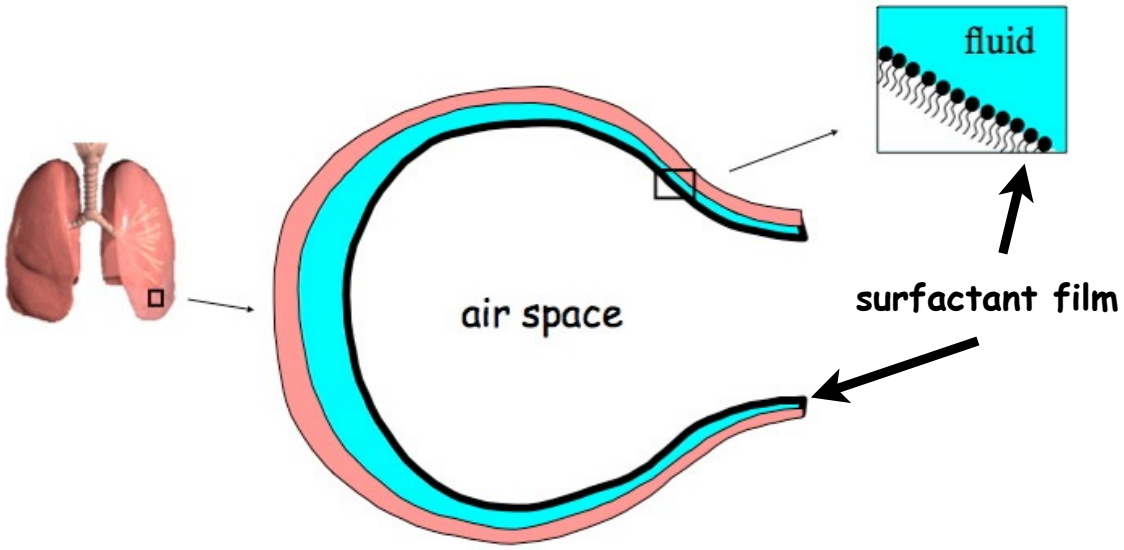

Figure 1: Schematic showing the inside of an alveolus and the position of lung surfactant inside.

During this process, gas exchange occurs in the alveoli. This is where the capillaries of the pulmonary circulation come into close contact with the inhaled air. The alveolar surface is coated with a 0.2 μm thick layer of water through which the respiratory gasses can diffuse [1]. While this water layer is a great system for preventing the dehydration of alveolar tissue, it does create the inherent problem of surface tension. Surface tension is a phenomena brought about when the molecules on the surface of a fluid are more attracted to each other than the external environment. Water has an especially high surface tension due to water molecules being exceptionally polar. The normal surface tension of water is approximately 70 mN/m. This creates a particular problem for the lungs. If left unchecked, the surface tension of the fluid layer in the alveoli would cause them to collapse [2]. This effect would be even more pronounced during the increased pressure of exhalation. Collapsed alveoli require a lot of work to be forced back open. Surface tension can be reduced if amphipathic molecules known as surfactant are arranged along the air-water interface (Figure 1). Being amphipathic, these molecules can interact with both the polar water and non-polar air space, which reduces the effect of surface tension. The lungs create their own surfactant called pulmonary surfactant.

1.2 Pulmonary Surfactant

Pulmonary surfactant is produced by the alveolar type II epithelial cells [3]. Its composition is comprised of mostly phospholipids, cholesterol and proteins (See Table 1). The phospholipids comprise 80% of the total mass of the pulmonary surfactant and make up the bulk of the amphipathic molecules that sit along the air-water interface in alveoli. These phospholipids are most responsible for lowering surface tension. A significant portion of the phospholipid fraction are phosphatidylglycerol (PG) species making up 10% the total mass of the surfactant [4]. These have negatively charged head groups and are responsible for giving pulmonary surfactant an overall negative charge which is probably important for the interaction between surfactant and positively charged surfactant proteins (see below). By far the most common phospholipid found in surfactant, however, is phosphatidylcholine (PC) species, which takes up approximately 70% of the total surfactant mass [5]. About half of this is dipalmitoylphosphatidylcholine (DPPC) [4]. DPPC is a phospholipid that contains choline, a zwitterionic head group and therefore has an overall neutral charge. The hydrophobic part consists of two palmitoyl chains, which are saturated fatty acids. These fatty acids allow for the tight packing of pulmonary surfactant, important during the compression of alveoli [6]. The problem with DPPC in biological membranes is that they have a relatively high melting point (~41°C). At the physiological temperature of 37°C, this would lead to tight packing of lipids which is important for the surfactant to reduce surface tension [7]. However, the tight packing results in reduced mobility which creates a problem when the surfactant must spread across the air-water interface. The mobility of lipids in surfactant is increased by the presence of unsaturated phospholipids and cholesterol, which comprises approximately

10% of the surfactant mass. However, the movement of surfactant to the interface is mostly dependent on the hydrophobic surfactant proteins, which make up about 3% [8] [9]. The remaining 7% is occupied by the hydrophilic surfactant proteins [10].

Table 1: Composition of Adult Human Lung Surfactant [4 5 8 9 10]

Category	Component	Percentage (by weight)
Phospholipids (~85%)	Phosphatidylcholine (PC)	~70%
	Phosphatidylglycerol (PG) Phosphatidylinositol (PI) (acidic phospholipids)	~15%
	Phosphatidylethanolamine (PE) Phosphatidylserine (PS) Sphingomyelin (SM)	Minor
Neutral Lipids (~5%)	Cholesterol	~5%
	Glycerides Free Fatty Acids	Minor
Proteins (~10%)	Surfactant Protein A (SP-A)	~6%
	Surfactant Protein B (SP-B)	~1.5%
	Surfactant Protein C (SP-C)	~1.5%
	Surfactant Protein D (SP-D)	~1%

A current model for pulmonary surfactant synthesis has the surfactant excreted from the Type II cells as lamellar bodies (LB) into the external water layer of alveoli (Figure 2) [3] [11]. Once outside the cells, these lamellar bodies become hydrated and unravel into an ordered crosshatched structure of tubules known as tubular myelin (TM) [12]. Pulmonary surfactant in tubular myelin structures could spread directly onto the air-water interface as a surface active film [13] [14]. However, it is more probable that they form a multi-layered, three dimensional structure of lipids [3] [8]. This multi-layered structure is associated with the surface active film and can act as a form of lipid reservoir [15]. These structures are stabilized by the hydrophobic surfactant proteins.

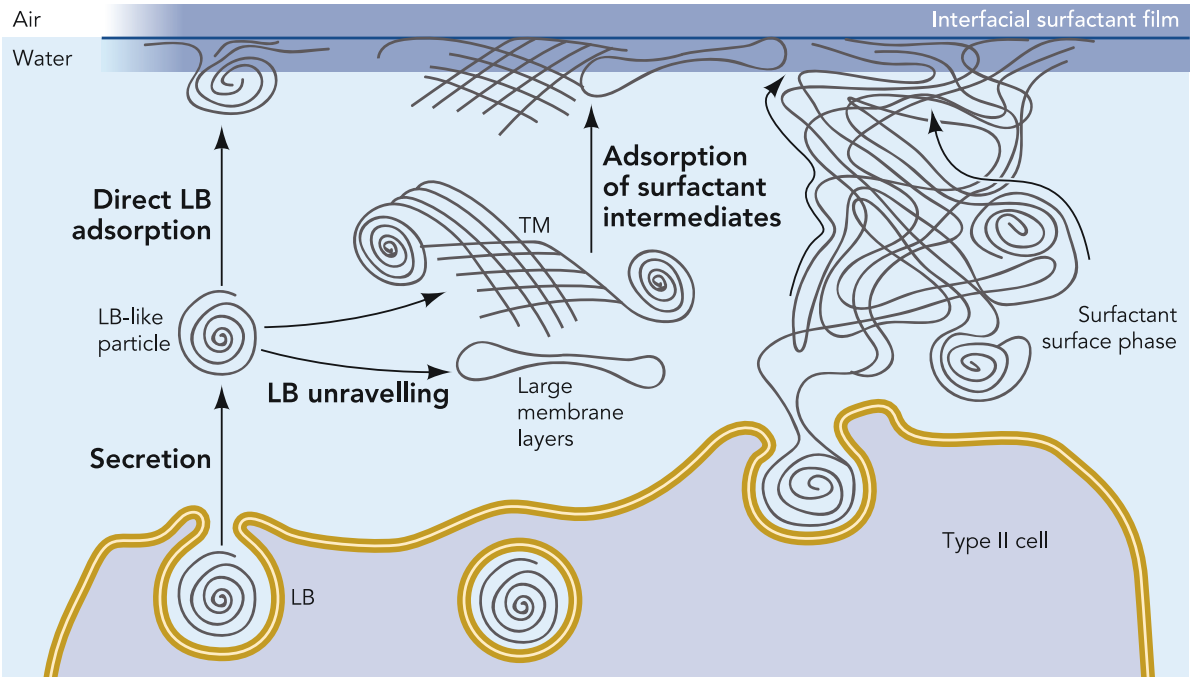

Figure 2: Models for the secretion and absorption of pulmonary surfactant. Adapted from Figure 2, Perez-Gil and Weaver, 2010 with permission from the publisher [16].

During breathing, the surface area of the air-water interface changes. During exhalation when the surface area is smallest, the pulmonary surfactant will be forced away from the interface (Figure 3). During inhalation, the surface area increases again and must be once again coated with pulmonary surfactant. These multi-layered, surface associated structures would fulfill these requirements in that they can provide a way for the surfactant to be stored during exhalation. They also allow for efficient re-spreading of the surfactant during inhalation. The formation and stability of these structures are thus of great physiological importance [8] [17].

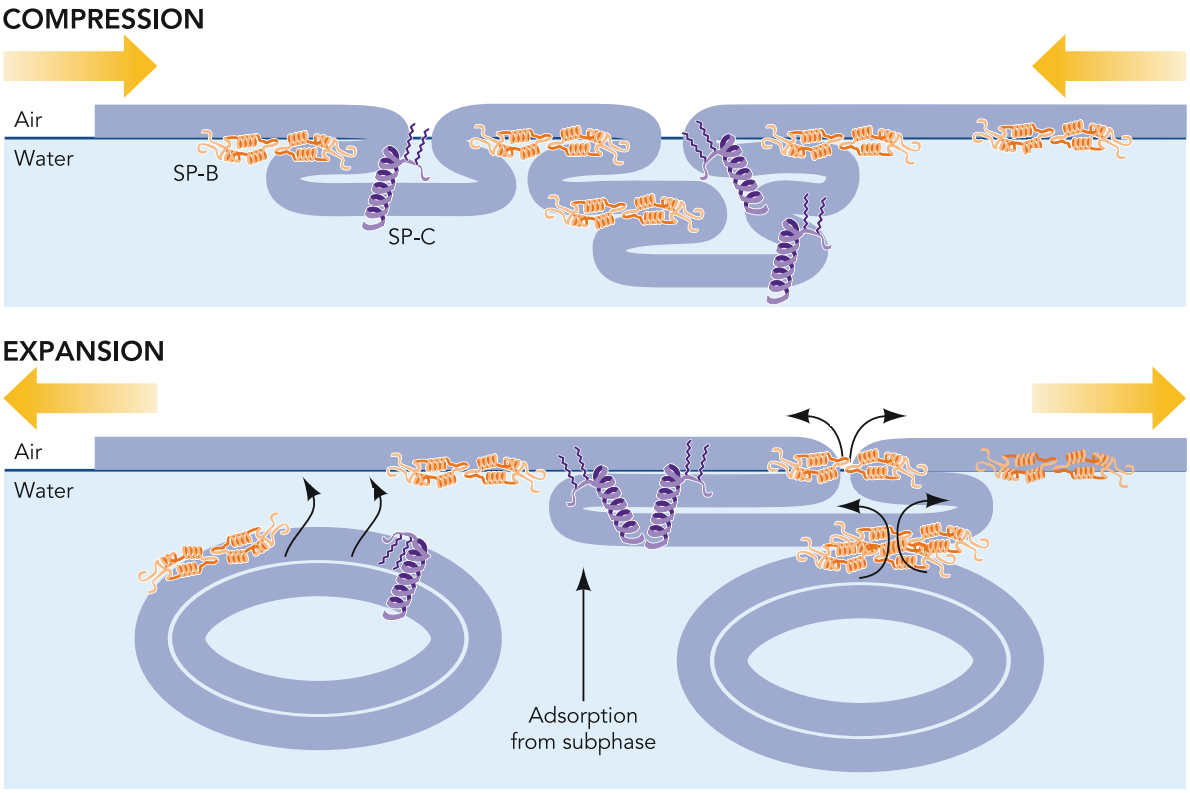

Figure 3: The hydrophobic surfactant proteins and their interactions with surfactant layers during compression and expansion. Adapted from Figure 3, Perez-Gil and Weaver, 2010 with permission from the publisher [16].

1.3 Surfactant Proteins

There are four surfactant proteins: surfactant protein A, B, C, and D (SP-A, SP-B, SP-C, SP-D). They were named chronologically with A being the first discovered and D being the last [18]. SP-A and SP-D are hydrophilic and mostly function as part of the innate immune defence system. SP-B and SP-C are small hydrophobic proteins that directly interact with the surface active films.

Along with reducing surface tension, pulmonary surfactant can help defend against inhaled pathogens. The lungs have a large surface area that is regularly exposed to the environment. To help combat this, the surfactant has evolved an immune function along with the surface active function. Its position along the air-water interface establishes a barrier that pathogens have difficulty getting past to reach the epithelial cells. Also, surfactant proteins A and D have been shown to have innate immune properties [19] [20] [21].

SP-A is the most abundant pulmonary surfactant protein. It consists of a carbohydrate-recognition domain and a collagen domain that forms a trimer [22]. Six of these trimers come together to form an octadecamer in aqueous solution, a structure that is consistent with the collectin family of proteins [23] [24] [22]. However, it has also been found to form smaller conformations when interacting with lipid or detergent micelles [25]. SP-A has the ability to bind to many possible ligands including Ca^{2+}, phospholipids, and carbohydrates allowing the protein to bind to a wide variety of pathogens including bacteria, viruses, and fungi [24] [26]. It can also attract alveolar macrophages to the pathogens in order to remove them [27]. Knockout of the SP-A gene causes increased vulnerability to infection [26]. Despite its relative abundance, the lack of a working SP-A

gene does not result in impaired breathing [28]. This suggests it is not essential to the surface activity of pulmonary surfactant. However, experiments show that SP-A assists in the formation of surface active films together with SP-B and SP-C. Also, these films perform better during compression-expansion dynamics when SP-A is present which suggests a cooperative function of SP-A by interacting with the hydrophobic surfactant proteins [29] [30].

SP-D is another member of the collectin family [22]. Its structure consists of a collection of trimers similar to SP-A. The quaternary structure of SP-D however, only consists of four trimers as opposed to the six in SP-A [10]. Both the structures of SP-A and SP-D were studied using X-ray crystallography for the CRD domains. Electron microscopy was used to complete the structure [31] [32]. Knockout of the SP-D gene also leads to a marked increase in the vulnerability to infection. However, this knockout has no observable effect on surface activity indicating that the presence SP-D is not important to surfactant function [33]. SP-D has been shown *in vivo* to help regulate the lipid homeostasis of surfactant [22].

Along with the immune function associated with SP-A and SP-D, surface tension reduction by pulmonary surfactant is also essential. Surface tension relies on the hydrophobic surfactant proteins SP-B and SP-C [8].

SP-C is a small, 35 residue alpha-helical peptide. As well as having many hydrophobic amino acids, it also has two sites of palmitoylation near the carboxy-terminus [34]. They combine to make SP-C one of the most hydrophobic proteins known. These features allow SP-C to interact directly with the lipid portion of the pulmonary surfactant. Through this interaction, SP-C could be helping to stabilize the multi-layered

surfactant reservoir and also aid in the spreading of surface active films [8] [35]. Despite this important function, the presence of a working SP-C gene is not necessary to start air-breathing life. Mice with a knockout of the SP-C gene display normal gas exchange and surfactant function [36] [37]. The presence of SP-B could be sufficient for surfactant to function normally. In humans however, SP-C deficiency has been found to lead to chronic lung impairment [38]. The full structure of SP-C in an organic solvent (chloroform/methanol), was determined through nuclear magnetic resonance (NMR) spectroscopy [39]. NMR was used instead of X-ray crystallography due to the inherent difficulty in getting hydrophobic proteins to crystallize. This difficulty is also seen with the other hydrophobic surfactant protein: SP-B.

1.4 Surfactant Protein B

SP-B is the most important surfactant protein. It is the only surfactant protein whose deficiency is absolutely fatal [40] [41]. SP-B is first synthesized as a soluble propeptide. It is processed to its mature form in the alveolar type II epithelial cells. This processing involves the action of multiple enzymes including pepsinogen C, cathepsin H, napsin A, and possibly others [42] [43] [44] [45]. The mature SP-B is a 79 residue, 8.7 kDa hydrophobic protein (Table 2). Like SP-C, it is one of the most hydrophobic proteins known. It is more hydrophobic than many integral membrane proteins. It also contains many cationic residues which give SP-B an overall +7 charge at neutral pH. Being positively charged could help SP-B interact with the large proportion of negatively charged lipids that form part of the pulmonary surfactant [46].

Most of what is currently known about SP-B function has arisen from biophysical experiments with SP-B isolated from lung lavages from porcine or bovine sources. It has been shown to promote membrane binding, fusion, and leakage [47] [48] [49]. SP-B can also be observed assisting the absorption spreading of lipid films to an air-water interface [50] [51]. Any or all of these activities could be the mechanism of SP-Bs contribution to the surface activity of pulmonary surfactant. Many current models have SP-B assisting the formation and stabilization of the multi-layered films that form underneath the air-water interface during exhalation [52]. It also facilitates the re-spreading of the surface active film during inhalation [53] [54]. Unfortunately, the mechanism of SP-B is incompletely understood due mostly to the lack of a three-dimensional structure.

SP-B is a member of the saposin superfamily of small lipid-binding proteins [55] [56]. SP-B has either four or five alpha helices. These are held together by three disulfide bonds between cysteine residues. This is a structure that is similar to proteins of the saposin family [57]. SP-B isolated from lung lavages has an observed size of about 17 kDa leading to the suggestion that it can form a dimer that is held together with an intermolecular disulfide bond [55]. While this much about SP-B structure is known, the full tertiary structure still remains a mystery. The difficulty with finding the structure of SP-B will be discussed below.

Table 2: Amino acid sequence of mature human surfactant protein B (SP-B)

1-10	Phe - Pro - Ile - Pro - Leu - Pro - Tyr - Cys - Trp - Leu
11-20	Cys - Arg - Ala - Leu - Ile - Lys - Arg - Ile - Gln - Ala
21-30	Met - Ile - Pro - Lys - Gly - Ala - Leu - Ala - Val - Ala
31-40	Val - Ala - Gln - Val - Cys - Arg - Val - Val - Pro - Leu
41-50	Val - Ala - Gly - Gly - Ile - Cys - Gln - Cys - Leu - Ala
51-60	Glu - Arg - Tyr - Ser - Val - Ile - Leu - Leu - Asp - Thr
61-70	Leu - Leu - Gly - Arg - Met - Leu - Pro - Gln - Leu - Val
71-79	Cys - Arg - Leu - Val - Leu - Arg - Cys - Ser - Met

1.5 Pulmonary Surfactant Disorders

Being of such vital importance, impairment of pulmonary surfactant can lead to a detrimental effect on gas exchange and lung function in general. There are several disorders that involve pulmonary surfactant but the most common are respiratory distress syndrome (RDS), and acute respiratory distress syndrome (ARDS).

RDS is also commonly known as neonatal respiratory distress syndrome due to it affecting babies who have had a premature birth. If born without enough time to properly develop a functional pulmonary surfactant, breathing can be extremely impaired [58]. RDS can currently be treated with a combination of mechanical ventilation and the application of exogenous surfactant. This treatment only has to last long enough for the infants to produce their own surfactant normally. Treatment with exogenous surfactant has decreased the mortality rate of premature birth by half. However, RDS remains the leading cause of death of premature infants [59].

The exogenous surfactant used in treatment for RDS usually comes from natural sources. These sources are commonly bovine and include the most common exogenous treatment in Canada: bovine lipid extracted surfactant (BLES) [60]. The composition of surfactant from this source is similar to normal human surfactant with the exception of the hydrophilic proteins (SP-A and SP-D) and neutral lipids (glycerides, cholesterol). The BLES does contain the hydrophilic proteins SP-B and SP-C which are crucial to surface activity. The sequence of the surfactant proteins are highly conserved amongst species. The relative expense of BLES is not an obstacle here, at least in developed countries, because of the very small amount needed to saturate premature

lungs. This is not the case for the surfactant disorders afflicting adults including ALI and ARDS.

ALI and the more severe ARDS are acute disorders which lead to the inactivation of pulmonary surfactant. There can be many different causes for this. These include inflammation, mechanical stress, oxidative stress, or the leakage of blood serum proteins into the alveolar space [61]. ARDS is much more complicated to treat than RDS.

Mechanical ventilation leads to problems in that the stress can exacerbate the condition. In fact, people who are hooked up to mechanical ventilators for a significant amount of time can develop ARDS [62]. Treatment with exogenous surfactant is very difficult. Unlike neonatal lungs, adult lungs are much larger and require much more surfactant to be effective. Also, people with ARDS likely already have collapsed alveoli which need more surfactant to force them open. Both of these reasons cause sufferers of ARDS to require a lot of exogenous surfactant for it to have a chance to be effective. Natural sources of surfactant are much too expensive to provide a viable treatment [63]. An artificial source of a surfactant treatment has long been a goal of surfactant researchers. To date, no artificial surfactant treatments have shown any improvement for ARDS patients [64]. This is partly due to the conditions already present in the lungs during ARDS also inactivating the exogenous surfactant [65]. Furthermore, the inability to artificially produce SP-B, which is critical to proper surfactant function, reduces the efficacy of any artificial surfactant treatment. For these reasons, with current treatments, the mortality rate from ARDS is 50% [66]. The development of an artificial source for SP-B could lead to artificial surfactant that could act as a successful treatment for ARDS. Also, it would support solving the three-dimensional structure of SP-B which could lead

to a better understanding of its mechanism and result in the development of new ARDS treatments.

1.6 Structural Studies of Proteins

As mentioned before, the most common method for the structural determination of proteins is X-ray crystallography. This is a powerful tool that can determine protein structure down to the atomic level. Unfortunately, this method requires proteins to be crystallized in an ordered fashion. With the right conditions, this can be done relatively easily with soluble proteins. Hydrophobic proteins, however, are resistant to crystal formation, partly because the detergents that are commonly used to isolate hydrophobic proteins prevent crystal lattice formation [67] [68]. For this reason, only 1% of protein structures in the Protein Data Bank (PDB) are hydrophobic or membrane proteins [68]. SP-B is an extremely hydrophobic peptide. As a result of this, all attempts to produce an SP-B crystal have failed.

The other method most commonly used to determine protein structure is solution NMR. Specifically, this is done using techniques such as three dimensional total correlation spectroscopy (TOCSY) and nuclear Overhauser effect spectroscopy (NOESY). Application of these techniques to all but the smallest proteins requires the replacement of the carbon and nitrogen atoms of a protein with ^{13}C and ^{15}N isotopes. These isotopes have half-spin nuclei and can produce a signal with NMR. These spins can interact with each other through-bond (TOCSY) and through-space (NOESY). The frequencies of the pairs of nuclei involved in these interactions are then determined, a process called "assignment". Then, the NOESY spectra are used to generate a long list

of pairs of hydrogen nuclei that are close in space. With enough of these distance restraints, a computer program can calculate possible structures of the protein [69] [70]. The advantage of this technique over X-ray crystallography is that there is no crystallization requirement and hydrophobic proteins can be analyzed in the presence of lipid or detergent micelles. Interaction with these micelles would provide a more physiologically relevant structure as many hydrophobic proteins like SP-B interact with lipids. The main disadvantage is the need for ^{13}C and ^{15}N labelled protein. These can be obtained through the recombinant expression of the protein in *E.coli.*

1.7 Recombinant Expression of Proteins

The recombinant expression of proteins is a common artificial source for proteins. If the genetic sequence of the protein is known, that gene can then be inserted into a bacterial expression vector which can then be transfected into an *E.coli* culture. These plasmids vary depending on the protein being expressed but they usually contain some common features including resistance to a certain antibiotic (such as ampicillin or kanamycin) and a promoter than can act as a genetic “switch”. The antibiotic resistance is to reduce competition and contamination from other bacteria. When grown in the presence of the antibiotic, only the bacteria that contain the plasmid should grow [71]. The promoter is used to achieve some control over the expression of the gene of interest. In many cases, this promoter is the lac operon. This is a promoter already found in some bacterial species. In the presence of lactose, the promoter is activated, leading to the expression of genes involved with lactose metabolism. In recombinant systems, the lac operon is placed in front of the gene of interest. Instead of lactose, an

analog known as isopropyl-β-D-1-thiogalactopyranoside (IPTG) is used. Like lactose, IPTG can activate the lac operon and thus induce expression of the gene. Unlike lactose, it will not degrade, resulting in a constant concentration of IPTG over the course of protein expression [72]. This system of continuous activation of the gene is known as over-expression and produces much more protein than the *E.coli* would normally produce. This induction also inhibits bacterial growth as all available resources are used to produce the protein.

Several variables have to be optimized in order to maximize protein yield, such as the timing of induction, which is usually done during the log phase of bacterial growth. Next, the concentration of IPTG to use for induction must be determined and finally, the expression time must also be optimized. While there is usually some idea of the appropriate ranges for each variable, the optimization requires a lot of trial and error [73].

Recombinant expression in *E.coli* is very efficient in producing soluble proteins. However, problems arise when trying to over-express hydrophobic proteins. Recombinant hydrophobic proteins can be toxic to the *E.coli* through possible competition with native membrane proteins and disruption of the membrane as a whole [68] [73]. Because of this, it is difficult to get large yields of recombinant hydrophobic proteins. There are, however, techniques to overcome these difficulties. First, several bacteria strains have been developed to resist the toxicity of hydrophobic proteins. One of these strains, C43, directs the expressed proteins into inclusion bodies making them incapable of membrane disruption [74]. Also, the protein can be expressed as a fusion with a large hydrophilic protein which would increase the solubility of the protein being

over-expressed and prevent it from disrupting the bacterial membrane. Common fusion partners include maltose binding protein (MBP), glutathione S-transferase (GST) and staphyloccal nuclease (SN) [73] [75] [76].

1.8 Purification of Recombinant Proteins

The next step in producing recombinant protein is to purify it from native *E.coli* proteins as well as other biomolecules such as lipids and DNA. The cells can be lysed through various methods including the use of a French press and sonication. Different cellular components can be separated through the use of different solvents and centrifugation. It is possible to enrich the sample from the soluble, membrane, and insoluble inclusion bodies fractions. Depending on the nature of the expressed protein, it can be located in one or more of these fractions and should be located before further work.

The recombinant protein can be further purified using affinity chromatography. Some hydrophilic fusion proteins also have a binding function. Taking advantage of this fact, chromatography resin loaded with a ligand specific for the fusion protein can be used to isolate the fusion complex. These fusions include MBP and GST which bind to maltose and glutathione respectively [73] [75]. Alternatively, recombinant proteins can be isolated through the use of a histidine tag. A sequence of at least six histidine (6xHis) residues can bind to a nickel charged resin in a technique known as immobilized metal affinity chromatography (IMAC) [77]. The 6xHis tag can be expressed as a part of the protein. Using these chromatography methods, the recombinant protein (as a fusion or otherwise) can be sufficiently enriched.

If the recombinant protein was expressed without any fusions then this would be the final step. However, if the protein was expressed with a fusion protein then this must be removed before most structural studies can be done. To facilitate this, a cleavage site located between the fusion and the protein of interest is usually included in the design of the gene. This site is a particular sequence that can be targeted for cleavage by either enzymatic or chemical means. Enzymatic cleavage makes use of protease to cleave the fusion. Common proteases used in this way are trypsin, thrombin, and tobacco etch virus (TEV) protease [76 78 79]. These reactions have to take place under gentle buffer conditions so the enzyme remains folded and functional. However, under these conditions, hydrophobic proteins tend to aggregate which can block enzymatic action. One way around this is to switch to chemical cleavage which takes place under much more severe conditions. The most commonly used method of chemical cleavage uses cyanogen bromide (cleaves after methionine residues), which reacts in a solution of 70% formic acid [67]. Under these conditions, the fusion protein should be entirely unfolded and the cleavage sites sufficiently exposed. Another chemical that is routinely used for chemical cleavage is hydroxylamine [80]. While generally more efficient, the conditions for chemical cleavage renders proteins completely denatured and they must be carefully refolded to properly function.

The fusion construct has to be designed so that the specific cleavage site is not found anywhere in the protein of interest. If this were the case, the protein would get cleaved into pieces. For example, because cyanogen bromide cleaves after methionine residues, the protein cannot have any internal methionines. In this case, another

proteolytic agent would be used or the internal methionines could be mutated to another similar amino acid [67].

After proteolysis has taken place, the protein must be separated from the hydrophilic fusion protein. There might also be some undigested fusions present that must be removed if the reaction wasn't 100% efficient which is often the case. The separation may require many different techniques including organic extraction and chromatography. The production of a recombinant fusion protein and its subsequent purification is discussed in detail in this thesis.

1.9 Recombinant Expression of SP-B

Recombinant expression would be an excellent artificial source for SP-B for both research and clinical applications. It is a relatively cheap and quick way to produce proteins. Manipulation of the gene would permit the introduction of mutations allowing certain residues to be changed. Through observing the impact of these changes on SP-B function, we can gain some insight into which residues are critically important. Gene manipulation will also have applications in the clinical sense as certain genes can be designed to produce an SP-B derivative that is more resistant to inactivation in ARDS which can lead to possible treatment options. Furthermore, the *E.coli* can be grown in a media containing only ^{13}C and ^{15}N carbon and nitrogen sources producing the isotope-labelled SP-B that is required for NMR structural studies. Of course, before any expression can be attempted, a plasmid construct must be designed.

1.10 Designing the Plasmid Construct

The first step of recombinant expression is to design the plasmid that will be used to transfect the bacterial cells. Several things must be considered. First of all, will the protein of interest poison the bacteria? As mentioned above, hydrophobic proteins have a tendency to interfere with the normal expression in bacterial systems. Expressing the protein is only part of the process as the protein must also be isolated from the other bacterial proteins and other molecules including lipids.

The work presented in this thesis can be traced to work done with expression of SP-C [76]. Like SP-B, SP-C is a very hydrophobic protein and the expression was facilitated by expressing the SP-C as a fusion with staphylococcal nuclease (SN), which is a large hydrophilic protein. The purification was accomplished through the use of a poly-histidine tag at the amino-terminus of the fusion and a thrombin cleavage site was placed between the two proteins to remove the SN. To try and replicate the successful expression of SP-C with SP-B, the plasmid was modified to replace SP-C with SP-B. This plasmid was first produced by the Jesus Perez-Gil lab at the Universidad Complutense de Madrid and passed on to our lab. Attempts to produce a full length recombinant SP-B with this plasmid was discussed in the thesis of Mahzad Sharifahmadian [81], and did not yield high expression levels of SP-B. As suggested, a new gene was designed to attempt to improve expression.

This new gene, designated SN-Δ7NTΔM-SP-B-6His, was designed with several new features to aid in the expression and purification of SP-B (Figure 4). First of all, the thrombin cleavage site was removed in favour of a cyanogen bromide cleavage site (a methionine residue). The use of a cyanogen bromide digest also required the removal

of the internal methionines in SP-B which were changed to leucines similar to the work done in Gong et al. [67]. Another change to the SP-B was made in that the seven amino-terminal residues (FPIPLPY) were removed to aid in the expression as suggested by Sharifahmadian [81]. Finally, the 6-histidine tag was moved from the amino-terminus of the SN to the carboxy-terminus of the SP-B. The SP-B and 6-his tag were separated by another cyanogen bromide cleavage site to facilitate the removal of the tag.

The work presented here will demonstrate a new effort to express SP-B recombinantly using this new gene. The hypothesis is that these genetic modifications will allow SP-B to be expressed in an *E. coli* system. The goal is to express and purify SP-B for structural studies and for inclusion in improved therapeutics for ARDS.

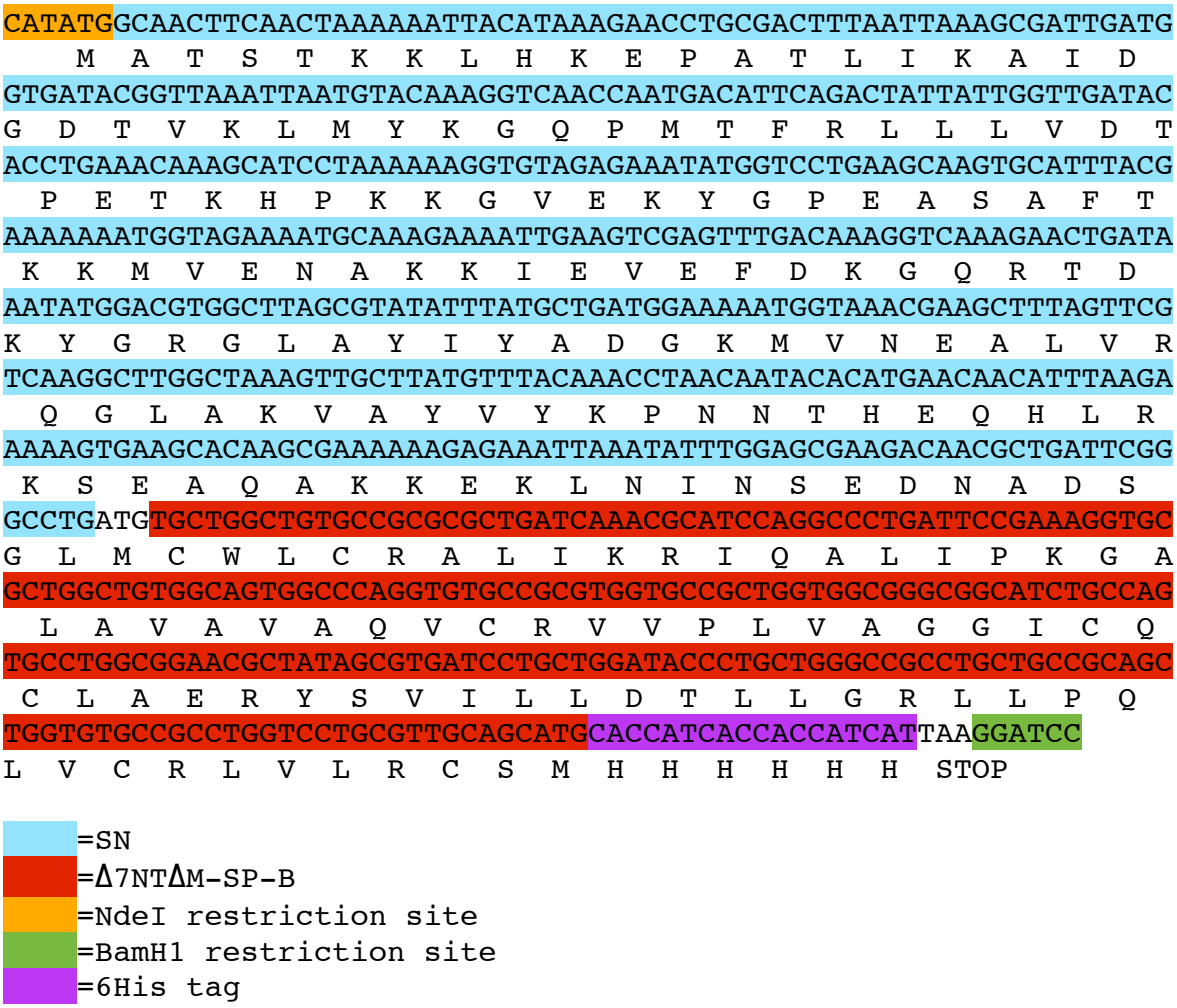

Figure 4: The SN-Δ7NTΔM-SP-B-6His plasmid construct (both the nucleotide sequence and amino acid sequence of the expressed fusion).

2. Materials and Methods

2.1 SDS Polyacrylamide Gel Electrophoresis (PAGE)

SDS PAGE was used throughout this work [82]. Two types of gels were used, a precast, 16.5% polyacrylamide gel (Mini-PROTEAN Tris Tricine Precast Gel, Bio-Rad, Hercules, CA, USA) and a hand-cast 18% polyacrylamide gel. The 18% gels were prepared by first creating a separating gel by mixing 6 mL of a 30% acrylamide, 0.8% bis-acrylamide solution with 4 mL separating buffer (91.3 g/L Tris, 2.1 g/L SDS, pH = 8.8). 100 µL ammonium persulfate (10%) and 20 µL tetramethylethylenediamine (TEMED) was then added and mixed well. The resulting solution was poured between two gel plates leaving enough room for the stacking gel. 50% ethanol was poured on top and the separating gel was allowed to set. Once set, the ethanol was discarded and the top of the gel was washed with deionized water. A stacking gel was prepared by mixing 0.65 mL of a 30% acrylamide, 0.8% bis-acrylamide solution with 4.35 mL stacking buffer (16.18 g/L Tris, 1.2 g/L SDS, 0.1 g/L sodium azide, pH = 6.8). 100 µL ammonium persulfate (10%) and 20 µL TEMED was then added and mixed well. The stacking gel was then poured on top of the separating gel. Before setting, a comb was placed in the stacking gel to create sample wells. After the stacking gel was set, the gels were either used immediately or stored in the fridge overnight.

The gels were placed in an electrophoresis tank which was filled with the appropriate running buffer: SDS buffer (2.4 g/L Tris, 11.25 g/L glycine, 1 g/L SDS, 0.1 g/L sodium azide) for the hand-cast 18% gels or Tris Tricine buffer (Bio-Rad, Hercules,

CA, USA) for the precast gels. Protein samples were dissolved in sample buffer (13% glycerol, 1.97 g/L Tris, 3.25 g/L SDS, 0.1 g/L sodium azide, 0.02% bromophenol blue) with or without a reducing agent (dithiothreitol (DTT)). These samples were then heated in boiling water for 2-3 minutes, and once cooled, applied to the gel. Two molecular size markers were usually loaded onto the gels as well. The markers were the Precision Plus Kaleidoscope Protein Standards and the Kaleidoscope Polypeptide Standards (Bio-Rad, Hercules, CA, USA).

The gel was run at 80 V until the tracking dye reached the separating gel at which point the voltage was increased to 180 V until the tracking dye reached the bottom of the gel. The gels were either stained with Coomassie Brilliant Blue (CBB) R-250 or silver.

2.1.1 CBB R-250 Staining

Completed gels were placed in a staining solution (0.25% CBB R-250, 40% ethanol, 7% glacial acetic acid) and agitated for 45 minutes. The gels were then transferred to a destaining solution (10% ethanol, 7% glacial acetic acid) and agitated until the protein bands were visible and the background was clear.

2.1.2 Silver Staining

Completed gels were placed in a fixing solution (40% ethanol, 10% glacial acetic acid) and agitated for 30 minutes. The gel was then transferred to an incubating solution (30% ethanol, 68 g/L sodium acetate trihydrate, 2 g/L sodium thiosulfate, 0.1% gluteraldehyde) and agitated for another 30 minutes. The gel was washed three times

with deionized water and placed in a silver solution (1 g/L silver nitrate) and agitated for a further 40 minutes. The gel was rinsed once with deionized water and placed into a developing solution (25 g/L sodium carbonate) until the bands were evident (5-15 minutes). The reaction was stopped by placing the gel in stop solution (14.6 g/L disodium ethylenediamine tetraacetate (EDTA)) and agitated for 15 minutes.

2.2 Western Blot

Western blot analysis was also used throughout this work [83]. Electrophoresis was performed as described above but instead of staining, the finished gel was placed in transfer buffer (10 mM CAPS,10% methanol, pH = 11) and agitated for 30 minutes. A polyvinylidene fluoride (PVDF) membrane (Millipore Corporation, MA, USA) was cut out and rinsed once with methanol, three times with deionized water, then soaked in transfer buffer for 30 minutes. Both the gel and membrane were placed in the electrophoresis apparatus and the protein was transferred to the membrane by applying a voltage of 60 V for two hours. Once complete, the gel was discarded and the membrane was soaked in a blocking solution (2% milk in TTBS) for one hour. After three washes with TTBS (150 mM Tris ,50 mM NaCl, 0.05% Tween-20 at pH = 7.6), the gel was soaked in a primary antibody solution overnight. In this research, the primary antibody used was an anti-SP-B rabbit antibody (Seven Hills Bioreagents, Cleveland, OH, USA) diluted 1:5000 in TTBS. The next morning, the primary antibody was decanted and stored in a -4°C freezer. The membrane was washed twice with TTBS and a secondary antibody was applied and stirred for one hour. An anti-rabbit IgG with alkaline phosphatase (Sigma-Aldrich, St. Louis, MO, USA) diluted 1:5000 in TTBS was

used. The secondary antibody is discarded and the membrane washed twice with TTBS. The colour reaction is performed in the dark using a solution of 60 µL BCIP and 120 µL NBT in 20 mL TTBS. Once complete, the colour reaction is stopped using Tris-EDTA (TE) buffer (10 mM Tris, 1 mM EDTA, pH = 8) All stages of this procedure were performed at 20°C.

2.3 Transformation of Plasmids into Cell Line

1µL of the 1 ng/µL plasmid DNA was added to 50µL of C43 (DE3) competent cells in a prechilled tube. The mixture was incubated on ice for 30 minutes then heat shocked at 42°C for 45 seconds. This was followed by a further incubation of 2 minutes, once again on ice. 500µL of 2xYT broth (16g/L tryptone, 10g/L yeast extract, and 5g/L NaCl at pH 7) preheated to 42°C was added to the cells and this was incubated at 37°C, 175 rpm for 1 hour. After incubation, the transformation mixture was plated onto two 2xYT agar plates containing ampicillin and incubated overnight at 37°C.

2.4 Determining the Cellular Extract Fraction Where the Expressed SN-Δ7NTΔM-SP-B-6His is Located

To ascertain in which cellular extract fraction the expressed SN-Δ7NTΔM-SP-B-6His fusion protein is located, a smaller scale expression was prepared. A small sample of transfected C43 cells was placed in 10 mL 2xYT broth + 0.1 mM ampicillin and incubated overnight at 37°C and 175 rpm. The overnight culture was then used to inoculate 1 L of 2xYT broth with 0.1 mM ampicillin in a 4 L flask. The flask was incubated at 37°C and 175 rpm until the OD_{600} (optical density at 600 nm) reached

approximately 0.6. The cells were induced with 0.4 mM IPTG and returned to the shaking incubator for a further 3 hours at 37°C. Induction was halted by centrifuging the cells suspension at 5000 rpm for 15 minutes at 4°C upon which the cells were resuspended in a Tris buffered saline (TBS) buffer + 5 mM phenylmethylsulfonylflouride (PMSF). The TBS buffer consists of 150 mM Tris and 50 mM NaCl at pH = 7.6. The cells were then lysed by passing them twice through a French press at 12,000 psi and the total extract was divided into three equal portions to correspond to the three different cellular extract fractions. These samples were not centrifuged. Sample 1 contained the extract in TBS buffer, sample 2 contained the extract in TBS buffer + 0.5% lauroyl sarcosine (LS), and sample 3 contained the extract in TBS buffer + 0.5% LS + 6 M urea.

To each sample, imidazole (5M stock) was added to 20mM and three nickel-charged IMAC columns (see below) were prepared, one for each sample. These columns were equilibrated with the appropriate solvent conditions + 20mM imidazole. Each sample blot was applied to a column at 20°C and washed with starting buffer. Any fusion protein was eluted using the starting buffer + 300mM imidazole. The relative amount of the fusion protein in each sample was determined by applying a portion (10 µL) of each sample to an 18% polyacrylamide gel (SDS PAGE).

2.5 Large Scale Expression of SN-Δ7NTΔM-SP-B-6His

A small sample of transfected C43 cells were placed in 75 mL 2xYT broth + 0.1 mM ampicillin and incubated overnight at 37°C and 175 rpm. The next morning, 10 mL of the starting culture was added to each of six 4 L flasks containing 1 L of 2xYT broth + 0.1mM ampicillin. The flasks were incubated at 37°C and 175 rpm until the OD_{600}

reached approximately 0.6. The cells were induced with 0.4 mM IPTG and returned to the shaking incubator for a further 3 hours. Induction was halted by centrifuging the cell suspension at 5000 rpm for 15 minutes at 4°C upon which the cells were resuspended in a TBS buffer + 5mM PMSF and frozen at -20°C until ready to lyse. The procedure changed for cell lysis during which the sonication step was eliminated and three passes through a French press at 12,000 psi was utilized. After lysis, no centrifugation takes place but LS and urea were added to the total cellular extract to make a concentration of 0.5% w/w and 6M respectively. Solubilization was achieved by mixing the cellular extract in this buffer for one hour. To remove anionic impurities, 1 g of DE52 anionic exchange cellulose resin (Whatman, Maidstone, Kent, UK) equilibrated with Buffer A (TBS, 0.5% LS, 6 M urea), was added to the total extract and mixed for another hour. The DE52 resin was then removed by centrifugation at 8000 rpm for 15 min at 15°C. The supernatant was decanted and imidazole (5M stock) was added to 10 mM. Approximately 5 mL nickel-charged resin (see below) equilibrated with Buffer A + 10 mM imidazole was then added to the supernatant and this mixture was then gently shaken for an hour. The mixing of resin directly into the cell extract was done instead of applying the extract to a column due to the increased thickness of the extract that is a result from this new procedure.

The nickel-charged resin with SN-SP-B fusion protein bound is removed from the rest of the extract by centrifugation at 8000 rpm for 15 minutes at 15°C. The supernatant is discarded and the resin is resuspended in a small amount of Buffer A + 10 mM imidazole at 20°C and applied to a column. This is followed by a washing of the column using 20 mL Buffer B (TBS, 0.2% LS, 6 M urea) + 10 mM imidazole. The fusion

protein is then eluted using a step-wise imidazole gradient with the application of Buffer B + 25 mM imidazole followed by 25, 50, 100, 200, and 300 mM imidazole (10 mL each). The elution was collected as approximately 1.5 mL fractions using gravity. The location of the fusion protein (and any other bound expression products) was determined using OD_{280} of the fractions followed by SDS PAGE with an 18% polyacrylamide gel. The presence of SP-B was confirmed using Western blot analysis with an anti-SP-B antibody. SP-B was confirmed in both 8 kDa and 26 kDa bands in the SDS PAGE gel. Fractions containing both samples were separately pooled and dialyzed overnight against water using 1000 Da dialysis tubing (Thermo Scientific, NC, USA) for the 8 kDa sample and 12-14 kDa dialysis tubing (Sigma-Aldrich, St. Louis, MO, USA) for the 26 kDa sample. The samples were lyophilized by transferring them into freeze-drying flasks (Labconco, Kansas City, MO, USA) and flash freezing them using liquid nitrogen. The flasks are then hooked up to a freeze drier overnight or until all the ice had evaporated leaving a dry protein powder. Both of the dried protein samples were then stored at 4°C.

2.6 Nickel-Bound Immobilized Metal Ion Affinity Chromatograhphy (IMAC)

To prepare the resin (IMAC Separose 6 Fast Flow, GE Healthcare Life Sciences, Piscataway, NL, USA), it was poured into a small column (1 cm diameter) and the fluid allowed to flow through. Ni ions in the form of nickel (II) sulfate (1/2 column volume of 0.1 M $NiSO_4$) was added to the resin which was then washed with excess deionized water and stored until ready for use. Before use, the column is equilibrated with one

column volume starting buffer. After use, the column is re-equilibrated with two column volumes starting buffer and stored at room temperature.

2.7 Cyanogen Bromide Digestion

The lyophilized protein samples were dissolved in 2 mL, 70% formic acid. An excess of cyanogen bromide was then added and the reaction was allowed to take place overnight at room temperature in the dark. Cyanogen bromide is a dangerous compound to work with so precautions must be taken such as wearing the proper safety equipment (ie. lab coat, gloves, and eye protection). Handling of the cyanogen bromide and the reaction itself must be completed in a fume hood. Accurate measurements cannot be obtained inside a fume hood so an obvious excess of cyanogen bromide was dissolved in the solution (ie. a small amount on the end of a spatula). The following day, 28 mL deionized water was added to the reaction mixture to create a 1:15 dilution. The sample was lyophilized and the resulting dry protein sample was stored at 4°C [84].

2.8 Enrichment of SP-B

Enriching the modified SP-B requires separating it from the SN fragments produced during cyanogen bromide digestion as well as any undigested fusions. The enrichment was a challenging endeavour which involved attempts of several enrichment techniques. All of the isolation work described below was done with the 26 kDa samples obtained from the expression of SN-Δ7NTΔM-SP-B-6His.

2.8.1 Organic Extraction

The first attempt to separate SP-B from the impurities was through the use of an organic extraction similar to that used to isolate recombinant SP-C [76]. The lyophilized cyanogen bromide digest was resuspended in 2 mL deionized water with 0.5% LS. To the suspension, one volume of methanol and one volume of chloroform were added. This mixture was vortexed and incubated at 37°C for 30 minutes, after which another volume of chloroform and one volume of deionized water were added. After vortexing, the layers were separated by centrifugation at 1500 rpm for 5 minutes at 15°C, during which an unexpected insoluble layer formed between the organic and aqueous phases. The bottom, organic layer was carefully removed and kept in a separate flask. To the remaining aqueous and insoluble phases, another two volumes of chloroform was added. The mixture was once again vortexed and centrifuged as before with the bottom, organic layer removed and pooled with the first organic sample. The insoluble precipitate was removed from the aqueous phase through centrifugation in a microcentrifuge. The aqueous layer was then decanted and lyophilized while the organic phase was dried under a stream of nitrogen. The protein content of all three phases: organic, insoluble, and aqueous were analyzed through SDS PAGE using an 18% polyacrylamide gel.

2.8.2 High Performance Liquid Chromatography (HPLC)

The next attempt at enriching the SP-B was through HPLC. A freeze dried, cyanogen bromide digested SN-SP-B sample was mixed into a 1 mL solution of 80% acetonitrile, 20% HPLC grade water, and 0.1% trifluoroacetic acid (TFA). The solution

was mixed gently in an attempt to dissolve as much protein as possible. After mixing, the cloudy solution was passed through a 25 mm syringe filter with a 1 µm glass fiber membrane (Pall Life Sciences, Ann Arbor, MI, USA). The resulting clear solution was then applied to a reverse-phase DYNAMAX C8 HPLC column (Varian Inc., St. Laurent, QC, Canada) at 20°C and eluted with an acetonitrile gradient (20% - 100%) pumped through the column at a rate of 15 mL per minute and collected as approximately 5 mL fractions. Fractions containing protein were identified using an OD_{280} profile and each separate elution was pooled. Each eluted sample was analyzed by SDS PAGE with an 18 % polyacrylamide gel to determine the location of SP-B.

2.8.3 Cationic Exchange Chromatography

A freeze dried, cyanogen bromide digested SN-SP-B sample was first dissolved in 6 M urea to break up the aggregates and allow the protein to solubilize. To this solution, PC was added to a 5:1 lipid to protein ratio and incubated for 10 minutes at 39°C followed by vortexing for one minute. This incubation/vortexing was repeated for a further 90 minutes after which the mixture was dialyzed against 4 L water overnight. 100 mg CHAPS (3-[(3-cholamidopropyl)dimethylammonio]-1-propanesulfonate) detergent (dissolved in 200 µL deionized water) was then added to the mixture and gently stirred until the solution was clear.

A starting buffer of 50 mM phosphate (5.74 g/L Na_2HPO_4, 1.2 g/L KH_2PO_4), 10 mM CHAPS, and 0.025 M NaCl, pH = 7 was prepared. This solution was used to dilute the protein/lipid sample to 10 mL and equilibrate a HiTrap cationic exchange column (GE Healthcare Life Sciences, Piscataway, NL, USA). The 10 mL of sample was applied

to the column at 20°C and the protein was eluted with a step-wise salt gradient using the same solution as the starting buffer except with increasing NaCl concentrations (0.025, 0.1, 0.25, 0.5, 0.75, and 1 M). 10 mL of each step was used and passed through the column using a peristaltic pump at about 2 mL per minute. The elution was collected in approximately 1 mL fractions and analyzed by OD_{280} and SDS PAGE with a 18% polyacrylamide gel. After use, the HiTrap cationic exchange column was washed with excess deionized water.

2.8.4 Sephadex LH20 Enrichment of SP-B from Cyanogen Bromide Digest

After dialysis, the products of the cyanogen bromide digest tend to heavily aggregate making them very insoluble. In an effort to force these aggregates into an organic solution required for certain separation techniques, a new solubilization procedure was tried. The digest was first dissolved in 5 mL, 6 M urea and DPPC was added in a 5:1 lipid to protein ratio. The mixture was incubated for 10 minutes at 39°C then vortexed for one minute, a cycle which was repeated over the course of 90 minutes to create DPPC vesicles. The mixture was then dialyzed against 4 L deionized water overnight and lyophilized. A 2:1 mixture of chloroform and methanol was added to the protein/lipid dried powder until it was successfully dissolved (solution turned clear), approximately 2 mL solvent.

Once this solution was created, LH20 chromatography was used in an effort to separate the SP-B from the impurities. A solvent resistant chromatography column (2.5 x 100 cm) was packed with Sephadex LH-20 resin (GE Healthcare Life Sciences, Piscataway, NL, USA). The column was equilibrated using 2:1 chloroform:methanol and

the 2 mL sample was applied at 20°C. The lipids and protein were eluted from the column with excess 2:1 chloroform:methanol and collected as 1.5 mL fractions without the use of a pump. The fractions were analyzed at OD_{240} and OD_{280} and those suspected of containing protein were dried under nitrogen gas and inspected by SDS PAGE on an 18% polyacrylamide gel. The presence of SP-B was confirmed using Western blotting with an anti-SP-B antibody and those fractions containing SP-B were pooled and stored at -20°C. After use, the LH20 column was washed with 2:1 chloroform:methanol.

2.9 Functional Studies of Recombinant SP-B

With a partially enriched recombinant SP-B, functional studies were undertaken to compare the expressed SP-B with native SP-B obtained from porcine lung lavages. These functional studies include membrane leakage and lipid mixing assays as well as surface activity studies with a captive bubble surfactometer (CBS). All of these studies were conducted in the Jesus Perez-Gil lab at the Universtidad Complutense de Madrid (Madrid, Spain).

2.9.1 Membrane Leakage Assay

This experiment required the production of large unilamellar vesicles (LUVs) with encapsulated fluorophores. The LUVs were made up of dipalmitoylphosphatidylcholine (DPPC), 1-palmitoyl-2-oleoyl-*sn*-glycero-3-phosphocholine (POPC), and 1-palmitoyl-2-oleoyl-*sn*-glycero-3-phosphoglycerol (POPG) in a 50:25:15 ratio. 10 mg/mL of this lipid mixture was added to a buffer of 5 mM Tris, 150 mM NaCl at pH = 7. The fluorophore

ANTS (8-aminonaphthalene-l,3,6-trisulfonic acid) and its quencher, DPX (p-xylene-bis-N-pyrimidinum bromide), were also added (12.5 mM and 45 mM respectively). Multilamellar vesicles (MLVs) were formed by alternating shaking and resting periods at 45°C for 90 minutes (ie. one minute shaking followed by 10 minutes rest). From these MLVs, LUVs were formed with five freeze-thaw cycles in liquid nitrogen. To ensure a consistent vesicle size as well as remove any remaining MLVs, the mixture was forced through an extruder with a 100 nm pore membrane. Because the LUVs were formed in a solution containing the fluorophores ANTS and DPX, these fluorophores will have been encapsulated inside the LUVs. To remove the free fluorophores not encapsulated, which would interfere with the leakage assay, the mixture was applied to a Sephadex G100 (GE Healthcare Life Sciences, Piscataway, NL, USA) gel filtration column (1.5 x 15 cm). The LUVs passed freely through the column while the free fluorophores were retained and eluted with excess buffer (5mM Tris, 150 mM NaCl, pH = 7) and collected in fractions. The lipid and fluorophores were tracked using OD_{400} (lipids), OD_{353} (ANTS), and OD_{259} (DPX). The lipid content of fractions containing LUVs were quantified using a phosphorous assay (see below) and used for the leakage assay.

The native SP-B was provided by the Jesus Perez-Gil lab while the recombinant SP-B was produced as described above. Both samples were stored in a solvent of 2:1 chloroform and methanol. As chloroform interferes with the fluorescence measurements, it had to be removed in favour of a methanol only solvent. Samples of both SP-Bs were slowly dried under nitrogen gas with the addition of excess methanol to prevent complete drying and protein aggregation. Chloroform is more volatile than methanol so will dry off first leaving the protein is a solution of methanol. Both SP-B

solutions, whose concentrations had previously been determined using amino acid analysis, were diluted to a final concentration of 60 μM.

The LUVs were diluted to a lipid concentration of 30 μM and 300 μL aliquots of this solution were added to cuvettes to analyze with the fluorimeter (SLM-Aminco AB2, Urbana, IL). The samples were excited at 353 nm (the excitation wavelength of ANTS) and emission at 520 nm (the emission wavelength of ANTS) was recorded. The emission at 520 nm of the LUVs alone was taken to be the minimal emission or leakage (F_0). The maximum leakage (F_{100}) was determined by adding 5 μL of the detergent Triton X-100 and recording the emission at 520 nm. Triton X-100 will dissolve the membranes of the LUVs allowing for total leakage.

The leakage experiments were performed for both the native and recombinant SP-B by adding 5 μL of the 60 μM SP-B solutions for a final concentration of 1 μM. Emission at 520 nm was recorded over a 10 minute period with the final emission recorded as Fp. This was repeated by adding another 5 μL SP-B to the cuvette to produce a 2 μM experiment, followed by a 3 μM and 4 μM experiment. The percent leakage (%L) was calculated using the formula:

$$\%L = 100\ (Fp - F_0) / (F_{100} - F_0)$$

where Fp is final emission, F_{100} is maximum emission, and F_0 is initial emission. To ensure the methanol of the SP-B samples was not interfering with the experiment, 20 μL of methanol alone was added to another 300 μL LUV sample and excited at 353 nm. No significant change in the emission at 520 nm was observed.

2.9.1.1 Phosphorous Assay

To determine the concentration of phosphorous containing lipids in several of the samples used during the functional experiments, a phosphorous assay was used. Standards were first made using different amounts of KH_2PO_4 (0.0037, 0.015, 0.026, 0.037, 0.092, 0.147 µmol). Experimental tubes containing different amounts of the unknown lipid solutions were also prepared. All tubes were dried down in a 250°C sand bath. 450 µL perchloric acid was added to each tube which were further incubated in the sand bath for 30 minutes at 250°C. 3.5 mL deionized water, 500 µL ammonium molybdate (2.5%), and 500 µL ascorbic acid (10%) were added to each tube and vortexed. The tubes were incubated in a 100°C water bath for 7 minutes after which the absorbance at 820 nm was determined for each tube. From this, a standard curve was generated. Using this curve and the absorbance of the experimental tubes, the lipid concentrations of the unknown samples were calculated.

2.9.2 Lipid Mixing

LUVs also had to be prepared for the lipid mixing experiments. This time, however, instead of encapsulated fluorophores, these LUVs would have fluorophores attached directly to the membrane and make use of the fluorescence resonance energy transfer (FRET) technique . The fluorophores in this case are the FRET donor, NBD (7-nitro-4-benzofurazanyl), and the FRET acceptor, Rhodamine. These fluorophores are attached to phosphatidylethanolamine (PE) which will allow them to be incorporated into the vesicular membrane. Both labelled and unlabelled LUVs were formed, made as before at a concentration of 50 µg/mL DPPC/POPC/POPG in a 50:25:15 ratio. These

labelled LUVs were made with NBD-PE and Rhodamine-PE (0.4 μM each) but were not subjected to chromatography and phosphorous assay steps. The same SP-B samples from the leakage experiments were also used.

For the lipid mixing experiments, the LUVs were mixed together in a 1:9 ratio of labelled to unlabelled, maintaining a total lipid concentration of 50 μg/mL. 300 μL of the mixture of vesicles was injected into a cuvette and placed into a fluorimeter at 37°C. The sample was excited at 450 nm (excitation wavelength of NBD) and the emission spectra from 500-650 nm was recorded to show FRET activity with no lipid mixing. This was followed with the addition of 5 μL of the 60 μM native SP-B sample for a final SP-B concentration of 1μM. The solution was mixed and allowed to rest for 5 minutes at which time another spectra from 500-650 nm was recorded. This was followed by the addition of more native SP-B to achieve 2, 3, and 4 μM SP-B concentrations. These experiments were repeated with the recombinant SP-B. To ensure the methanol of the SP-B solutions had no adverse effect on the experiments, a final trial was attempted with the injection of 20 μL methanol in 300 μL of the 50 μg/mL LUV sample.

2.9.3 Captive Bubble Surfactometer (CBS)

A captive bubble surfactometer (CBS) is a device used to mimic the environment inside an alveolus. It contains a chamber in which a small bubble can be created floating above a Tris buffered solution (5 mM Tris, 150 mM NaCl, 10% sucrose, pH = 7). The bubble can be observed with a camera and loaded into computer software which can calculate the surface tension of the bubble through its size and shape. The buffer contains sucrose to increase its density, allowing injected samples to float upwards to

the air-water interface of the bubble. The samples are injected through a small opening in the bottom of the chamber using a micro-syringe. The whole chamber is surrounded by a temperature-controlled water jacket which keeps the temperature of the system constant (37°C in the case of these experiments). In this thesis, three experiments are performed with the CBS: initial absorption, post expansion absorption, and dynamic simulation.

For these experiments, MLVs were formed in the presence of both native SP-B and recombinant SP-B. These MLVs were made of DPPC/POPC/POPG in a 50:25:10 ratio. The appropriate amount of SP-B was added to a solution of 25 mg/mL lipids in a Tris buffer (5 mM Tris, 150 mM NaCl) and the MLVs were prepared through alternating periods of shaking and rest at 45°C over the course of 90 minutes. For native SP-B, 1% and 2% (of total lipid mass) solutions were prepared while for recombinant SP-B, 5% and 10% solutions were used. A lipid only control sample containing just the 25 mg/mL lipids was also prepared for the upcoming experiments.

2.9.3.1 Initial Absorption (IA)

With initial absorption (IA) experiments, a bubble is first created in the chamber. Then the sample is injected and allowed to spread across the air-water interface. The change in surface tension this causes is recorded over the course of 5 minutes. This experiment was done for the lipids alone, native SP-B (1% and 2%), and recombinant SP-B (5% and 10%) samples. For the first trial, the samples were injected below the bubble and allowed to float upwards toward the air-water interface of the bubble. When

this proved problematic for the recombinant SP-B samples, the experiments were repeated by injecting the samples with the injector physically touching the bubble.

2.9.3.2 Post Expansion Absorption (PEA)

Post expansion absorption (PEA) experiments use the same bubbles described in the IA experiments above. After the IA experiment is completed, the chamber is sealed and expanded, creating a negative pressure. This causes the bubble to expand forcing the sample to spread across the increased surface area. The surface tension of the air-water interface was recorded over 5 minutes. These experiments were also completed with both injection procedures (touching the bubble and not touching the bubble).

2.9.3.3 Dynamic Simulations

After the PEA experiments, dynamic simulations were carried out. These experiments most accurately mimic the activity of an alveolus. The chamber remains sealed and is expanded and contracted which also causes this bubble to expand and contact. This is done at a rate of 20 cycles/minute which is the approximate breathing rate in humans. The surface tension changes in the air-water interface is recorded in the 1st, 10th, and 20th cycles. These dynamic simulation experiments were again completed with both injection procedures (touching the bubble and not touching the bubble).

3. Results

3.1 SN-Δ7NTΔM-SP-B-6His Expression Level and Cellular Location

After the plasmid was transfected into the C43 *E. coli* cells, it had to be determined if the fusion protein will express and identify which cellular fraction it is located in. This is important to know as it indicates which fractions should be used for the isolation procedure, and which should be discarded. Fusion proteins are typically designed to allow them to locate to the soluble fraction, however the very hydrophobic SP-B part could result in the fusion being directed into the membrane fraction and/or into insoluble inclusion bodies. The small one litre expression described in the Materials and Methods was split into three fractions highlighted in Table 3 and separated into soluble, membrane and inclusion body fractions as follows. Lauroyl sarcosine (LS) was used to solubilize the membrane fraction and urea was used to solubilize the inclusion bodies (insoluble).

Table 3: The different samples of cellular extracts of a small scale expression of SN-Δ7NTΔM-SP-B-6His and the solvent conditions of each sample. This was carried out in order to determine which sample (ie. fraction) contains the largest quantities of SN-SP-B fusion protein.

Sample	Cellular Extract Fraction	Solvent Conditions
1	soluble	TBS
2	soluble + membrane	TBS + 0.5% LS
3	soluble + membrane + insoluble	TBS + 0.5% LS + 6M urea

After running the fractions on a nickel bound IMAC column, portions of each were analyzed by SDS PAGE, shown in Figure 5. In each fraction, bands appeared around 26 kDa which is the approximate size of the expressed fusion protein. These bands were thus assumed to be the fusion protein indicating SN-Δ7NTΔM-SP-B-6His does express at detectable levels. This assumption would later be verified using Western blotting with an anti-SP-B antibody (Figure 8). Protein expression was detected in all fractions and the relative amounts in each fraction were determined by observing the size and amount of staining. The band from the soluble + membrane + insoluble fraction was the largest/darkest indicating that this fraction contained the most fusion protein. As a result, all future purifications of the SN-SP-B fusion were done using this fraction.

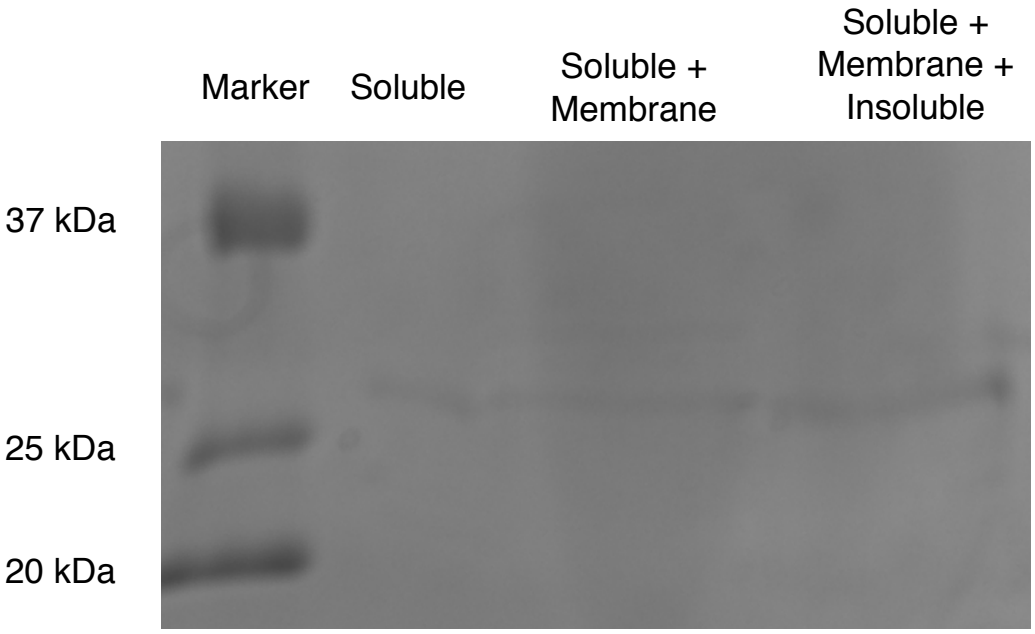

Figure 5: An 18% polyacrylamide gel showing the SDS PAGE of the different cellular extract fractions of a small scale expression of SN-Δ7NTΔM-SP-B-6His. Stained with Coomassie Brilliant Blue (CBB) R250.

3.2 Large Scale Expression of SN-Δ7NTΔM-SP-B-6His

Once I determined most of the protein was in the insoluble fraction, large scale (6 L) expressions were prepared. These cells were lysed and solubilized with the TBS, 0.5% LS, and 6 M urea, and the fusion protein (with 6xHis tag) was enriched using nickel-bound IMAC. After the lysate was loaded onto the column, it was washed with buffer containing 25 mM imidazole and then eluted in steps of 50, 100, 200, and finally 300 mM imidazole. Each step lasted about 10 mL or approximately 7-8 fractions. The elution profile was monitored by measuring the absorbance at 280nm (Figure 6). Peaks at fractions 4-9 (Peak A) and 10-16 (Peak B) can be observed. Further increases in absorbance at 280 nm can be seen after these peaks, however this is likely due to the increased imidazole concentration and not the presence of protein.

Figure 7 shows select fractions which were run on an SDS PAGE using an 18% polyacrylamide gel and CBB R250 staining. Two major bands appear, one from fractions 4, 6, and 8 with another from fractions 10, 12, and 14 with some crossover between the two. The first band is approximately 8 kDa while the second is about 26 kDa. These bands correspond to peaks A and B respectively.

A Western blot was also done on these fractions (Figure 8) to determine the identity of the bands. This Western blot was done using an anti-SP-B antibody. While the appearance is faint, SP-B is successfully detected in both fractions 6 and 12. These positive bands correspond to the strongest bands (1 and 2) from the SDS PAGE in Figure 7. It is unclear why there are two bands both positive for SP-B.

Theoretically, the SN-Δ7NTΔM-SP-B-6His plasmid construct should only produce a fusion protein of 26 kDa in mass. The second band from Figure 7 (ie. Peak B from

Figure 6) most closely resembles the expected size for the fusion. However, the first band from Figure 7, (ie. Peak A from Figure 6) at an apparent molecular mass of 8 kDa, is something other than the fusion. One possibility, that will be elaborated on in the discussion, is that Peak A corresponds to SP-B and a carboxy-terminal histidine tag that had been expressed without the SN fusion.

The fractions containing the fusion protein were pooled together and lyophilized in preparation for cyanogen bromide cleavage. The amount of undigested protein isolated in this step averaged about 10 mg per litre of culture. Fractions containing the SP-B expressed alone were also separately pooled and lyophilized. The protein isolated here averaged about 5 mg per litre of culture.

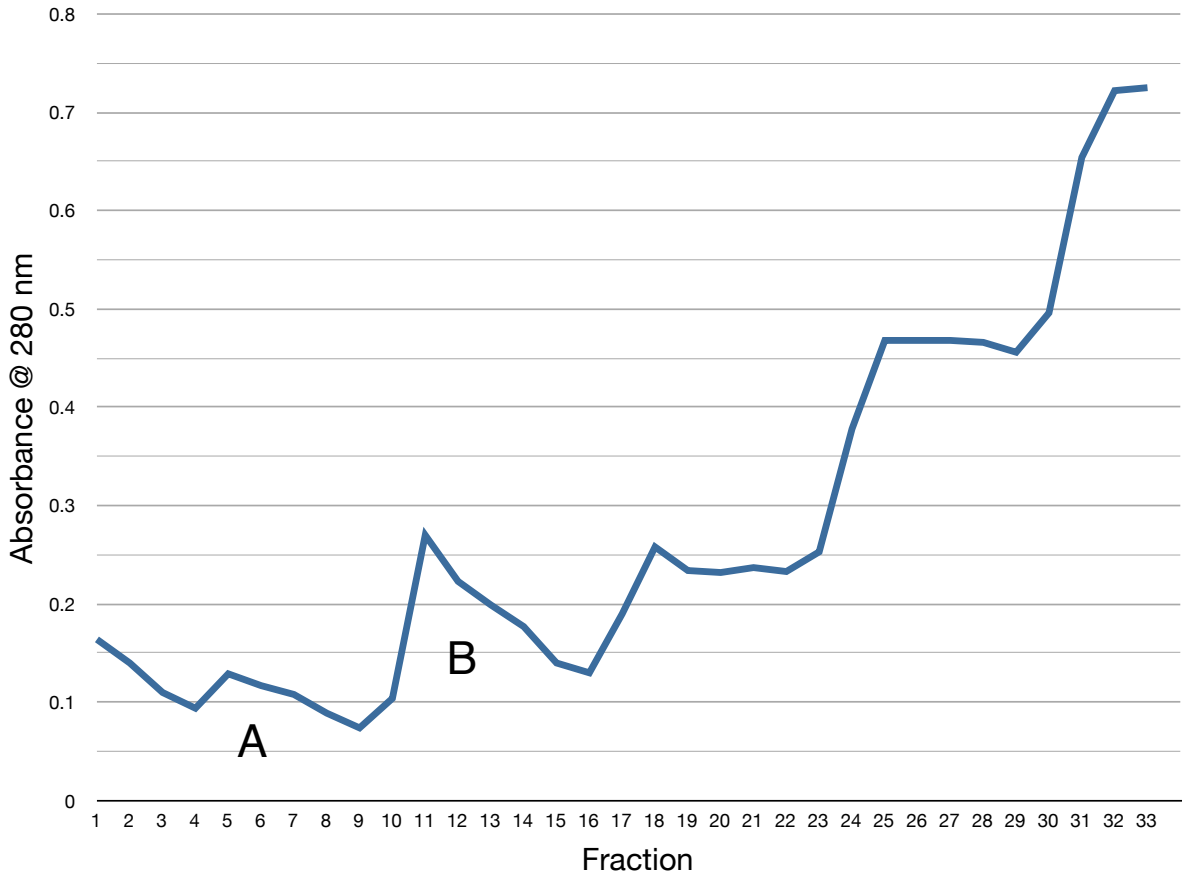

Figure 6: Elution profile from the nickel-bound IMAC column used to isolate the SN-SP-B fusion protein from the cellular extract. Protein was detected using an absorbance at 280 nm. Peaks A and B represent the two areas positive for protein. The subsequent peaks are the result of interference of the increased concentration of imidazole. Fractions 4-9 (Peak A) and fractions 10-16 (Peak B) were separately pooled as SP-B positive samples.

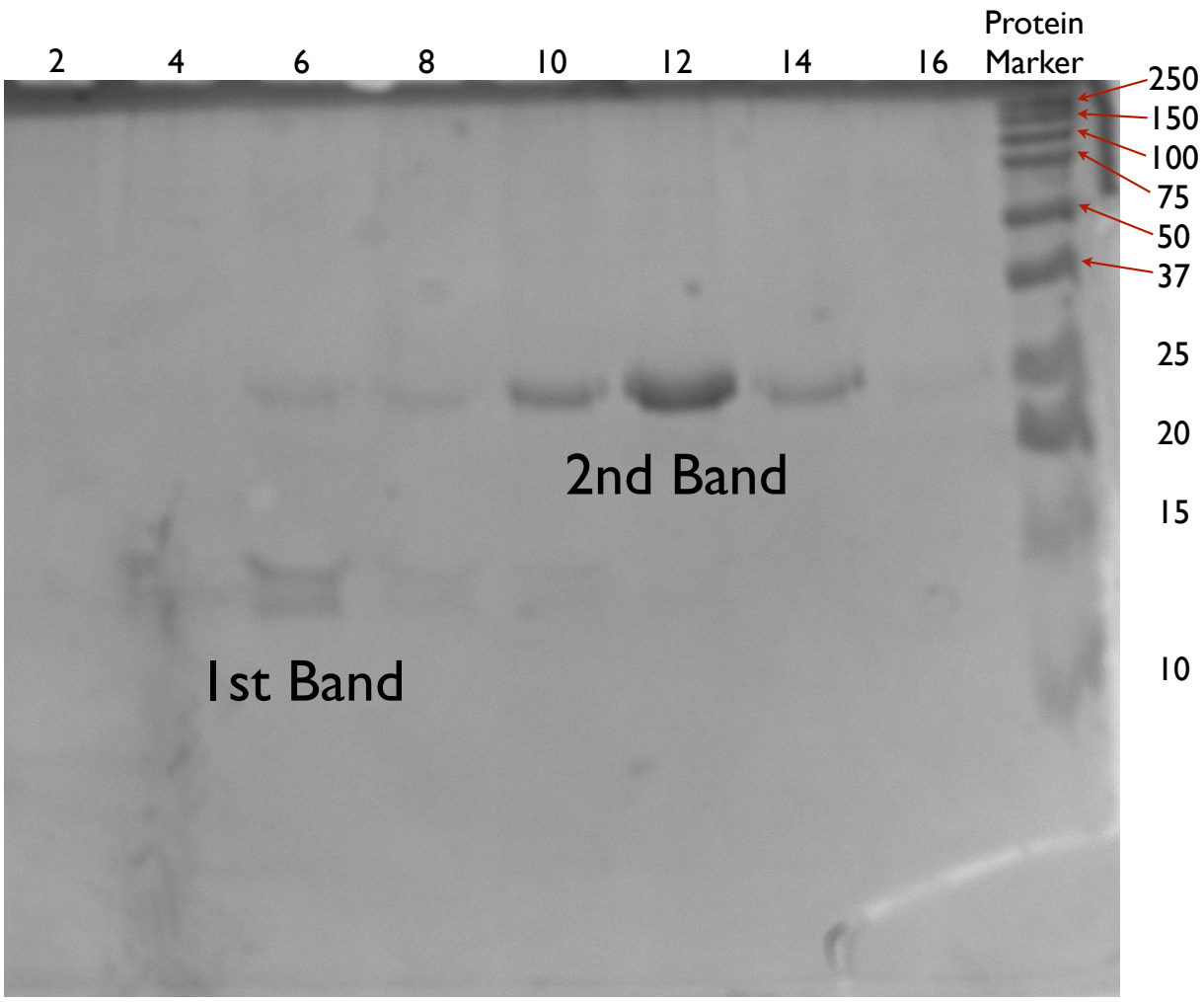

Figure 7: A precast 16.5% polyacrylamide gel showing the SDS PAGE of elution fractions from the nickel-bound IMAC column used to isolate the SN-SP-B fusion protein from the cellular extract. The fraction numbers are displayed across the top with the final lane containing a protein size reference marker. The size of each marker in kDa is displayed down the right of the gel. Stained with Coomassie Brilliant Blue (CBB) R250, two main protein bands were observed.

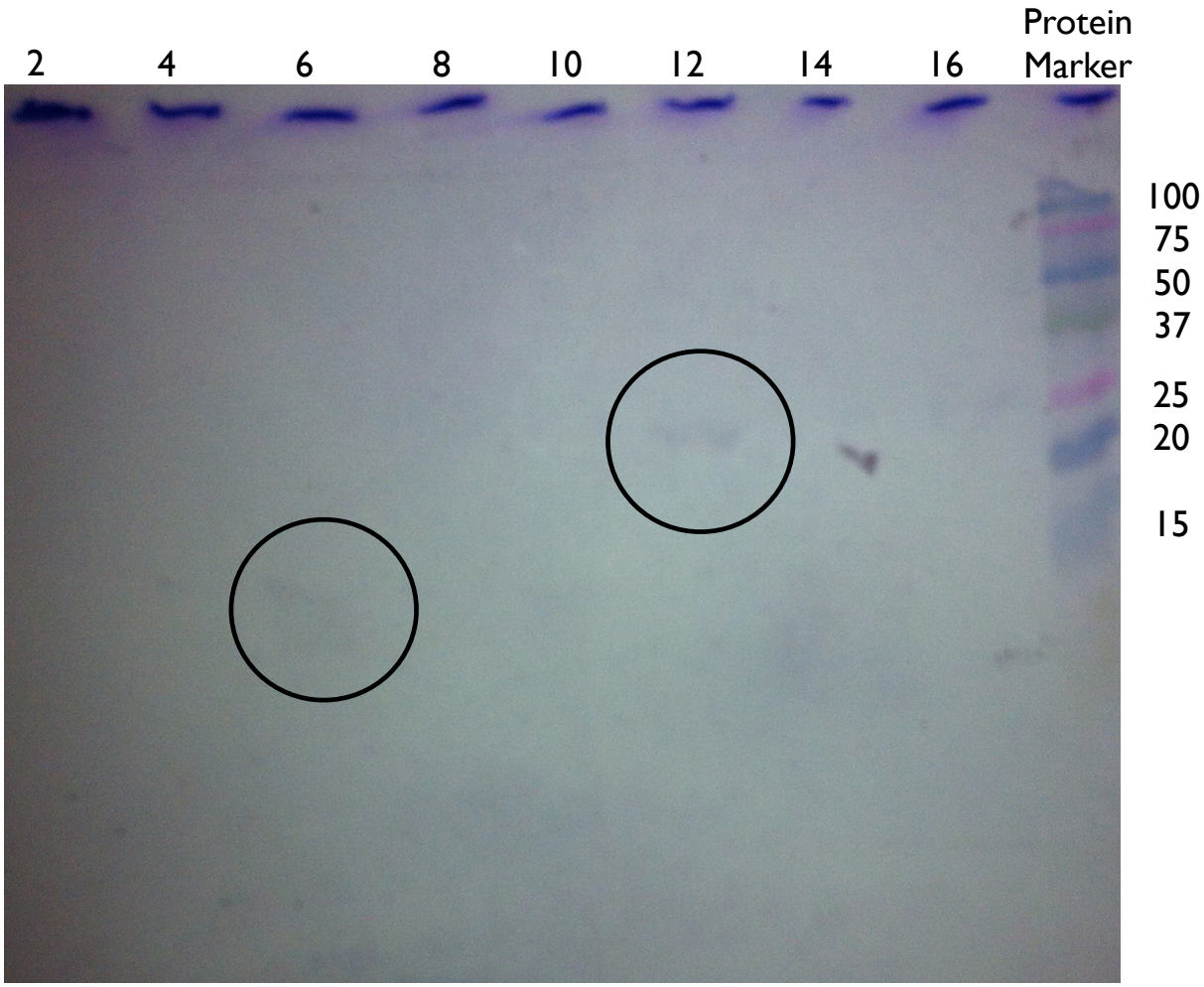

Figure 8: Western blot analysis of elution fractions from the nickel-bound IMAC column used to isolate the SN-SP-B fusion protein from the cellular extract, using the same sample from Figure 7. The fraction numbers are displayed across the top with the final lane containing a protein size reference marker. The size of each marker in kDa is displayed down the right of the membrane. The circled bands represent the antigen-antibody binding of the anti-SP-B antibody. The dark bands at the top are markers used to identify the lanes.

3.3 Cyanogen Bromide Cleavage

The lyophilized SN-SP-B fusion protein was then cleaved using a cyanogen bromide digest, as described in the Materials and Methods. As seen in Figure 4, there are cyanogen bromide cleavage sites (ie. methionine residues) positioned between the SN and SP-B as well as between the SP-B and histidine tag. There are also four methionine located throughout the SN sequence which would also result in the SN protein being digested into several pieces. This cleavage reaction will thus result in a recombinant SP-B that is no longer attached to anything. While the cyanogen bromide reaction is very efficient, there is the possibility of incomplete digestion. In other words, there could still be some SP-B that remains attached to SN fragments that would add another complication to the enrichment of SP-B. Cyanogen bromide will not cleave after a methionine that has been oxidized. Therefore, the presence of oxidized methane could present another source of incomplete digestion. Ideally, this enrichment would lead to a SP-B sample that is relatively pure of SN fragments, the histidine tag, and incomplete digests, however, this would prove to be very difficult to achieve.

Figure 9 shows a Western immunoblot of the SN-SP-B fusion sample before and after cleavage using an anti-SP-B antibody. Before cleavage, two positive SP-B bands appear, one identified as the fusion at about 26 kDa (with respect to the protein marker) and another below this. The lower band is approximately 8 kDa (with respect to the peptide marker) and is in all likelihood the SP-B that is expressed alone. As observed in Figure 7 there is always some crossover between the two expressed SP-Bs and thus contamination of the SN-SP-B with SP-B alone in inevitable. Because the end goal is to achieve an enriched sample of SP-B alone, this contamination is irrelevant.

After the cyanogen bromide cleavage, the 26 kDa band entirely disappears and the lower 8 kDa band's signal becomes stronger. This indicates that the cleavage was a success leading to an increase in SP-B alone. However, two weaker SP-B positive bands can be observed above the 8 kBa band but below the original 26 kDa band. These other bands likely arise from incomplete cleavage and thus, along with the SN fragments and histidine tag, must be removed during enrichment. Also worth noting is the presence of SP-B positive bands above 26 kDa. This is likely due to the oligomerization of SP-B which has been observed previously.

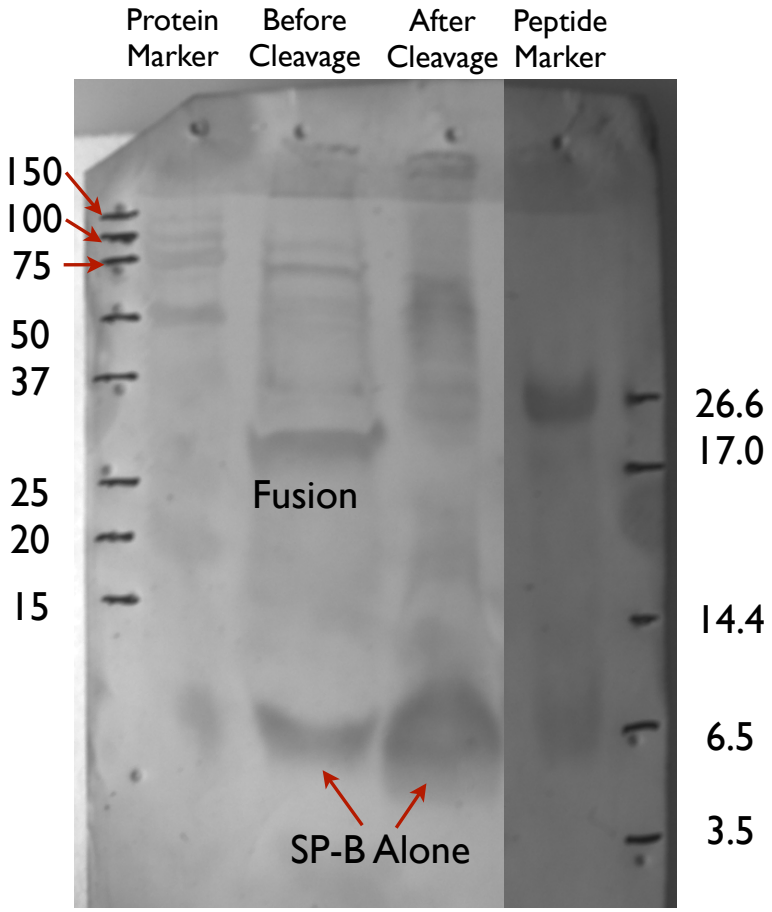

Figure 9: Western blot analysis of the isolated SN-SP-B fusion before and after cyanogen bromide cleavage. The outside lanes contain size reference markers. The sizes of each marker in kDa are displayed down the sides of the image. The bands represent the antigen-antibody binding of the anti-SP-B antibody. All lanes are from the same Western blot. The darker colour of the peptide marker lane is due to the middle lanes being removed from this image. Other bands are likely due to unspecific binding of the antibodies.

3.4 Enrichment of Recombinant SP-B

3.4.1 Organic Extraction

After the successful cleavage of the fusion protein, the next step was to attempt to isolate the SP-B from other cleavage products. Because SP-B is very hydrophobic and the SN fragments and histidine tag hydrophilic the most obvious enrichment method to use would be organic extraction. The completion of an organic extraction of the cyanogen bromide digest should, in theory, result in the SP-B being dissolved in organic solvent with the other impurities dissolved in a separate aqueous layer. Where the incomplete digests would appear is harder to predict as they have both hydrophobic and hydrophilic parts. If they were to appear in the organic solvent with the SP-B they could possibly be removed through a subsequent chromatography step.

The organic extraction carried out on the cyanogen bromide cleavage products yielded an unexpected result (see Figure 10A). An insoluble precipitate formed between the organic and aqueous phases. Samples from the organic, inorganic, and aqueous phases were analyzed using SDS PAGE (see Figure 10B). Nothing appears to have dissolved in the organic phase, while protein is present in both the insoluble and aqueous phases. This is likely the result of aggregation of the SP-B. Due to its very hydrophobic nature, SP-B has a tendency to stick to itself and other proteins which makes work with this protein extraordinarily difficult. SP-B is most likely the band just above 6.5 kDa and as can be seen in the gel, neither the insoluble nor inorganic phases offered any significant enrichment. As a result, the use of this method was discarded.

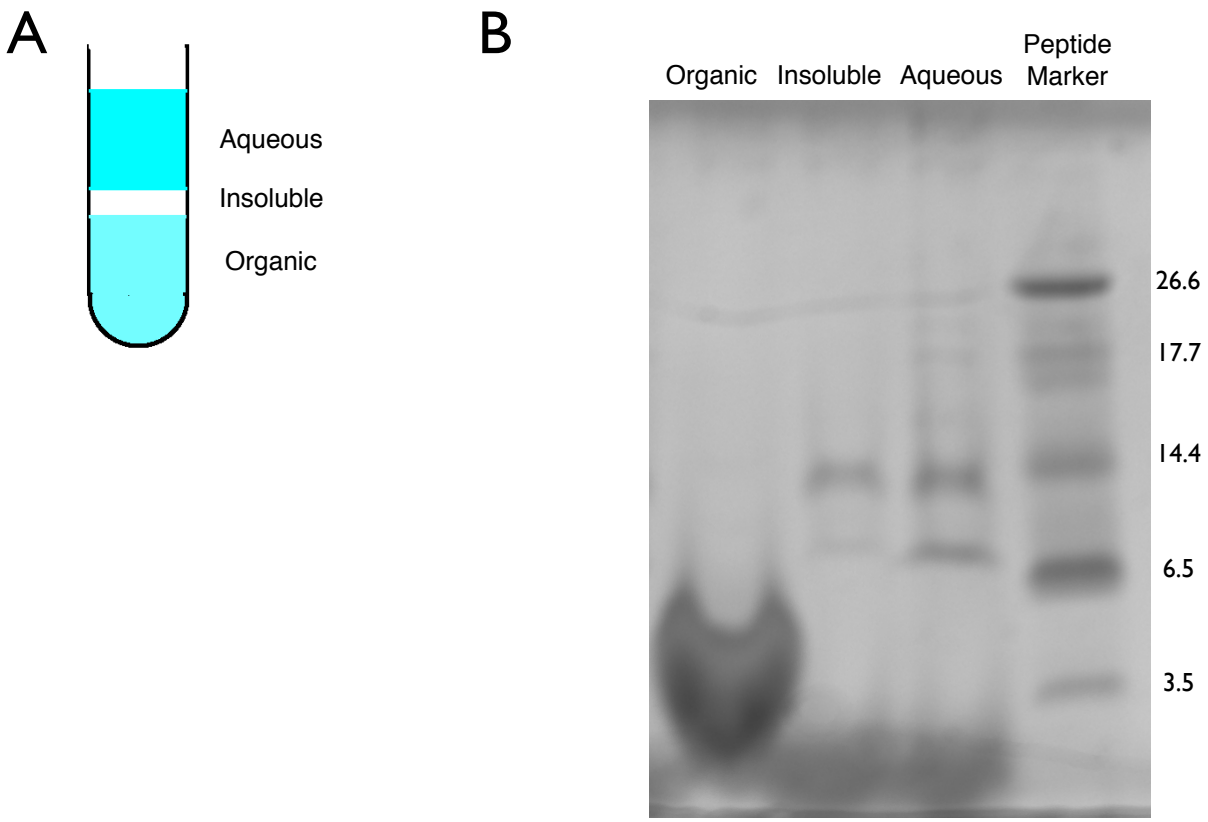

Figure 10: Organic extraction of cyanogen bromide digest. a) A schematic of what results in a glass tube when an organic extract is performed on the cyanogen bromide cleavage products of the SN-SP-B fusion protein. b) A precast 16.5% polyacrylamide gel showing the SDS PAGE analysis of the three portions of the organic extraction seen in Figure 7A. The final lane contains a size reference marker with the size of each marker in kDa displayed down the right side of the gel. The gel is stained with CBB-R250. The large smear in the organic lane is likely due to the presence of lipids in the sample.

3.4.2 High Performance Liquid Chromatography (HPLC)

The next method that was attempted to separate SP-B from the impurities was HPLC, using a C8 column which has 8 carbon chains attached to resin. The use of such a column is called reverse phase chromatography and allows for separation of proteins based on hydrophobicity. Hydrophobic proteins (in this case SP-B) will stick to the resin while the rest will flow through the column. The SP-B was eluted using an organic solvent (acetonitrile) gradient. The C8 column was used as opposed to the much more common C18 because SP-B is so hydrophobic it will bind strongly to the C18 resin and not elute. The elution was collected in fractions and a profile was generated (see Figure 11). Each peak was pooled and samples from each were analyzed through SDS PAGE (see Figure 12).

Almost nothing showed up on the gel and the dried fractions yielded little to no protein. This is likely the result of the filtration of the sample before application to the column. After the protein was mixed in the 80% acetonitrile solution, the sample was cloudy. However, after filtration, the sample became clear and colourless. With the result from the organic extraction in mind, it is likely that the SP-B did not dissolve in the acetonitrile/water mixture and as a result, was lost during filtration [85]. Like organic extraction, HPLC did not help enrich SP-B and therefore, a different method was approached.

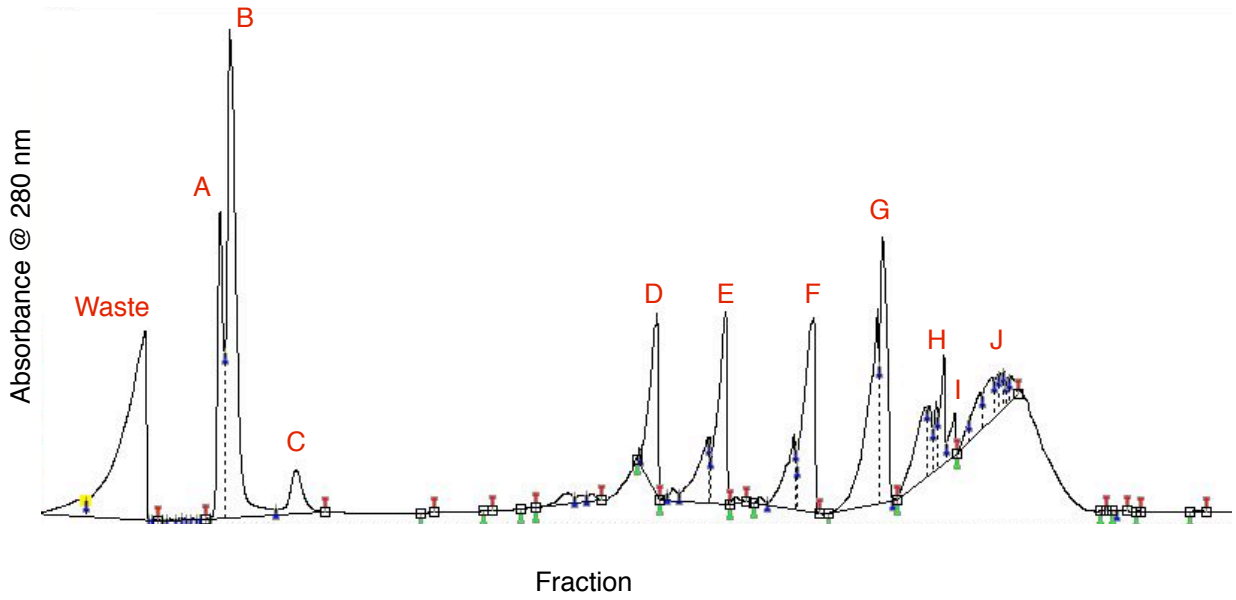

Figure 11: Elution profile of fraction taken from the HPLC of the cyanogen bromide digest. Protein was detected using an absorbance of 280 nm. The peaks analyzed with SDS PAGE are labelled A-J.

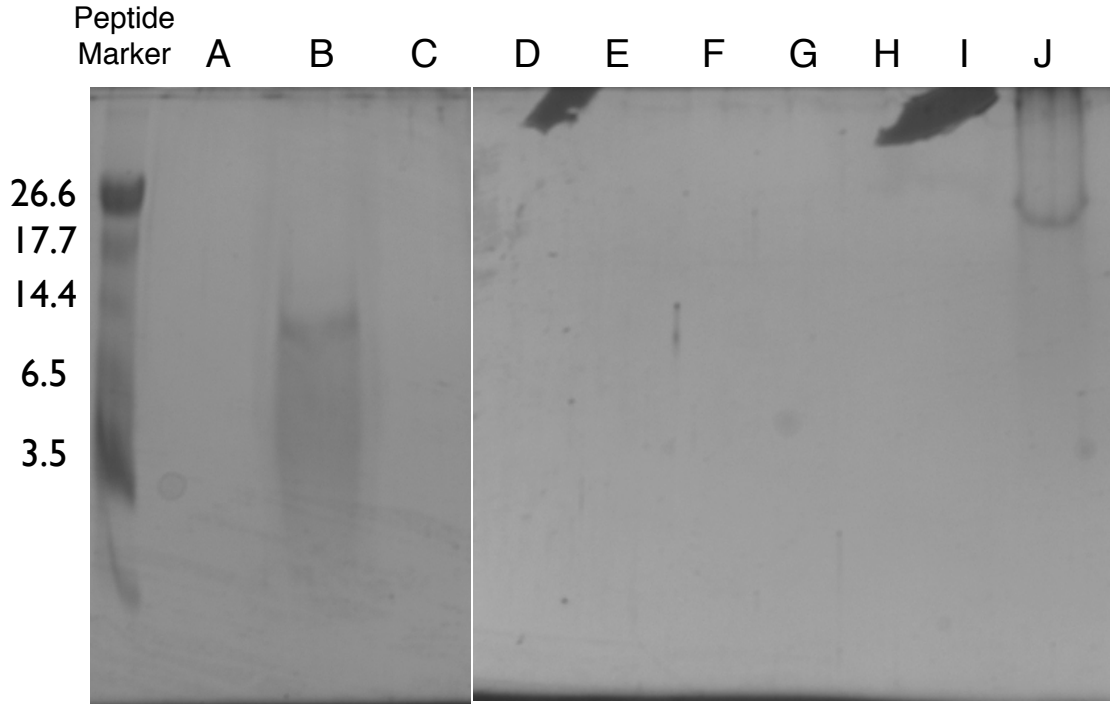

Figure 12: Precast 16.5% polyacrylamide gels showing the SDS PAGE of various elution fractions from the HPLC of the cyanogen bromide digestion products of the SN-SP-B fusion. The different fractions are displayed across the top and represent the same fraction from the elution profile in Figure 11. The first lane contains a size reference marker with the size of each marker in kDa displayed down the left side of the gel. The gels were stained with CBB-R250.

3.4.3 Cationic Exchange Chromatography

The next attempt at enriching the SP-B was through the use of cationic exchange chromatography. This chromatographic method utilizes resin that has a negative charge. Positively charged molecules, like SP-B (+7 at neutral pH), should bind to the resin allowing others to pass through. The bound cations are then eluted using a salt gradient. While some SN fragments will also be positively charged, they are less positive than SP-B and therefore should elute from the column earlier. The detergent CHAPS was used to try to dissolve SP-B in an aqueous buffer and unlike HPLC, the sample did not need to be filtered before applying to the column, therefore loss of sample should not be an issue. The elution was collected as fractions and a profile was generated (see Figure 13). Select fractions were also analyzed using SDS PAGE (see Figure 14).

From the profile in Figure 10, you can see a high absorbance from the first 10 fractions. Analysis of fraction 3 (Figure 14) shows that this large peak contained most of the CHAPS detergent (CHAPS appears as a large smear on SDS PAGE) as well as most of the proteins (the two large distorted bands above the smear) indicating that very little of the protein had bound to the column. The little protein that did bind eluted gradually with no separation, which can be seen in the other lanes of the gel in Figure 14. Aggregation of the protein in the digested sample could possibly lead to the blockage of the charged portions of SP-B and therefore rendering it unable to bind to the anionic resin. Once again, the failure of cationic exchange chromatography to improve enrichment has led me to look elsewhere.

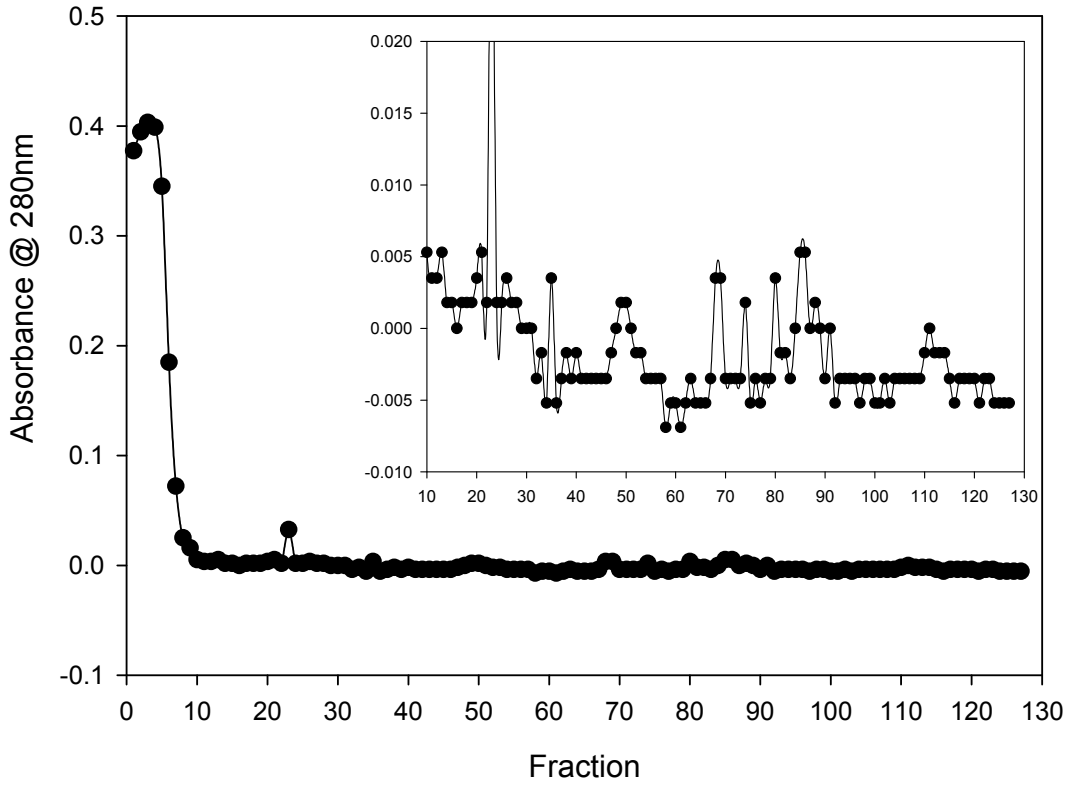

Figure 13: Elution profile from the cationic exchange chromatography of the cyanogen bromide digestion products of the SN-SP-B fusion protein. Protein was detected using an absorbance at 280 nm. The inset contains an expanded look at fractions 10-130.

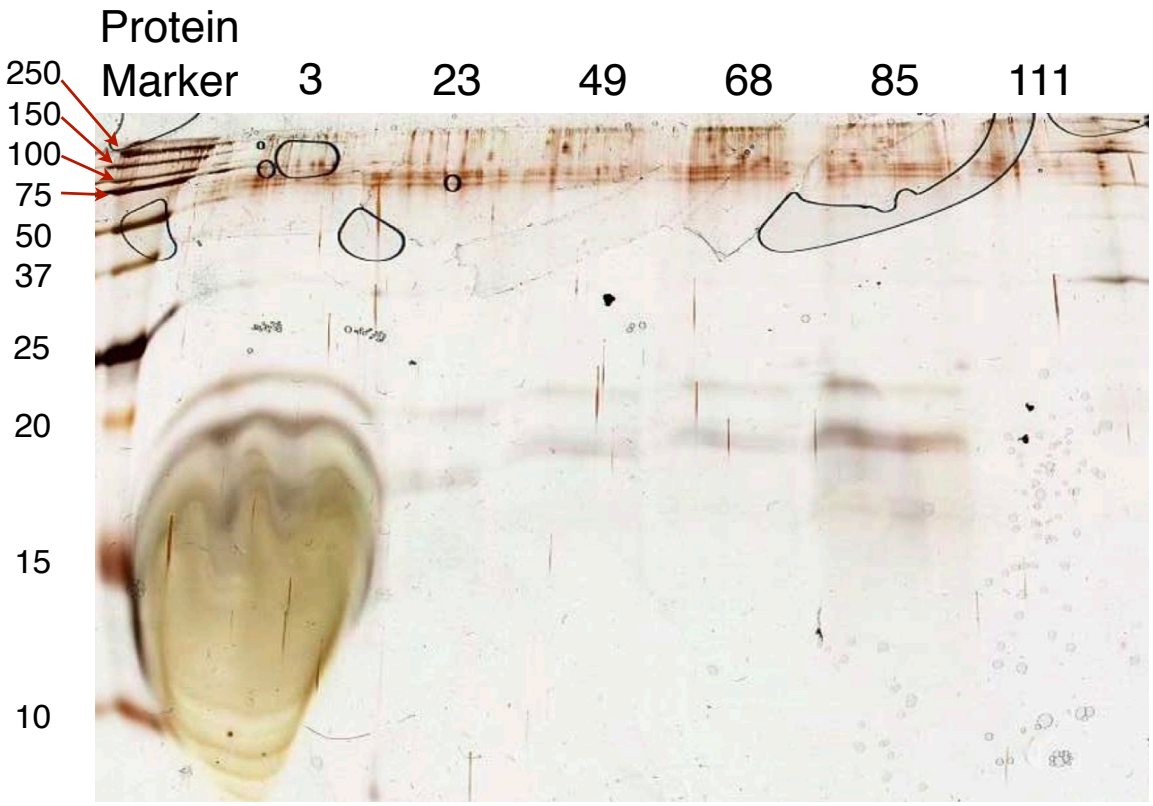

Figure 14: An 18% polyacrylamide gel showing the SDS PAGE of various elution fractions from the cationic exchange chromatography of the cyanogen bromide digestion products of the SN-SP-B fusion. The different fractions are displayed across the top and represent the same fractions from the elution profile in Figure 10. The first lane contains a size reference marker with the size of each marker in kDa displayed down the left side of the gel. The second lane (Fraction 3) contains a large smear caused by the CHAPS. Despite this, thick distorted protein bands can be observed above the smear. The gel was stained with silver staining.

3.4.4 Sephadex LH20

What was obvious at this point was that the SP-B and other digestion products were very insoluble. The likely culprit of this insolubility is protein aggregation. I have found that a high concentration of urea is capable of breaking up these protein aggregates. While the denaturing property of urea makes this possible, it is also the denaturing effect that makes it undesirable for any structural or functional work which is the ultimate goal of this work. A resolution to this problem was found using a new solubilization procedure with DPPC vesicles that is described in detail in the Materials and Methods. This procedure involved first dissolving the protein aggregate in high molar urea and then adding the DPPC vesicles. The hydrophobic SP-B should bind to these vesicles and after a period of dialysis the urea is removed leaving only the SP-B bound vesicles. Once lyophilized, this protein-lipid mixture dissolved readily in a organic solvent of 1:1 chloroform and methanol. Once dissolved in this solvent, I was able to apply the sample to a chromatography column containing LH20 resin which is a size exclusion column able to withstand the harsh conditions of organic solvent.

The first attempt at an LH20 chromatography was made using a sample of the SP-B expressed alone (ie. the 8 kDa band from Peak A in Figure 6). This sample was digested with cyanogen bromide (to remove the carboxy-terminal histidine tag) and solubilized using the urea/DPPC vesicle method. The LH20 profile featured in Figure 15 shows at least four major peaks which contain protein and lipids. Samples from these peaks were analyzed using SDS PAGE and Western blot (Figure 16). There is one visible band present from fraction 75 and tested positive for SP-B using anti-SP-B in the Western blot. While this is a very encouraging result, low yields of the SP-B expressed

alone resulted in too little enriched protein to do any meaningful research with. Because of the inability to increase this yield, the same method was applied to the SN-SP-B fusion digest which was expressed in much larger quantity.

The resulting profile of the LH20 chromatography with the fusion digest can be seen in Figure 17. As before, select fractions were analyzed with SDS PAGE and Western blotting (Figures 18 and 19) using duplicate gels. A thick band appears from fraction 77 in the gel in Figure 18. This was confirmed to be SP-B in the Western blot with anti-SP-B in Figure 19. The gel appears inconsistent with the chromatography profile in that the protein was present at a very small absorbance (about 0.05) whereas the large peaks centred around fractions 111 and 200 contained yielded no protein on the SDS PAGE/Western blot. These large peaks could be from other molecules present in the elution.

Once again, the enrichment of SP-B from the LH20 column was achieved and this time in larger quantities than the SP-B that had expressed by itself. This larger yield came at a price, however, as other bands present from fraction 77 (Figure 18) indicate the SP-B is not completely enriched. While this is an impediment to structural studies through solution NMR, it should be pure enough to undergo functional studies. Fractions 72-83 were pooled and dried. The total rSP-B isolated through this process was determined to be approximately 150 µg. This value was measured using amino acid analysis. Therefore the total yield of enriched rSP-B was 25 µg/L of culture.

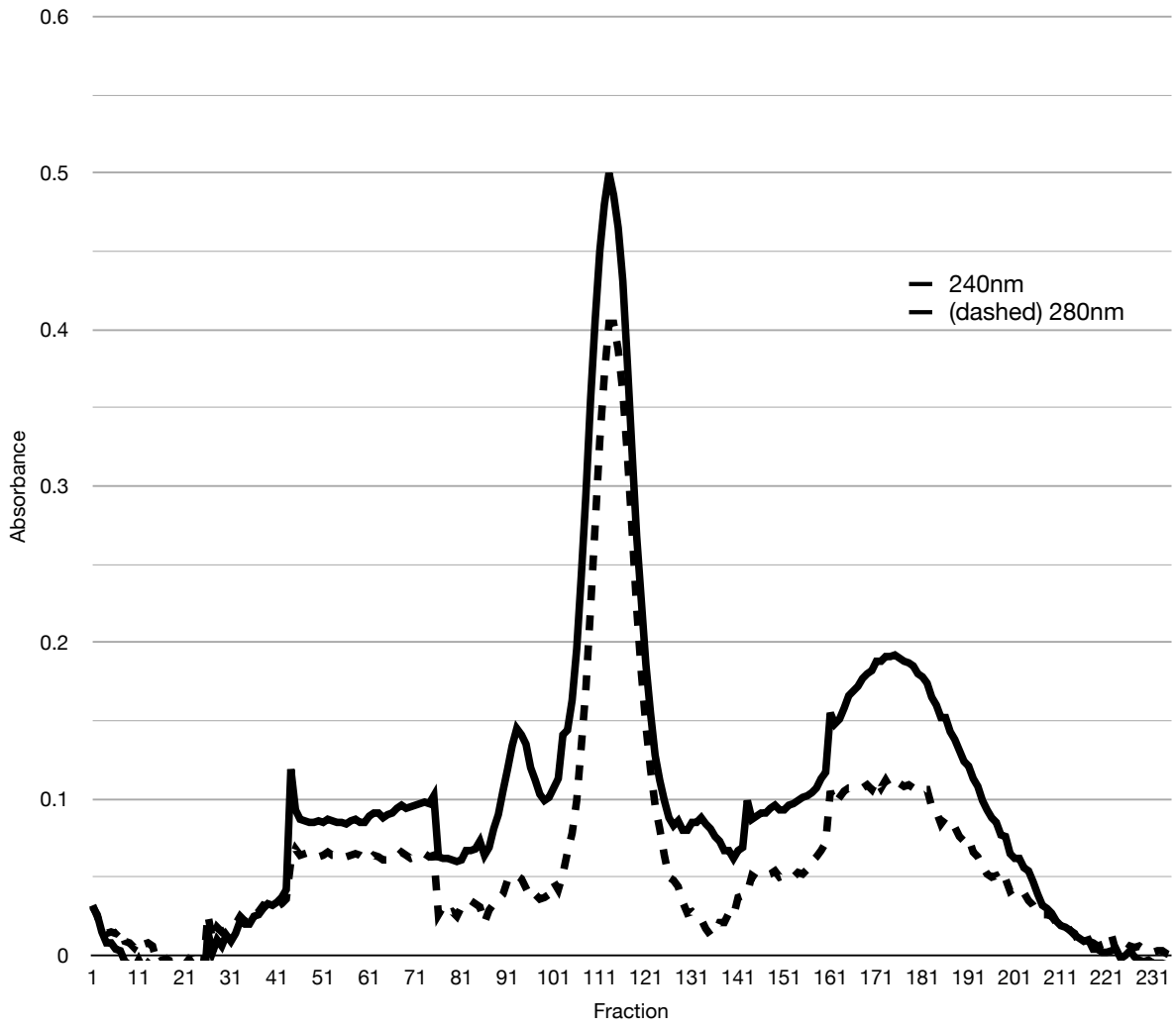

Figure 15: Elution profile from the LH20 size exclusion chromatography of the cyanogen bromide digestion products of the SP-B-expressed-alone sample. Protein was detected using absorbance at 240 and 280 nm. The fractions contained approximately 1.5 mL.

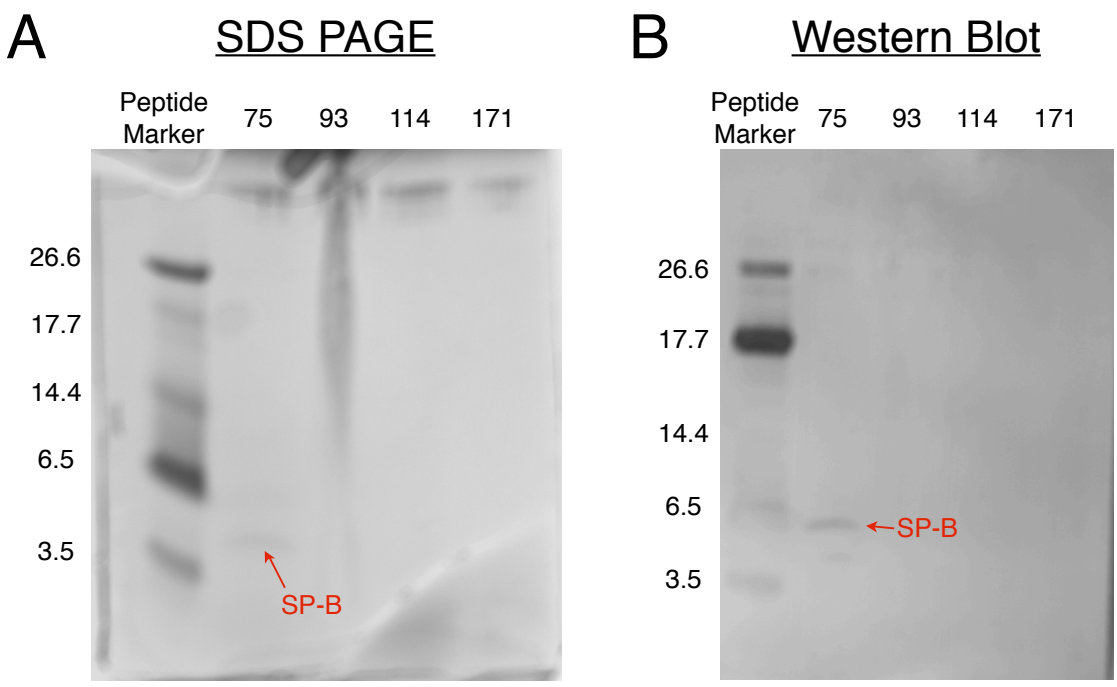

Figure 16: Analysis of Sephadex LH20 chromatographed SP-B-expressed-alone by SDS PAGE and Western blotting. A) A precast 16.5% polyacrylamide gel showing the SDS PAGE of various elution fractions from the LH20 size exclusion chromatography of the cyanogen bromide digestion products of the SP-B expressed alone sample. The gel was stained with CBB R250. B) A Western blot analysis of various elution fractions from the LH20 size exclusion chromatography of the cyanogen bromide digestion products of the SP-B expressed alone sample. The bands represent the antigen-antibody binding of the anti-SP-B antibody. The different fractions in both figures are displayed across the top and represent the same fractions from the elution profile in Figure 15. The left-hand lanes in each contain a size reference marker with the size of each marker in kDa. These were created using duplicate gels.

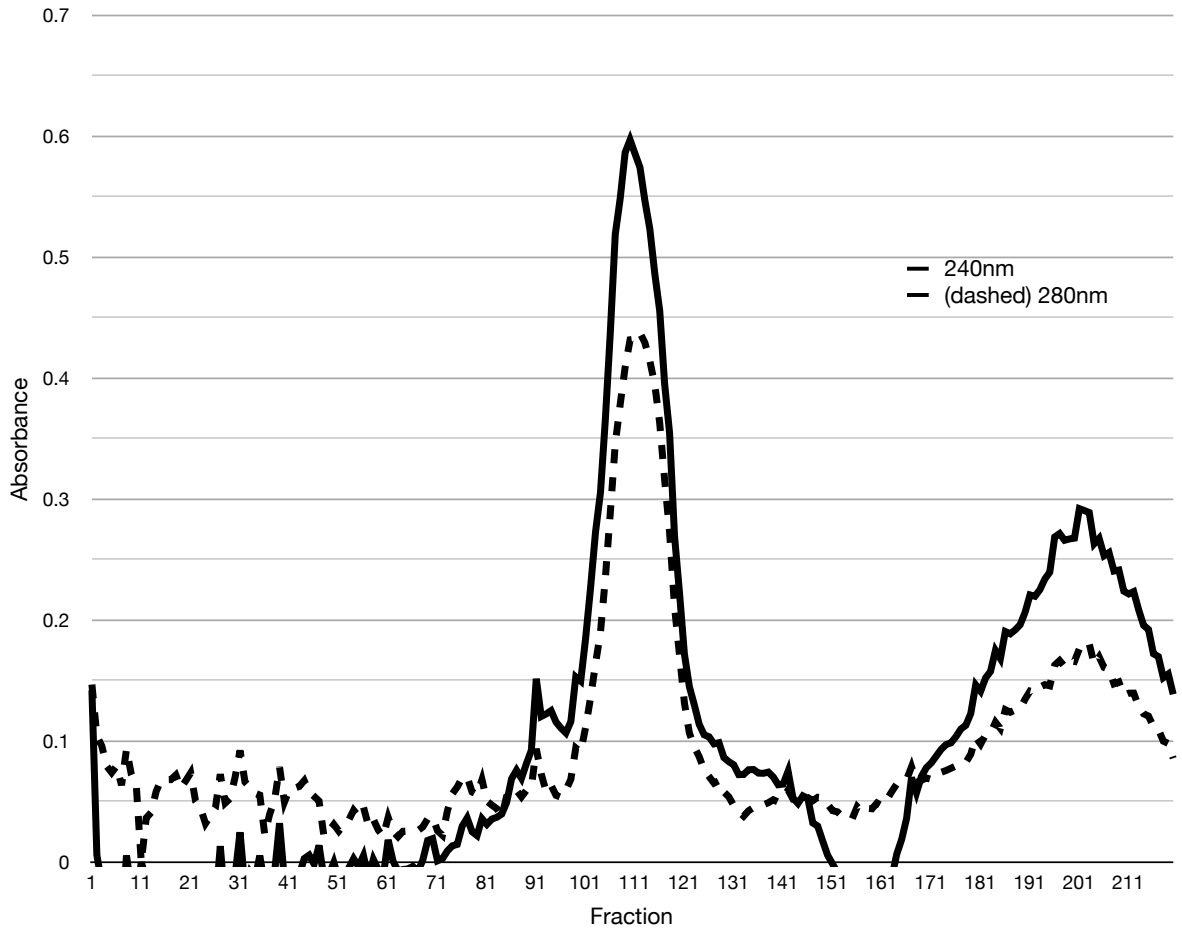

Figure 17: Elution profile from the LH20 size exclusion chromatography of the cyanogen bromide digestion products of the SN-SP-B fusion protein. Protein was detected using absorbance at 240 and 280 nm. The fractions contained approximately 1.5 mL. Fractions 72-83 were pooled.

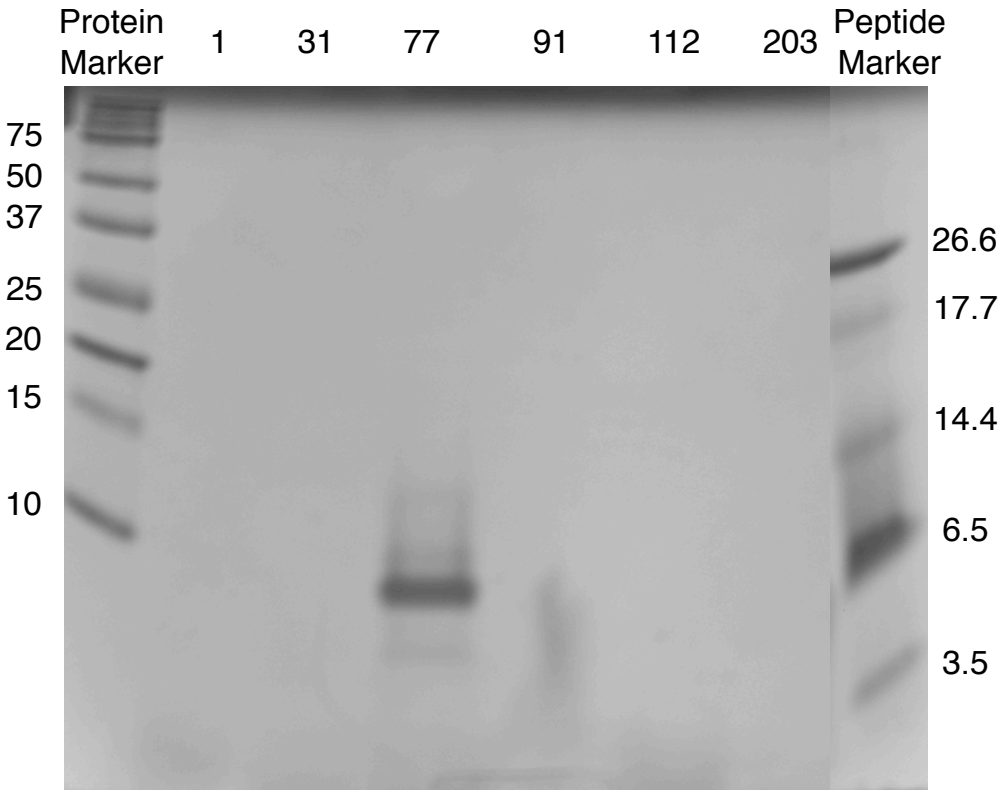

Figure 18: A precast 16.5% polyacrylamide gel showing the SDS PAGE of various elution fractions from the LH20 size exclusion chromatography of the cyanogen bromide digestion products of the SN-SP-B fusion protein. The different fractions are displayed across the top and represent the same fractions from the elution profile in Figure 17. The outside lanes contain size reference markers with the size of each marker in kDa displayed down the sides of the gel. The gel was stained with CBB R250. The break between the last two lanes is due to a portion of the gel being removed from the image.

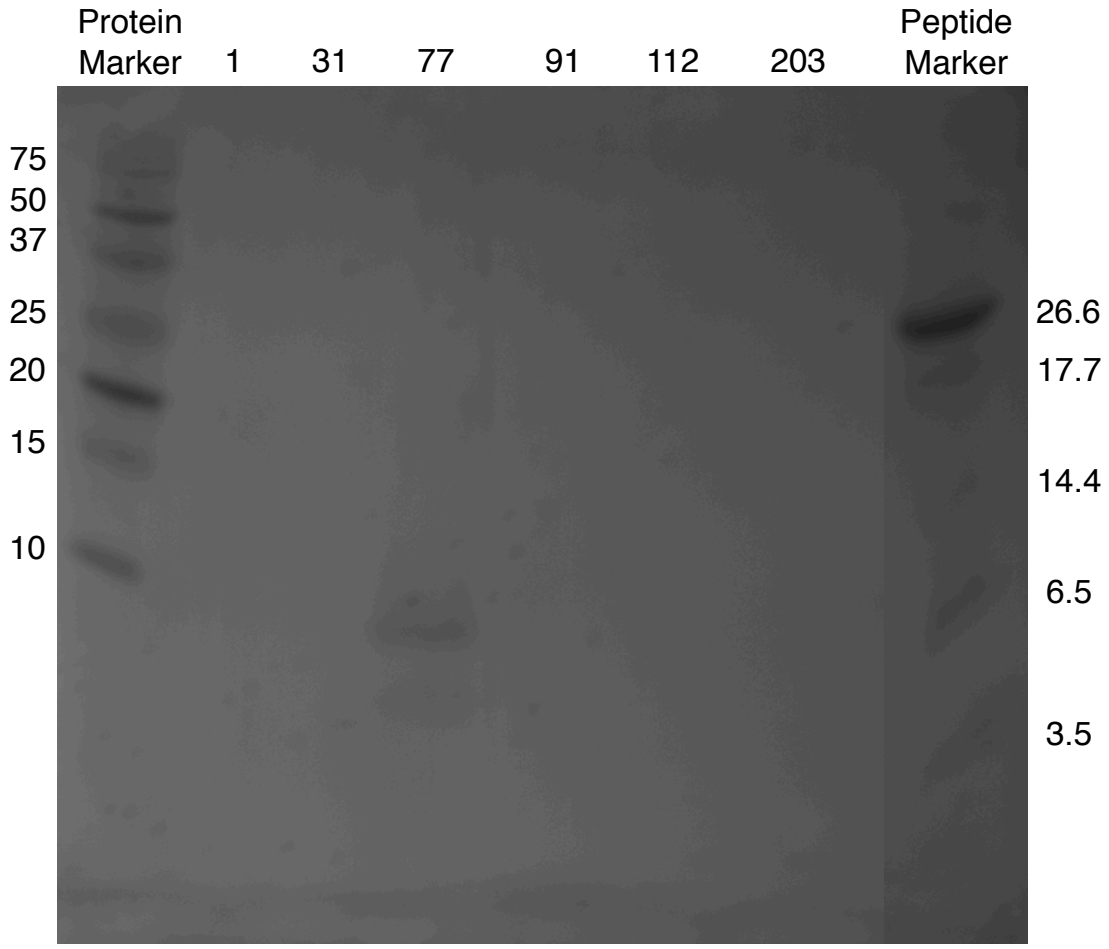

Figure 19: A Western blot analysis of various elution fractions from the LH20 size exclusion chromatography of the cyanogen bromide digestion products of the SN-SP-B fusion protein. The bands represent the antigen-antibody binding of the anti-SP-B antibody. The different fractions are displayed across the top and represent the same fractions from the elution profile in Figure 17. The outside lanes contain size reference markers with the size of each marker in kDa displayed down the sides of the membrane. The break between the last two lanes is due to a portion of the membrane being removed from the image.

3.5 Functional Studies of Recombinant SP-B

With a partially enriched recombinant SP-B, I moved onto functional studies. These studies were done to compare the activity of the expressed SP-B with native SP-B obtained from porcine lung lavages to ensure this recombinant expression was a viable source for functional SP-B. These functional studies include membrane leakage and lipid fusion assays as well as surface activity studies with a captive bubble surfactometer (CBS). All of these studies were conducted in the Jesus Perez-Gil lab at the Universidad Complutense de Madrid (Madrid, Spain).

3.5.1 Leakage Assay

This experiment is designed to measure the ability of a molecule to disrupt a membrane enough to cause the interior environment to leak out. It is measured through the use of the fluorophores ANTS and DPX which are encapsulated inside LUVs (see Figure 20). While encapsulated, they are in enough proximity to one another for DPX to quench the fluorescence of ANTS. If these fluorophores were allowed to escape to the exterior environment, the diffusion would release ANTS from the quenching effects of DPX and an increase of ANTS fluorescence (520 nm) can be measured if excited at a wavelength of 353 nm. From this measurement, the percent leakage can be calculated.

Figure 21 compares the percent leakage of both the native and recombinant SP-B samples. As the amount of SP-B increases (shown here as a protein:lipid mass ratio), the percent leakage also increases for both samples. However, the native SP-B causes more leakage than its recombinant counterpart. At an SP-B to lipid weight ratio of 0.13,

leakage has almost reached 100% whereas at the same amount the recombinant SP-B has only caused less than 60% leakage.

Figures 22 and 23 on the other hand show how percent leakage of both the native and recombinant SP-Bs respectively change over a period of five minutes. Once again this shows that while both cause leakage, the native SP-B does so much more efficiently. Interesting to note here is how the leakage of the native SP-B continues to increase over the full five minutes where in the recombinant SP-B experiment there is a sudden increase which promptly levels off. This seems to indicate that the native SP-B is creating a permanent pore in the membrane allowing continuous leakage to occur. This effect does not occur with the recombinant SP-B which only allows leakage to occur during an initial disruption of the membrane.

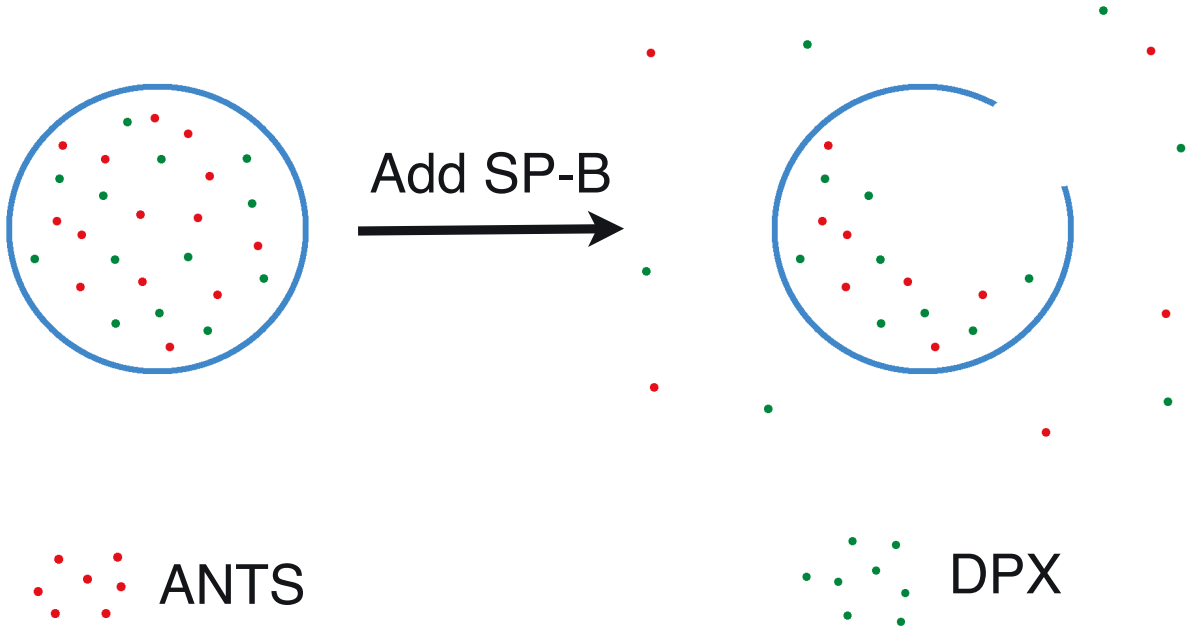

Figure 20: A schematic of the leakage assay. The blue circle represents the membrane of a LUV while the red and green dots represent the fluorophores. After the addition of SP-B the membrane opens and the fluorophores leak out to the surrounding environment.

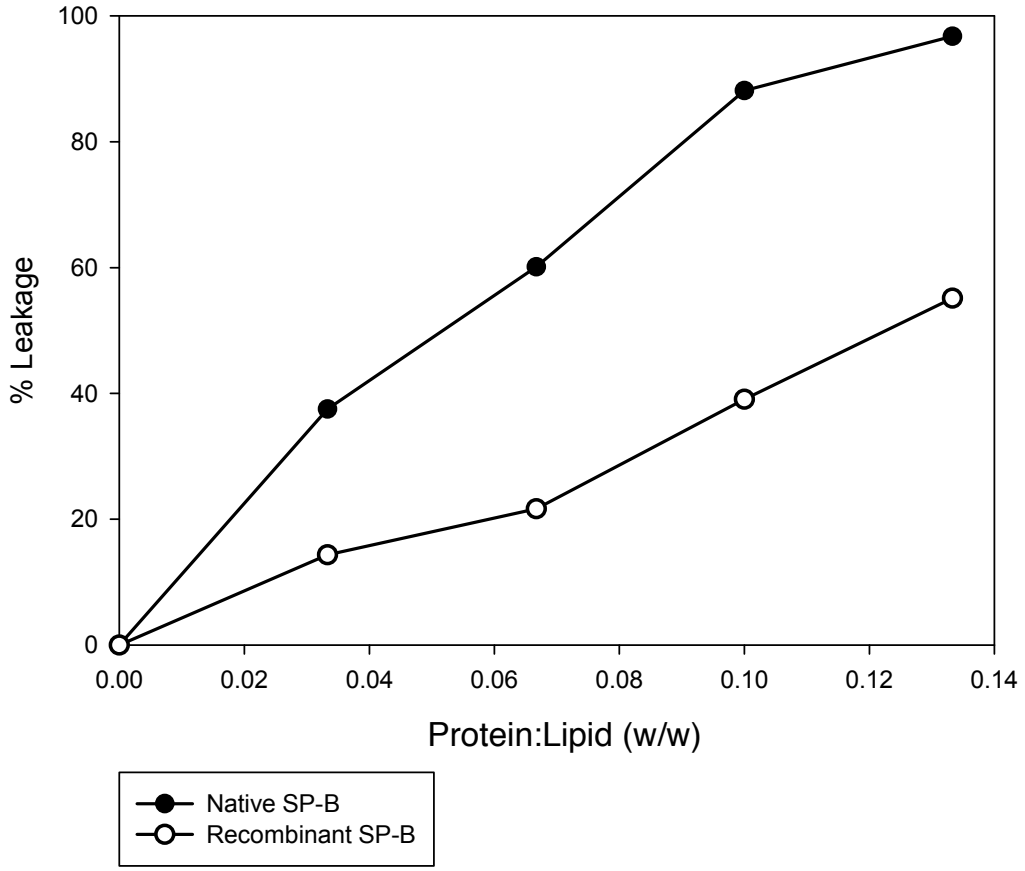

Figure 21: The final percent leakage of both the native SP-B and recombinant SP-B leakage assays.

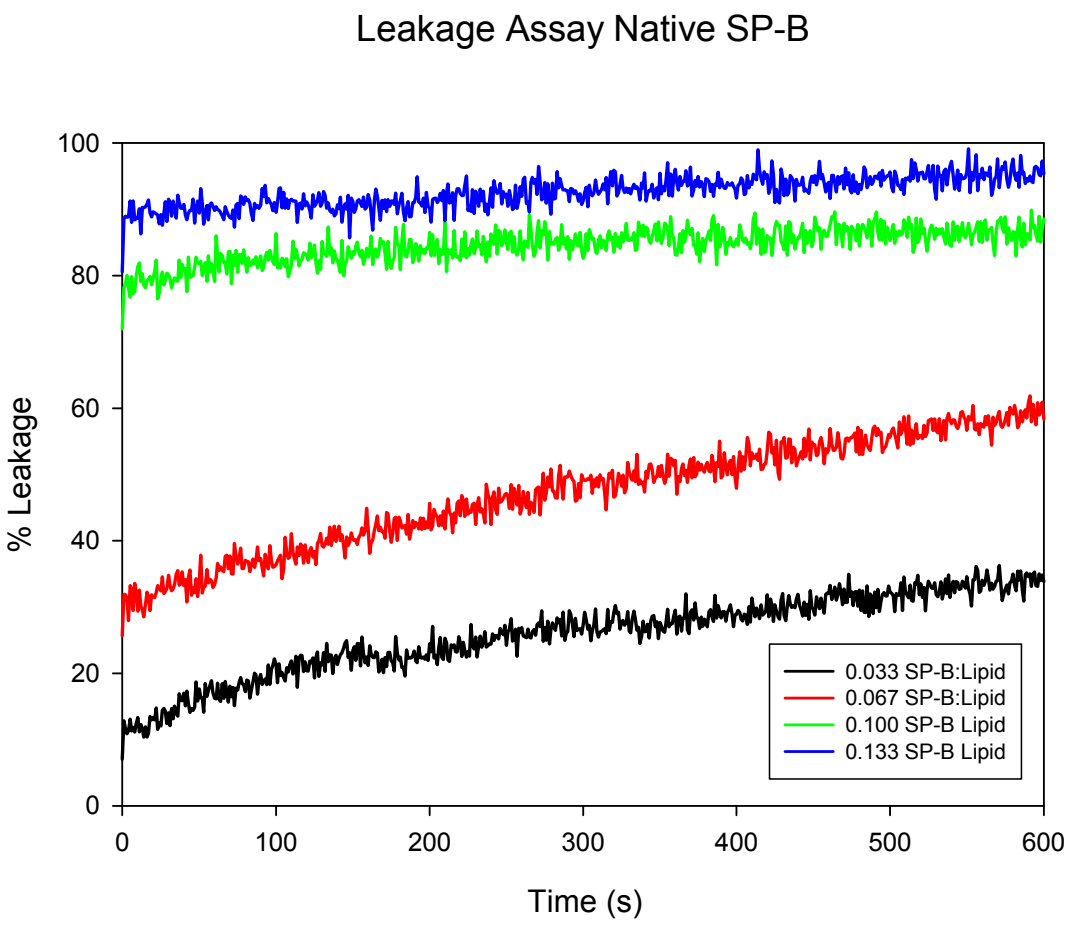

Figure 22: The percent leakage as a function of time of the leakage assay using native SP-B.

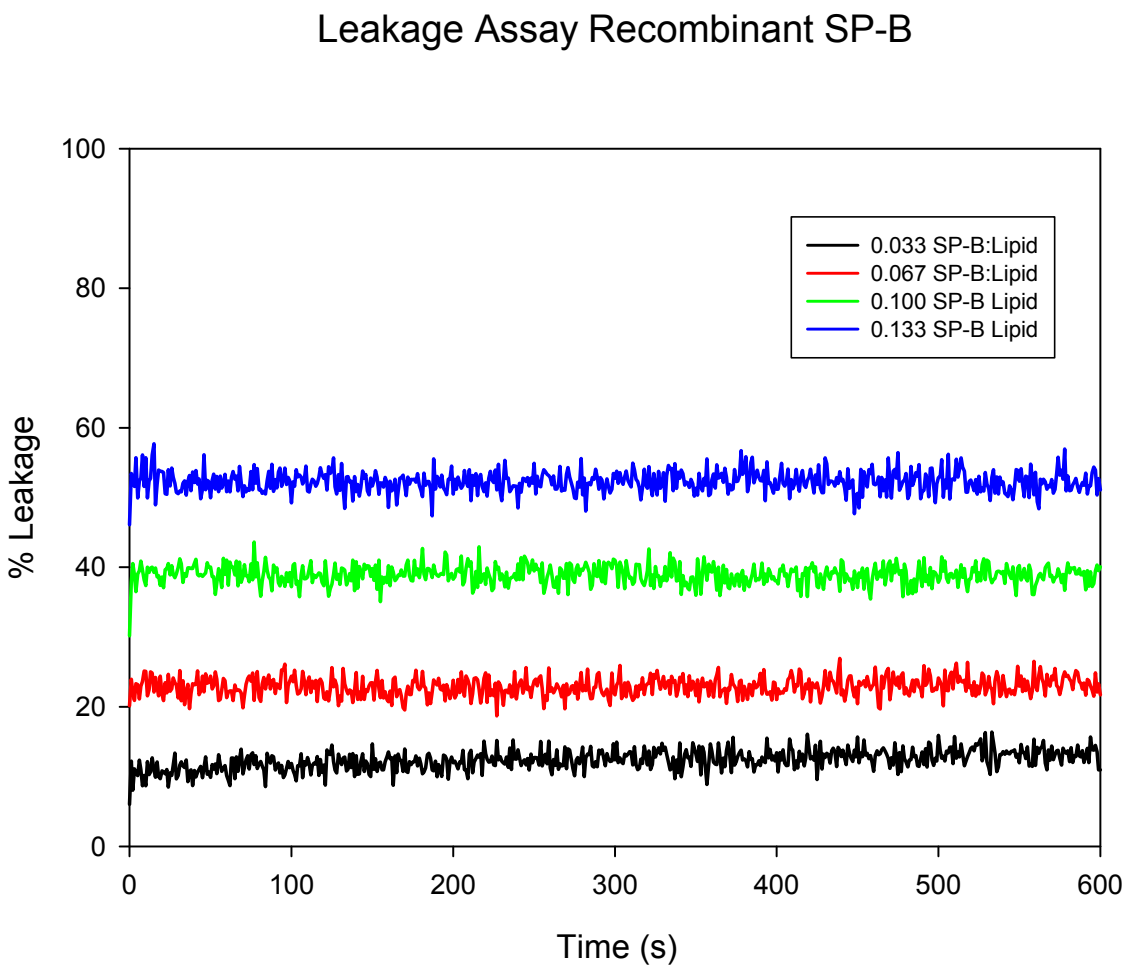

Figure 23: The percent leakage as a function of time of the leakage assay using recombinant SP-B.

3.5.2 Lipid Mixing

Like the leakage assay, lipid mixing also makes use of LUVs, however, this experiment measures the ability of a molecule to cause the lipids in the vesicles to mix. LUVs are formed with the FRET pair Rhodamine and NBD embedded directly into the membrane. FRET (fluorescence resonance energy transfer) is a technique in which the energy of a donor fluorophore is transferred to acceptor fluorophore in a radiation-less process. This will only occur if the fluorophores are in close enough proximity to one another. In this case, NBD is the donor fluorophore and Rhodamine is the acceptor fluorophore. When the average distance between these molecules is small enough, an emission close to the normal emission of Rhodamine (585 nm) can be measured. However, when the average distance increases, the 585 nm measurement will decrease while an emission close to that of NMD alone (470 nm) will increase.

During the initial phase of the experiment, labelled LUVs are mixed with an excess on unlabelled LUVs. Because both NBD and Rhodamine are contained within the membranes of the labelled vesicles, they are close enough for the FRET phenomenon to occur. However, if lipids are allowed to freely exchange between the vesicles, then the fluorophores will be diluted throughout the entire lipid mixture and the average distance will increase. This will be observed as a decrease in the 585 nm emission peak and an increase in the emission peak at 470 nm.

Figure 24 shows the fluorescent emission profile of the lipid mixing experiment using native SP-B. As the amount of SP-B increases, the Rhodamine peak (585 nm) decreases while the NBD peak (470 nm) increases. This demonstrates how SP-B is effective at causing lipid mixing. Figure 25 shows the same experiment with the

recombinant SP-B. While the same effect can be observed, it takes 4 μM of recombinant SP-B to achieve the same decrease in emission at 585 nm induced by only 2 μM of native SP-B. This indicates that while the recombinant SP-B has SP-B activity, it is not as effective as the native SP-B.

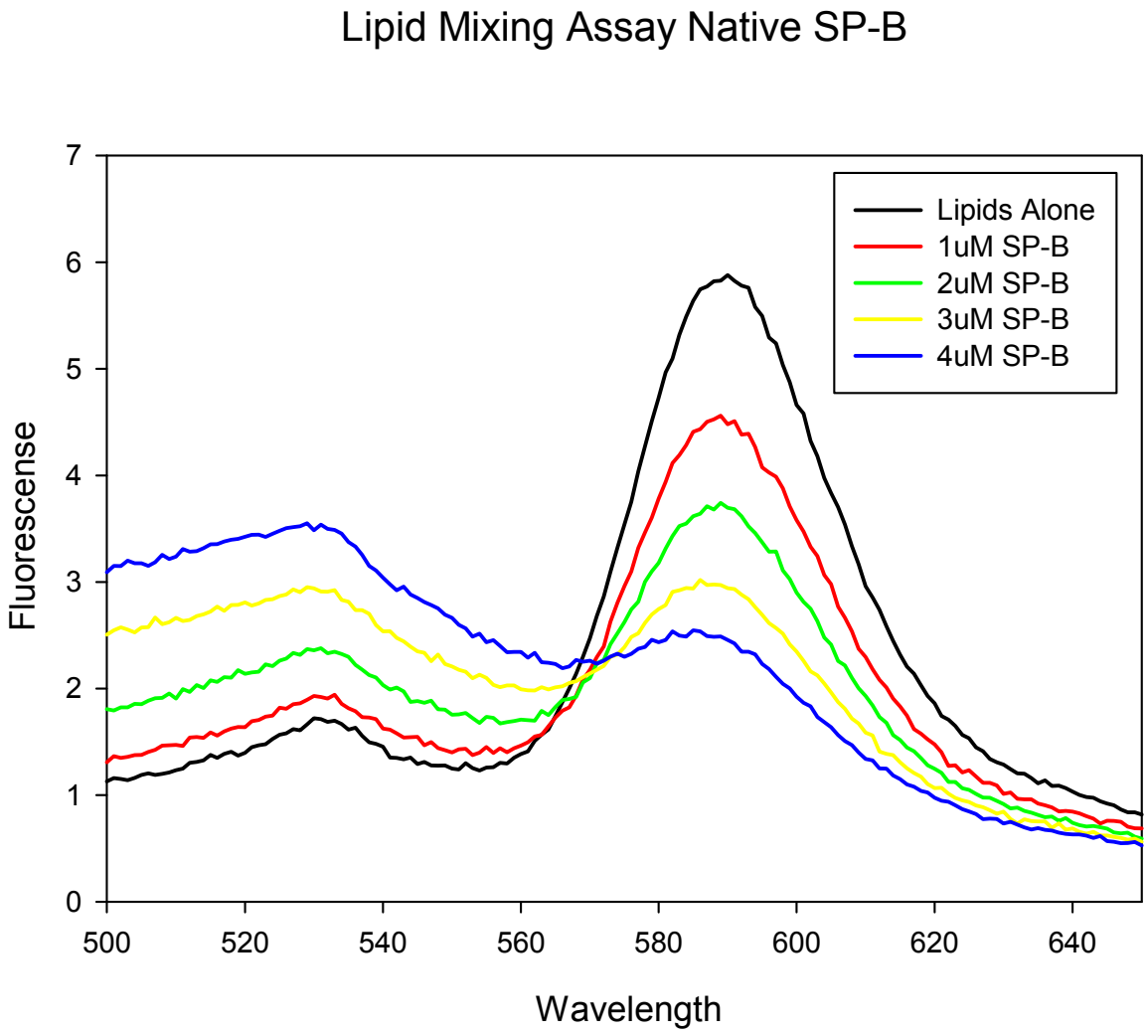

Figure 24: The fluorescent profile of the lipid mixing assay with native SP-B at different concentrations. The fluorescence is a relative value and the wavelength is in nm.

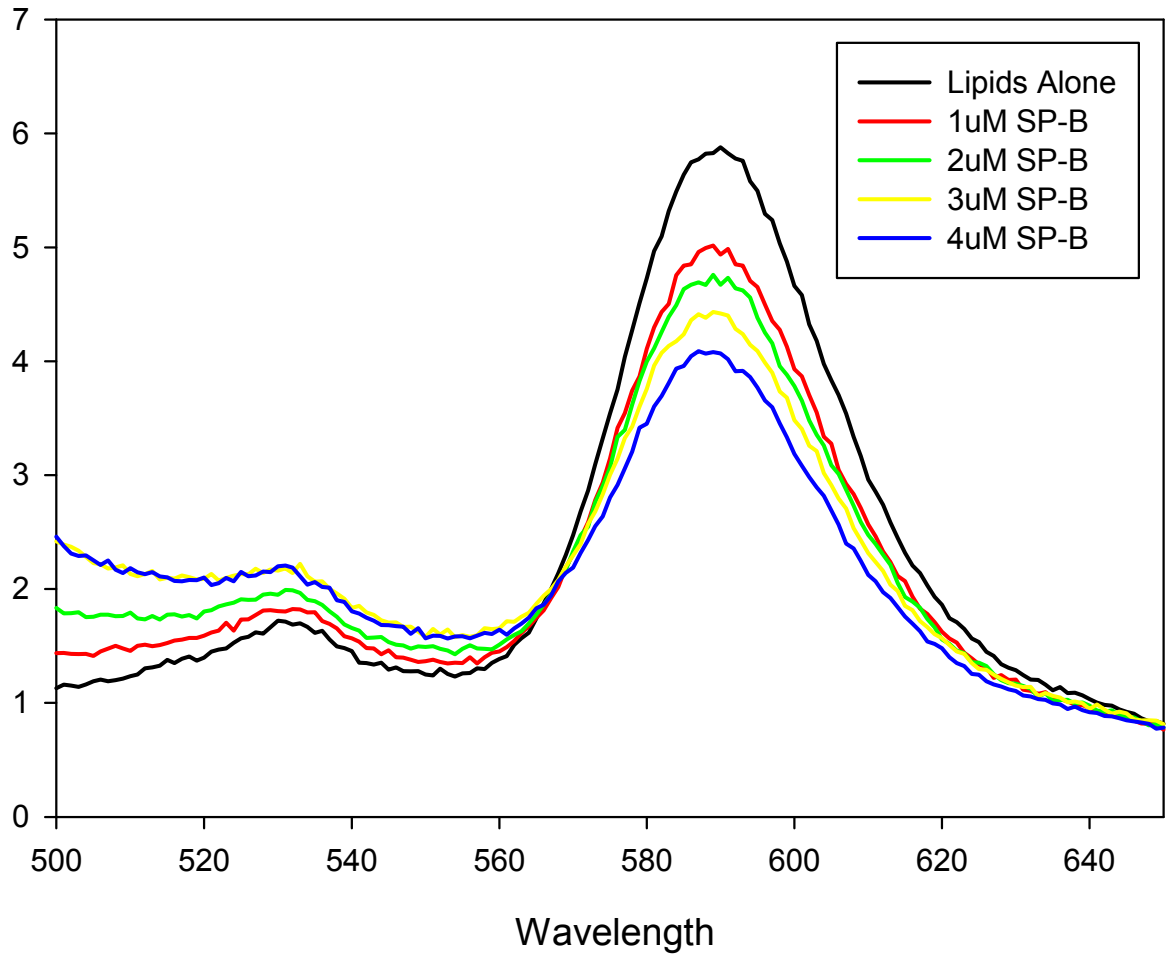

Figure 25: The fluorescent profile of the lipid mixing assay with recombinant SP-B at different concentrations. The fluorescence is a relative value and the wavelength is in nm.

3.5.3 Captive Bubble Surfactometer (CBS)

The captive bubble surfactometer is a device used to measure the surface tension of a bubble sealed in a chamber. This bubble can act as a mimic of the inside of an alveolus and thus produces some of the most physiologically relevant experiments when working with lung surfactant. I have performed three different experiments with the CBS. These include initial absorption (IA), post expansion absorption (PEA), and dynamic simulations. As mentioned in the Materials and Methods, the recombinant SP-B samples displayed an inability to adhere to the air-water interface when injected below the bubble. This problem was partially mediated by injecting the sample directly into the air-water interface by touching the bubble with the micro-syringe during injection. Because of this, the data displayed below includes both injection techniques (touching bubble and not touching bubble).

3.5.3.1 Initial Absorption (IA)

With initial absorption experiments, the sample was injected and the surface tension measurements begin immediately and continued for 5 minutes. This experiment measures the ability of the sample to adhere and spread across an air-water interface and reduce its surface tension. This is much like what occurs when newly formed surfactant must locate and spread across the air-water interface in alveoli. Figures 26 and 27 show the surface tension changes during this experiment. The surface tension generally starts at around 70 mN/m which is the normal surface tension of water. In both experiments, lipids alone do little to affect the surface tension of the interface which indicates that any pronounced change is due to the protein in the sample. In the not

touching bubble experiment (Figure 26), 2% native SP-B (nSP-B) reduces the surface tension to around 25 mN/m which is about the same level achieved by normal lung surfactant. The recombinant SP-B (rSP-B) is much less effective in this regard. Even at an amount of 10% of the total lipid mass, the surface tension is much greater than that achieved by the native SP-B. However, when the samples were injected directly into the air-water interface (Figure 27), the recombinant SP-B performs much better and is seen producing surface tensions as low as normal surfactant. However, much more recombinant SP-B is required than the native SP-B (10% vs. 1%). While the recombinant SP-B can reduce surface tension in this experiment, it is less effective than native SP-B.

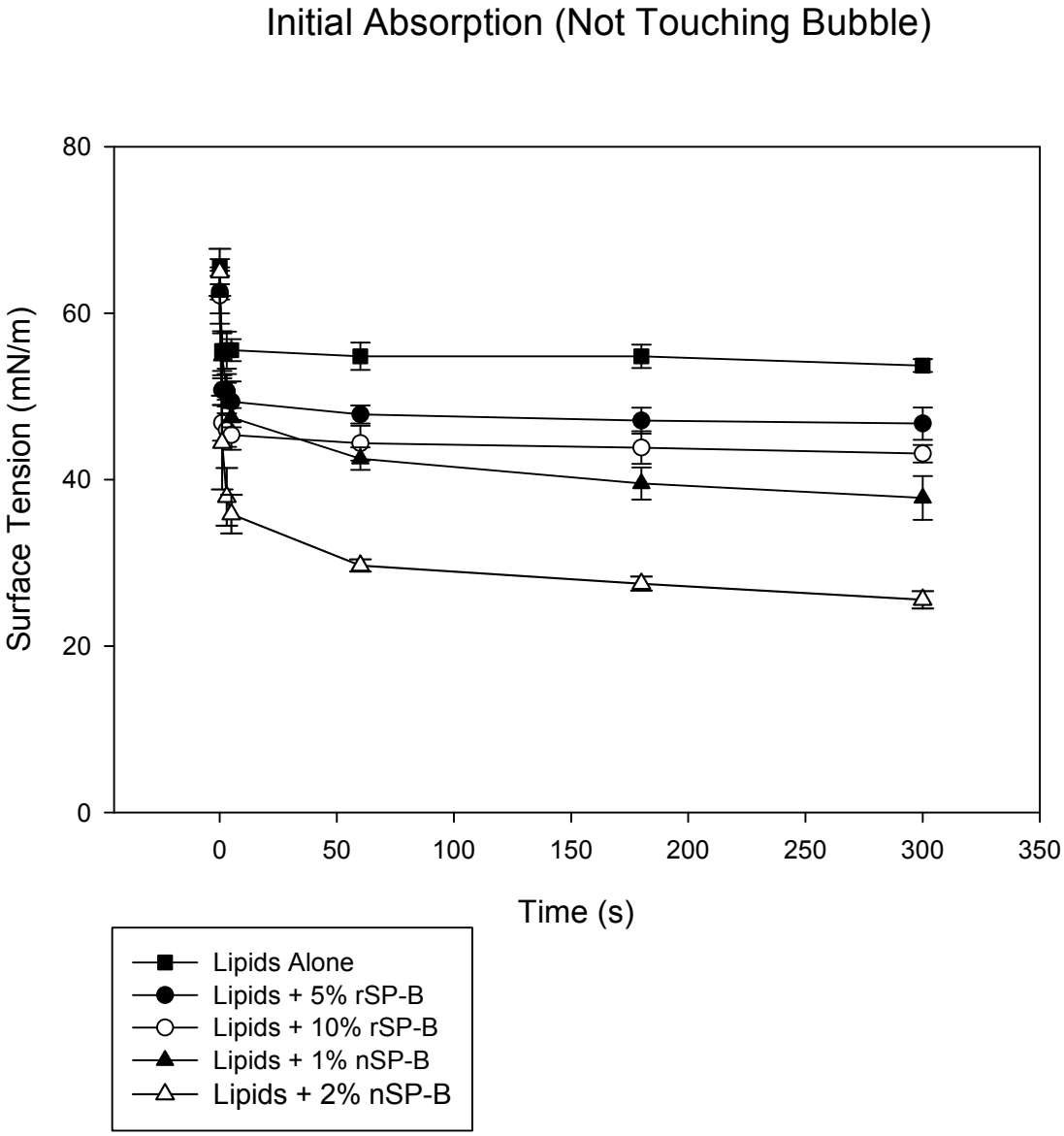

Figure 26: The changes in surface tension during the initial absorption experiments (not touching bubble). These samples have been injected below the air-water interface. Error bars represent one standard deviation with a sample size: n=3.

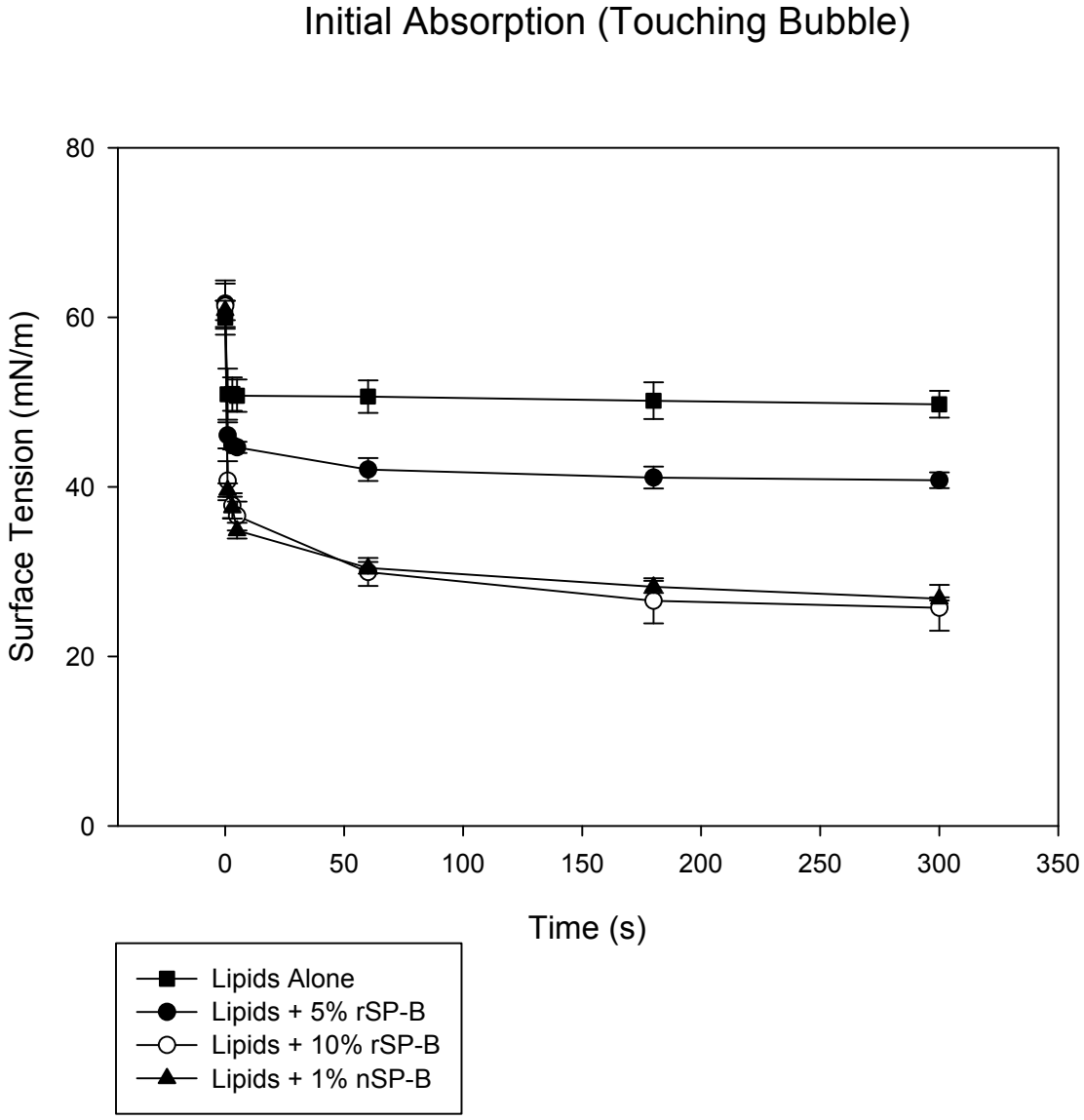

Figure 27: The changes in surface tension during the initial absorption experiments (touching bubble). These samples have been injected directly into the air-water interface. Error bars represent one standard deviation with a sample size: n=3.

3.5.3.2 Post Expansion Absorption (PEA)

Post expansion absorption uses a bubble that already has a sample spread across its air-water interface. The bubble is expanded, effectively increasing the surface area of the interface, and the surface tension is measured over the course of five minutes. What this experiment studies is the ability of the sample to diffuse across this enlarged surface area and reduce the surface tension of the interface back to normal. This is analogous to what occurs inside an alveolus when a deep breath is taken. The results of this experiment can be seen in Figures 28 and 29. Once again, the lipids alone do very little, indicating surface activity observed in the other samples require protein as well as the lipids. Like the IA experiments, the recombinant SP-B is not very effective unless the sample had been injected directly into the interface. When injected this way, both the recombinant and native SP-B allow the surface tension to return to rest at about 25 mN/m, which is similar to native surfactant. However, much more recombinant SP-B is required to be as effective as the native (up to 10 times). The same conclusion from the IA experiments can be drawn here. While not as effective as native SP-B, the recombinant SP-B still shows signs of being capable of normal surfactant function.

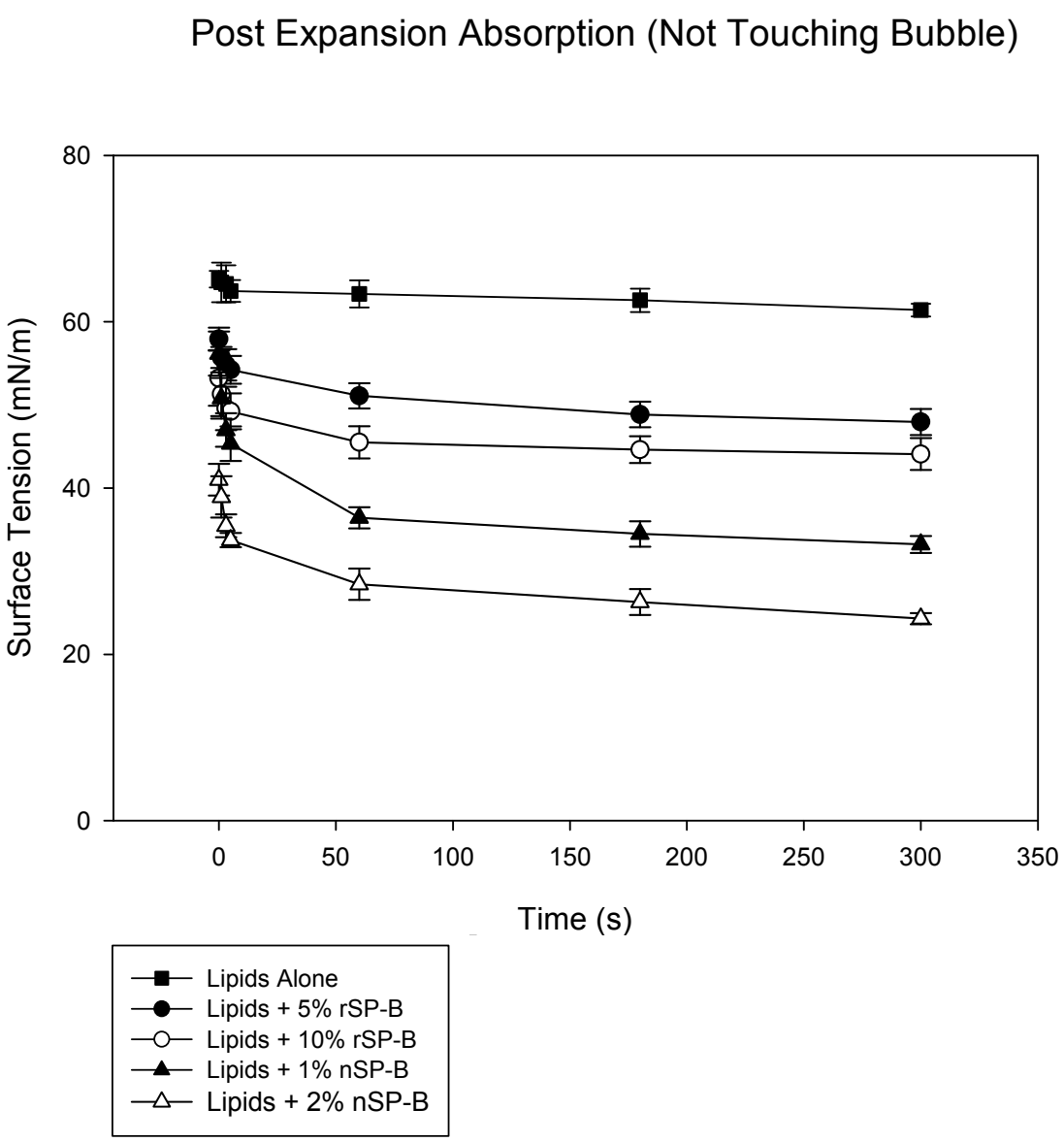

Figure 28: The changes in surface tension during the post expansion absorption experiments (not touching bubble). These samples have been injected below the air-water interface. Error bars represent one standard deviation with a sample size: n=3.

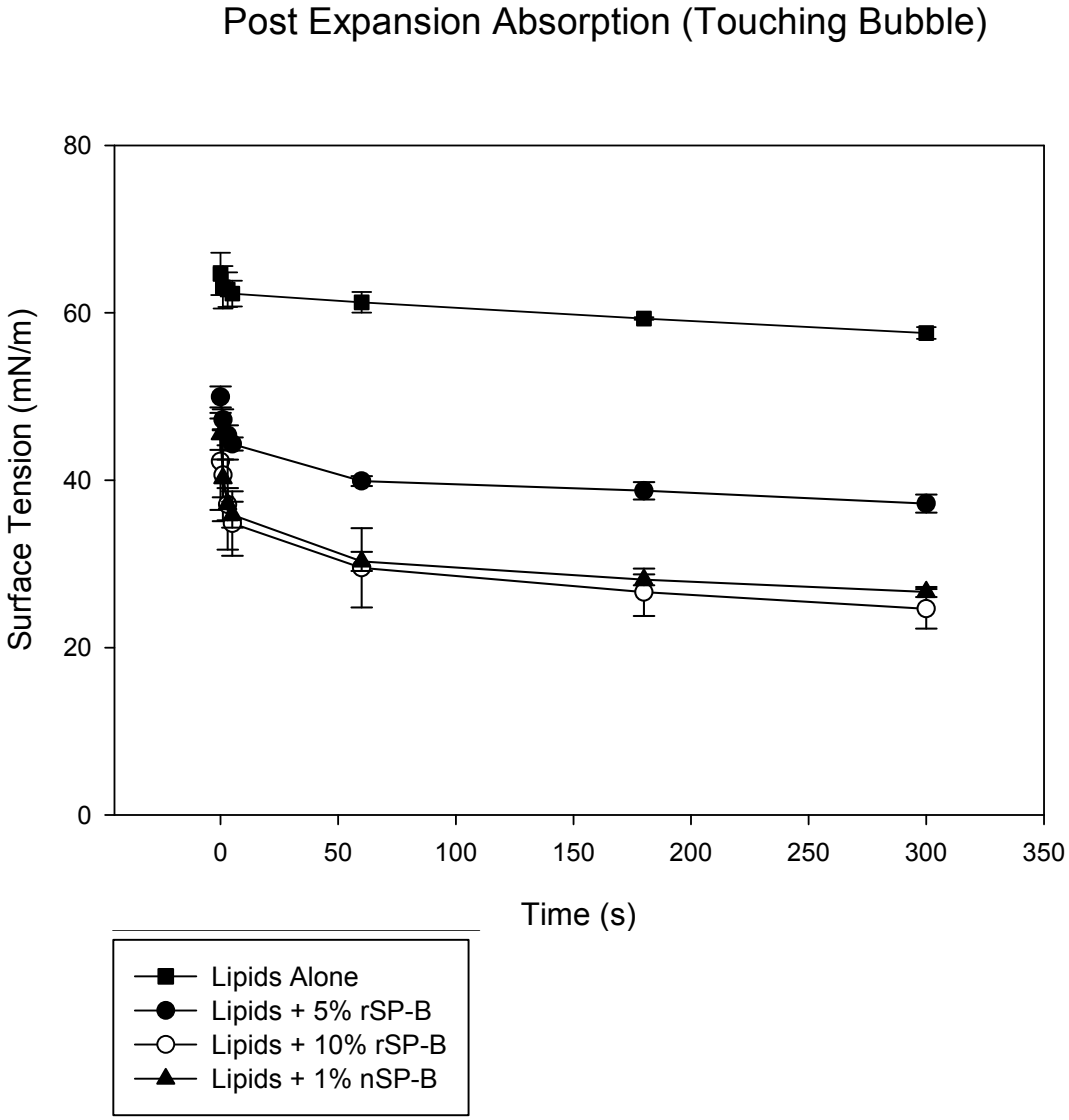

Figure 29: The changes in surface tension during the post expansion absorption experiments (touching bubble). These samples have been injected directly into the air-water interface. Error bars represent one standard deviation with a sample size: n=3.

3.5.3.3 Dynamic Simulation

With dynamic simulation experiments, the bubble already has a sample spread across the air-water interface. The bubble is then contracted and expanded 20 times over the course of a minute, which is the same rate as normal human breathing. This experiment imitates the alveolar environment during breathing and measures the changes in surface tension and relative surface area of the interface. Results from the dynamic simulation experiments are shown in Figures 30–38.

There are three things to look for in these experiments to assess if the surfactant is working properly. The first is maximum surface tension, which should not rise above the normal resting levels, which for normal surfactant is around 25 mN/m. The second is minimal surface tension, which should drop to almost 0 mN/m. The final thing to look for is the absence of hysteresis. Hysteresis is work applied to the bubble that does not result in a decrease in surface tension. In other words, it is a change in the relative area without change in the surface tension and can be observed in the following data as space between the compression and expansion lines. Normal working surfactant produces minimal hysteresis. If all three criteria are met, the sample is acting as an effective surfactant.

It is important to note here that the first cycle is usually less efficacious than the subsequent cycles and results in considerable hysteresis. This is due to the formation of multi-layered structures that are assembled underneath the interface during the first compression cycle and were discussed in the introduction (Figure 3). These structures create a reservoir for the surfactant to be stored during compression and allow the surfactant to easily re-spread along the interface during expansion. After the first cycle,

the formation of the multi-layered structures will occur more easily and will result in the disappearance of the hysteretic effect if the surfactant is functioning normally.

Figure 30 and 31 show the effect of lipids alone during compression-expansion cycles. None of the three criteria mentioned above are met in either trial. The maximum and minimum surface tension is too high and considerable hysteresis can be observed in every cycle. Therefore, the positive effect produced in the following experiments involving SP-B must be the result of the protein present in the samples.

The native SP-B produces positive results in almost every experiment (Figures 32-34). The best results can be seen Figure 32. Other than the first cycle, all three criteria of a functional surfactant are met. The surface tension does not rise much above 25 mN/m and drops to nearly 0 mN/m during compression. There is no space present between the expansion and compression lines in cycles 10 and 20, therefore no hysteresis is produced.

The results indicate the recombinant SP-B samples were not nearly as effective (Figures 35-38). Both 5% samples and the 10% not touching bubble samples produced results similar to lipids alone indicating that in these cases the SP-B was almost entirely not functional. However, some positive results can be seen in the 10% touching bubble experiment (Figure 38). Here we see the maximum surface tension rise not far above 40 mN/m and drop to close to 0 mN/m during compression. This could, however, be due to over compression of the sample during the experiment.

These experiments show that surface activity can be observed using recombinant SP-B. However, in order to achieve this activity, much more protein is required and the sample must be directly applied to air-water interface. Even with these

added requirements, the effectiveness of recombinant SP-B never reached that of the native SP-B in dynamic simulation experiments.

These functional studies show the recombinant SP-B produces normal SP-B activity. This is encouraging as it demonstrates that a functional SP-B can be produced in a recombinant system which has never been done before. However, while effective, it is never achieves the same results as native SP-B. Reasons for this are explored in the upcoming discussion.

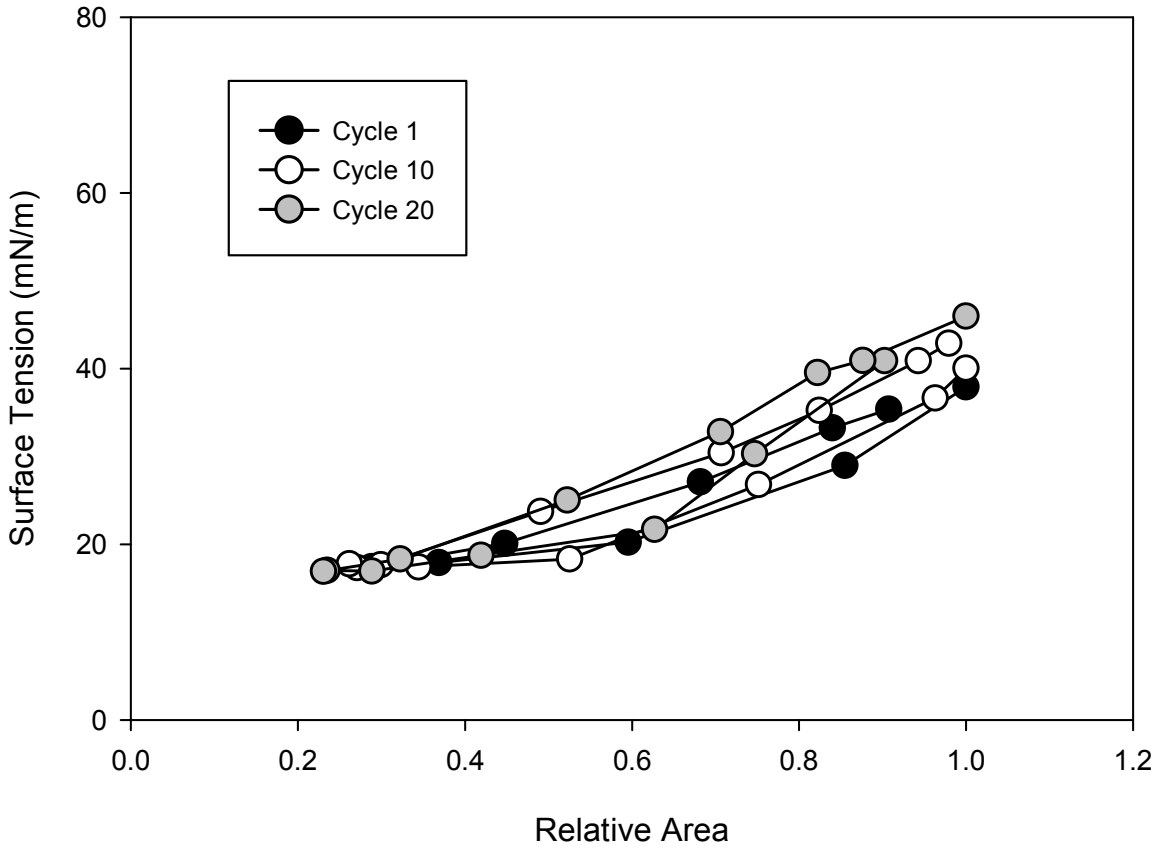

Figure 30: The dynamic simulation of the lipids alone sample that had been injected below the air-water interface (ie. not touching the bubble). The graph shows the surface tension and surface area changes of the air-water interface during cycles 1, 10, and 20.

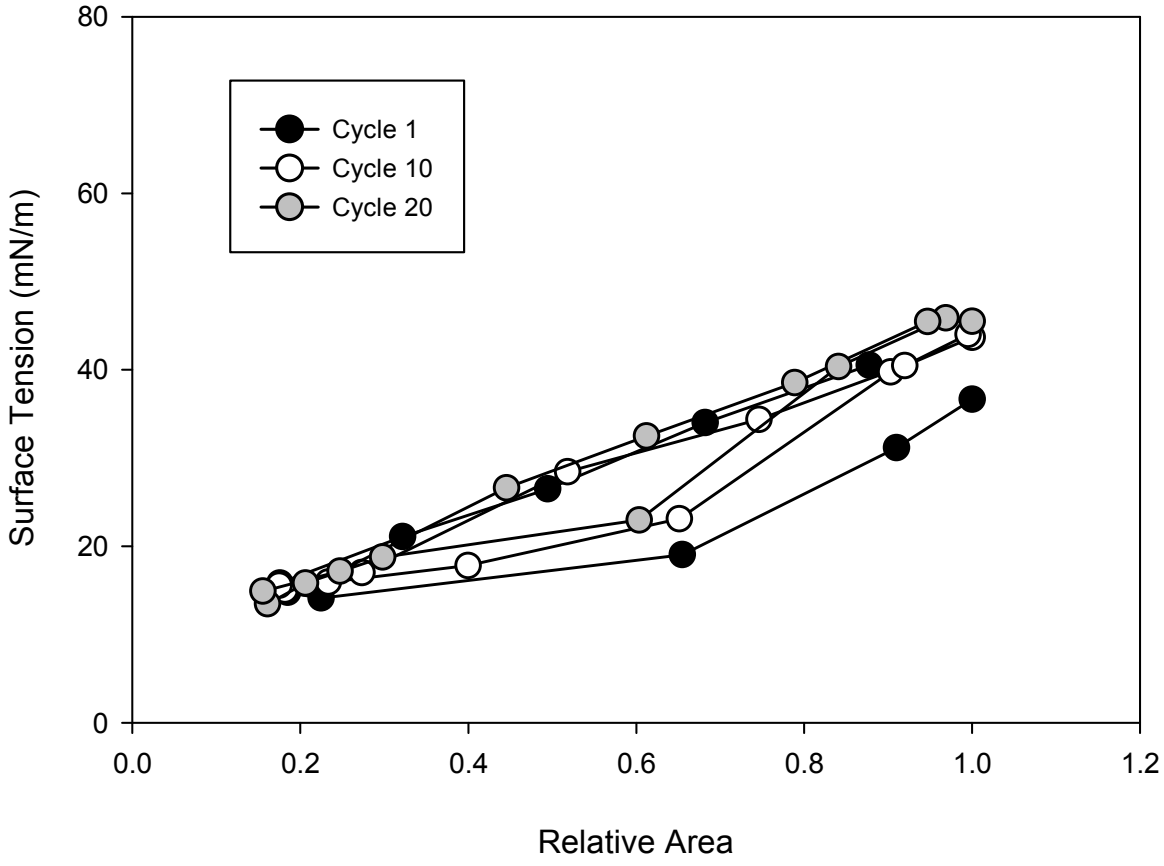

Figure 31: The dynamic simulation of the lipids alone sample that had been injected directly into the air-water interface (ie. touching the bubble). The graph shows the surface tension and surface area changes of the air-water interface during cycles 1, 10, and 20.

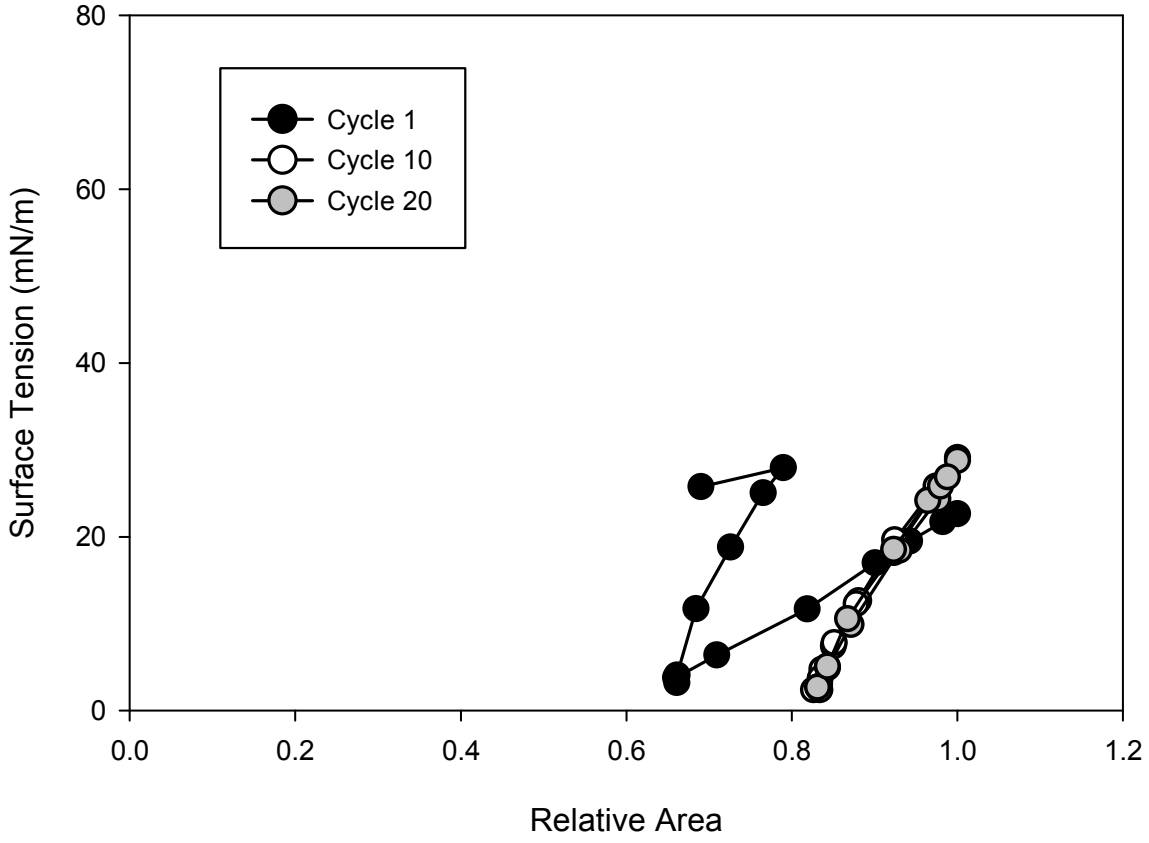

Figure 32: The dynamic simulation of the 1% native SP-B sample that had been injected below the air-water interface (ie. not touching the bubble). The graph shows the surface tension and surface area changes of the air-water interface during cycles 1, 10, and 20. The SP-B concentration is a percentage of the total lipid mass.

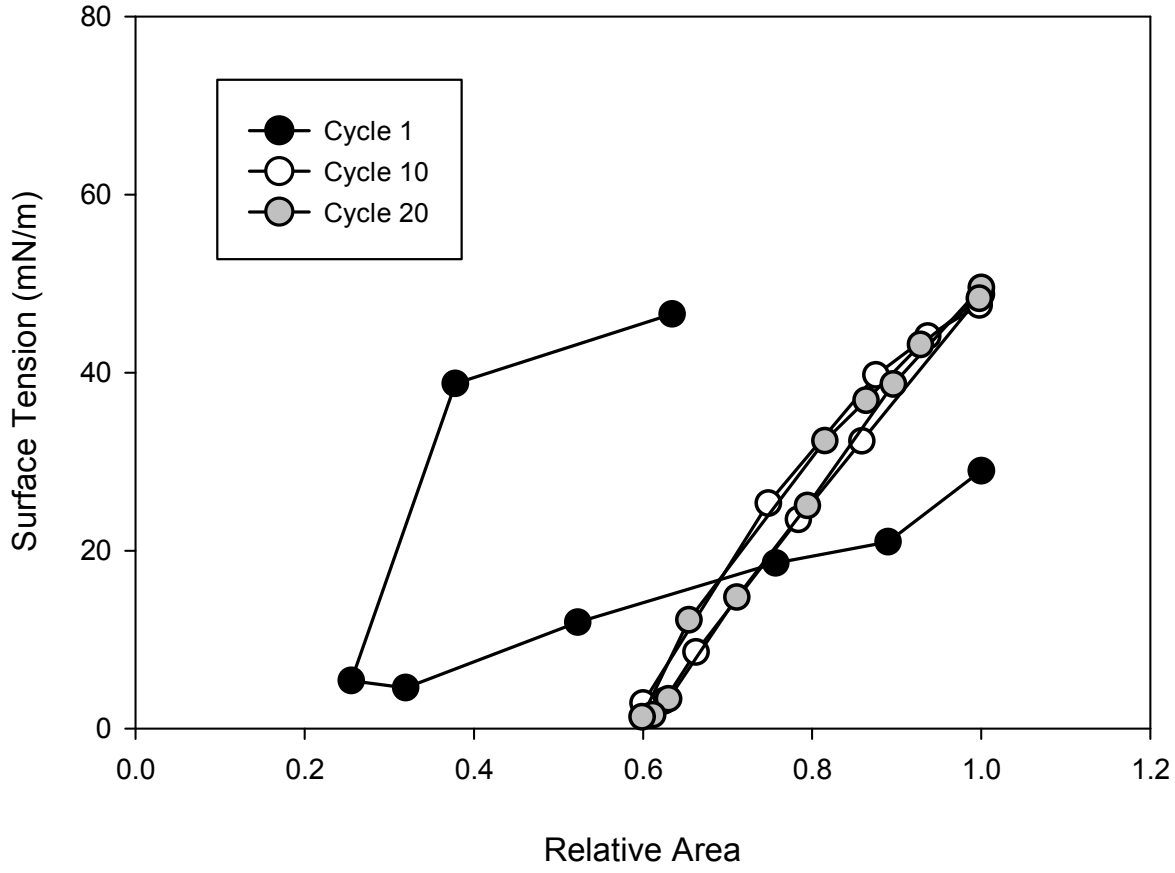

Figure 33: The dynamic simulation of the 1% native SP-B sample that had been injected directly into the air-water interface (ie. touching the bubble). The graph shows the surface tension and surface area changes of the air-water interface during cycles 1, 10, and 20. The SP-B concentration is a percentage of the total lipid mass.

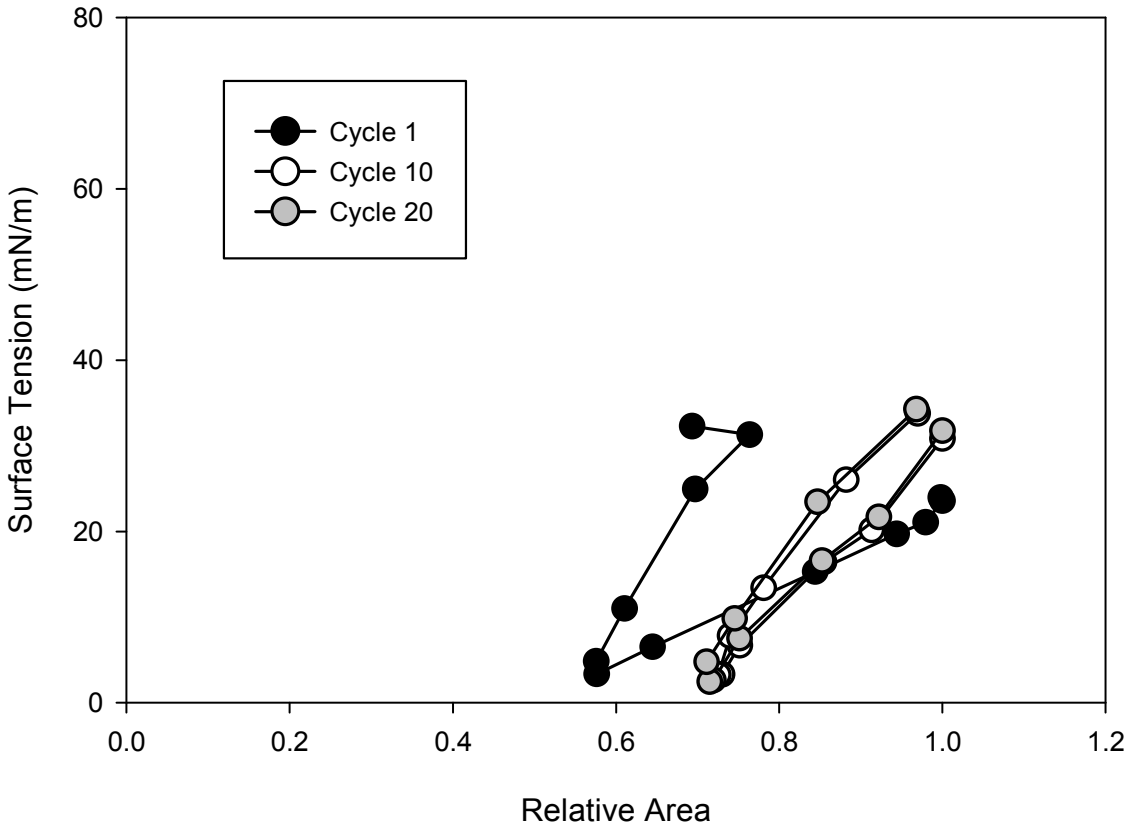

Figure 34: The dynamic simulation of the 2% native SP-B sample that had been injected below the air-water interface (ie. not touching the bubble). The graph shows the surface tension and surface area changes of the air-water interface during cycles 1, 10, and 20. The SP-B concentration is a percentage of the total lipid mass.

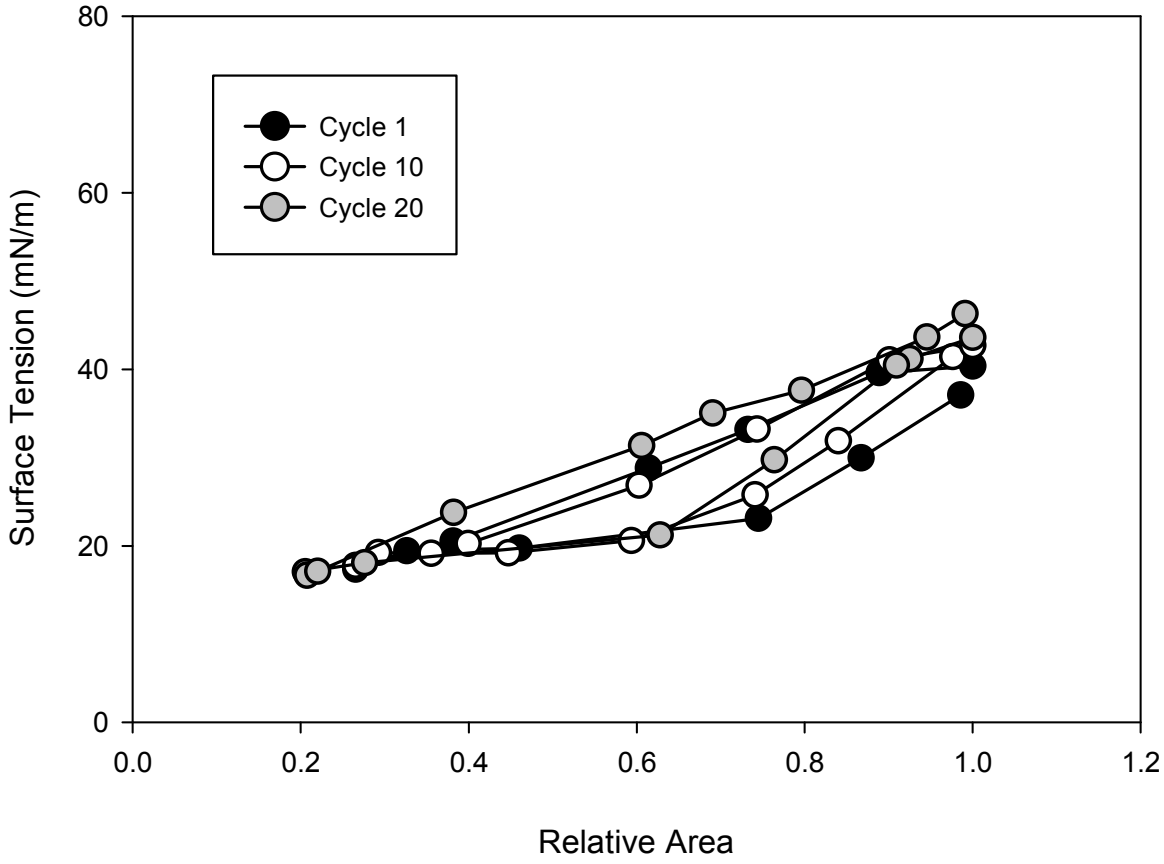

Figure 35: The dynamic simulation of the 5% recombinant SP-B sample that had been injected below the air-water interface (ie. not touching the bubble). The graph shows the surface tension and surface area changes of the air-water interface during cycles 1, 10, and 20. The SP-B concentration is a percentage of the total lipid mass.

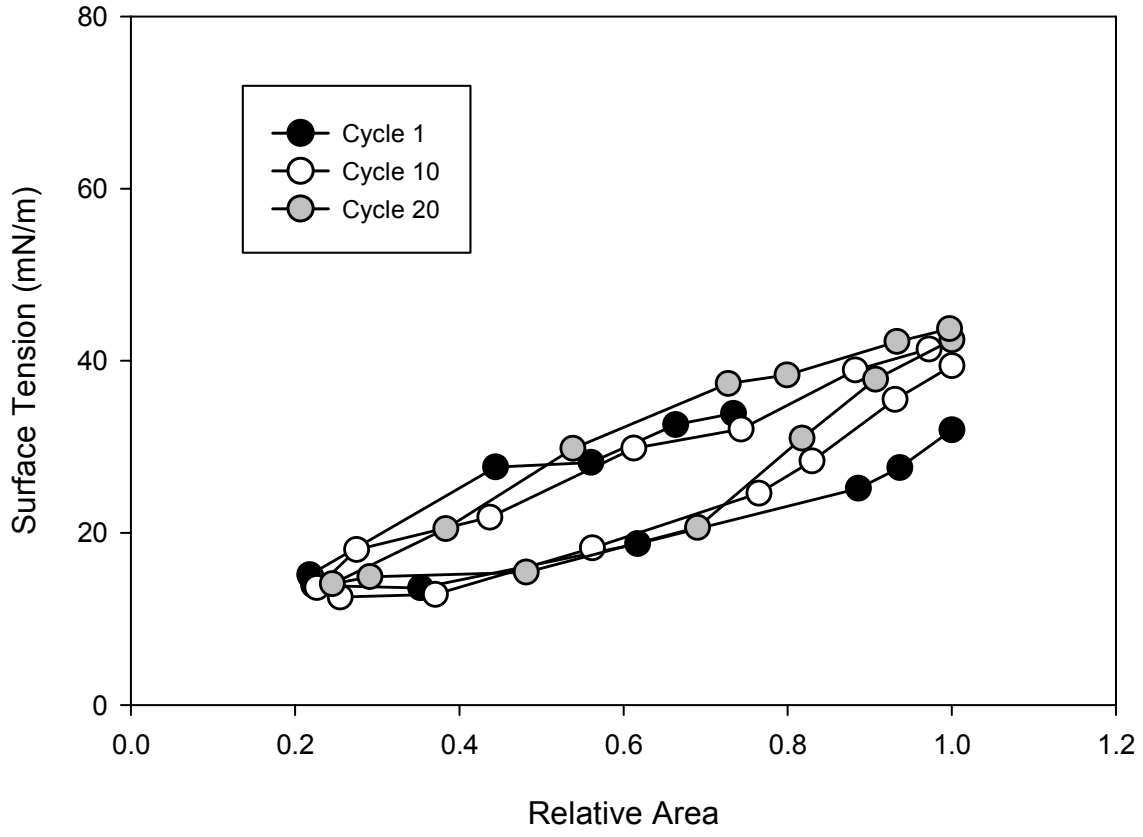

Figure 36: The dynamic simulation of the 5% recombinant SP-B sample that had been injected directly into the air-water interface (ie. touching the bubble). The graph shows the surface tension and surface area changes of the air-water interface during cycles 1, 10, and 20. The SP-B concentration is a percentage of the total lipid mass.

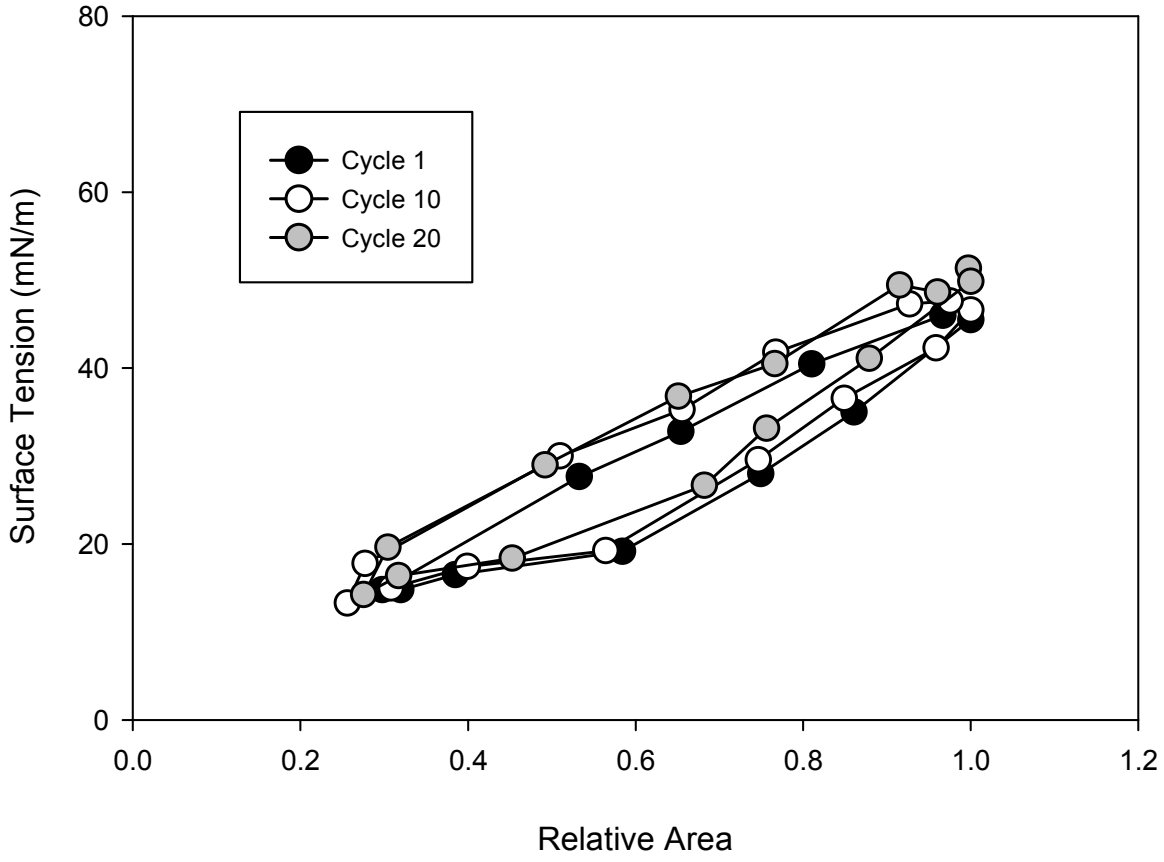

Figure 37: The dynamic simulation of the 10% recombinant SP-B sample that had been injected below the air-water interface (ie. not touching the bubble). The graph shows the surface tension and surface area changes of the air-water interface during cycles 1, 10, and 20. The SP-B concentration is a percentage of the total lipid mass.

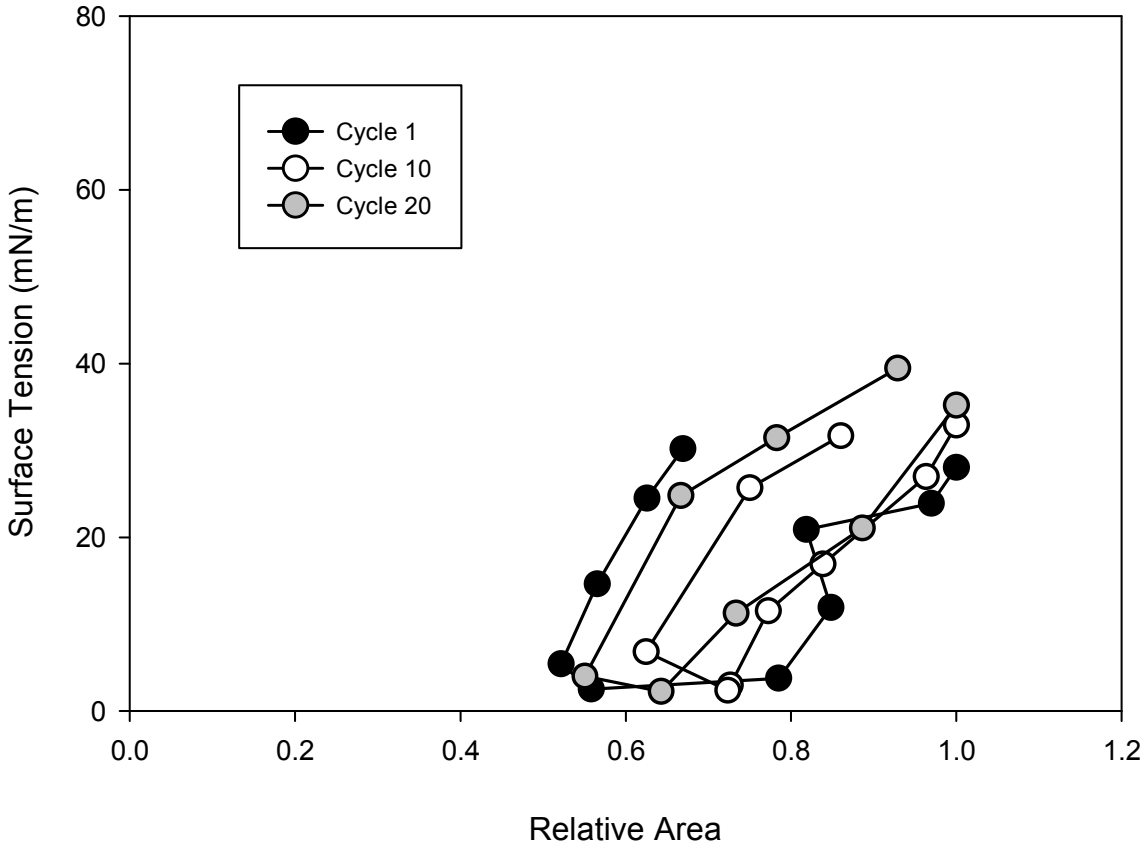

Figure 38: The dynamic simulation of the 10% recombinant SP-B sample that had been injected directly into the air-water interface (ie. touching the bubble). The graph shows the surface tension and surface area changes of the air-water interface during cycles 1, 10, and 20. The SP-B concentration is a percentage of the total lipid mass.

4. Discussion

In order to gain further understanding of lung surfactant function, it is crucial to determine the mechanism of SP-B. A prerequisite to a mechanistic understanding of a protein is to first determine its three dimensional structure as the structure and function of proteins are forever tied together. SP-B is a rare case in that it is an essential protein that does not yet have a solved three dimensional structure. The absence of a structure is not from a lack of trying, however, as researchers have been attempting to solve this problem for many years. Reasons why this has failed were discussed in the introduction and include the difficulty of getting SP-B to crystallize (which is required for X-ray crystallography) and the difficulty with recombinant expression (which is required for three dimensional NMR). In this thesis, I have discussed a renewed effort in the latter.

Previous attempts to produce a recombinant SP-B involved the fusion to SN with a thrombin cleavage site between them. Only a small amount of expression was achieved [81]. As mentioned in the results, a new plasmid was designed that replaced the thrombin cleavage site with a cyanogen bromide cleavage site (methionine residue). Also the histidine tag was moved from the amino-terminus to the carboxy-terminus and seven residues were deleted from the amino-terminus of SP-B. Once transformed into C43 *E. coli*, these changes resulted in an increased expression of the SN-SP-B fusion, much of which was present in insoluble inclusion bodies (see Figure 2). The new cyanogen bromide cleavage also produced positive results (see Figure 6) in which the fusion protein is almost entirely cleaved and SP-B alone and can be observed on a Western blot with an anti-SP-B antibody. This is the first time that a recombinantly

expressed SP-B has been observed on a SDS polyacrylamide gel or Western blot. While not yet purified, this was a very encouraging result.

While working with the new plasmid, something unexpected occurred. Another protein from the cellular extract was binding to the nickel-bound IMAC column and eluting just before the SN-SP-B fusion (see Figures 6 and 7). Western blotting with an anti-SP-B antibody confirms that this other peptide contains SP-B (see Figure 8). The size estimates seem to indicate that this alternate peptide could be SP-B expressed alone. This alternate expression was very puzzling as the plasmid was designed to only allow production of the SN-SP-B fusion and earlier studies have shown that a similar plasmid with no SN produces no detectable levels of SP-B. To try to arrive at a possible explanation, original SN-Δ7NTΔM-SP-B-6His plasmid construct (Figure 39) was studied. An important feature to the plasmid construct is the ribosome binding site (also known as the Shine-Delgarno sequence) which is located 3' (upstream) of the start codon (ATG) [86]. After the gene undergoes transcription, the resulting mRNA is directed to a ribosome which binds at the ribosome binding sequence before translation takes place. In this construct, the ribosome binding site is the sequence GAAGGAG and its location is highlighted in Figure 40. To see if SP-B could be expressed without the fusion, I scanned the plasmid upstream of the SP-B gene for another possible ribosome binding site. I found a possible site that has the sequence GGAG and is also highlighted in Figure 39. While only a partial match for a ribosome binding site, it has previously been demonstrated that small fragments of ribosome binding sites can lead to alternate gene expressions [86]. If this sequence does act as a secondary ribosome binding site, then translation would begin at the next start codon (ATG) which in this case would the

ATG in between the SN and SP-B genes that normally encodes the cyanogen bromide cleavage site. If translation were to occur here, it would produce SP-B with the carboxy-terminal histidine tag. This would produce a protein that would stick to the nickel-bound IMAC resin and would explain the presence of the SP-B positive band in the Western blot.

Another possible explanation for the alternate expression would be uncontrolled proteolysis inside the cell. The identity of this alternate expression could be found using accurate mass analysis or amino-terminal sequencing.

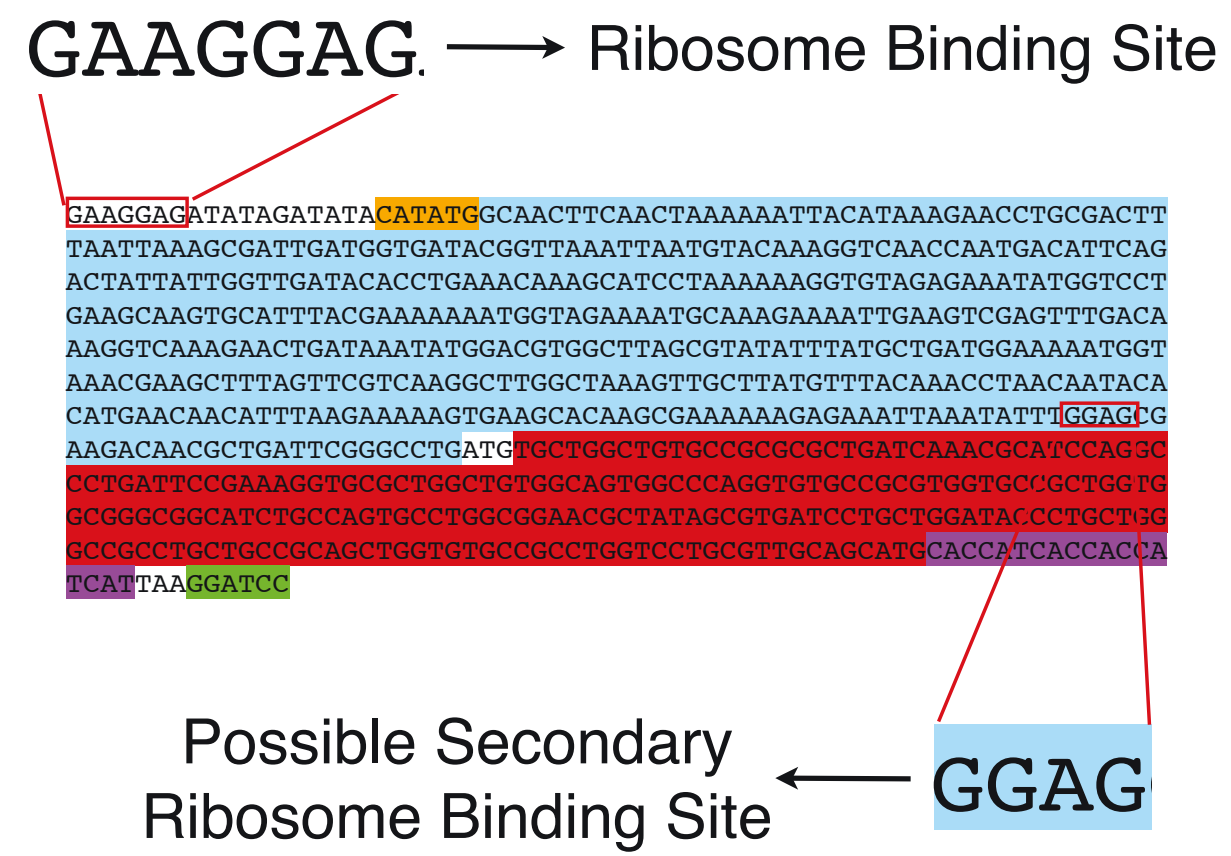

Figure 39: The SN-Δ7NTΔM-SP-B-6His plasmid construct with ribosome binding site. This figure is similar to Figure 1 except the amino acid sequence is omitted and part of the DNA sequence 3' (upstream) of the start of the SN gene is included to show the location and identity of the ribosome binding site. Also highlighted here is a possible secondary ribosome binding site that is located within the SN sequence 3' to the start of the SP-B gene which could be responsible for SP-B-6His expression.

While the successful expression and cleavage of the recombinant SP-B was very promising, the SP-B had to be separated from the SN fragments and other impurities to be of any use for experimental and clinical applications. The enrichment of recombinant SP-B would prove to be very difficult. Unsurprisingly, due to SP-Bs high hydrophobic content, it has a tendency to aggregate. After the cleavage and subsequent dialysis, it is probable that the SP-B formed large protein aggregates, which resulted in a sample that was very difficult to work with and remained insoluble in most aqueous and organic solvents. This led to many problems during isolation procedures that can be seen in the work done with organic extraction, HPLC, and cationic exchange chromatography (see Figures 10-14). A breakthrough occurred with a new solubilization procedure in which the protein was first dissolved in a high concentration of urea and dialyzed in the presence of DPPC vesicles, followed by lyophilization. The solubilized SP-B had presumably bound to the vesicles and remained inside the dialysis tubing while the urea diffused out. The dried protein/lipid powder was then easily solubilized in organic solvent. Being in solution with organic solvent does not help with many of the techniques tried (ie. HPLC, anionic exchange chromatography) as the solvent is not compatible with these methods. However, this breakthrough allowed the use of LH20 resin, which is resistant to organic solvent, to achieve partial enrichment of the recombinant SP-B (see Figures 17 and 18). While not completely isolated, this was the highest enrichment of recombinant SP-B yet obtained, so it was decided to proceed with functional studies to find out if the recombinant SP-B had the ability to function like native SP-B. This is very important for any possible clinical applications.

The problem with partial enrichment could be addressed by making a new construct where the his-tag is retained on the SP-B after SN cleavage. The SP-B could then be enriched using another Ni column thus circumventing the LH20 chromatography altogether.

Functionally, we already know that SP-B has the ability to bind and disrupt membranes, fuse membranes together, and reduce surface tension of air-water interfaces [47] [48] [49] [50] [51]. Going into the functional work, it was known that the function of the recombinant SP-B could be impaired. First of all, the impurities still present could have an impact. Also, there was as yet no attempt to ensure the recombinant SP-B was properly folded. Structural work has yet to be accomplished so it is entirely possible that during the harsh conditions of purification, the recombinant SP-B could be folded in a non-native state which would impair its functional ability. Lastly, and possibly the most important, is the amino-terminal deletion.

As mentioned in the results, this new SN-Δ7NTΔM-SP-B-6His the seven amino-terminal residues of SP-B was removed from the plasmid construct due to a suggestion by Sharifahmadian (2013) that this modification could allow for SP-B to be more easily expressed [81]. As the primary goal of this work is to solve the three-dimensional structure of SP-B, it was decided that these seven residues were not necessary. It is already known that these residues have to remain outside the first alpha helix of SP-B due to its proline rich structure (FPIPLPY) so its removal should have very little impact on the overall tertiary structure. It is thought that these residues will form a kinked, poly-pro like structure that will stick out from the rest of the protein [48] [87]. While not impacting the tertiary structure of SP-B, this amino-terminal region has been shown to have a large

functional impact. The lack of an amino-terminal region has been shown to impact the ability of SP-B to cause membrane leakage and lipid mixing [48], as well as lowering SP-Bs ability to reduce surface tension in CBS experiments [17] [87]. Molecular dynamics simulations suggest that the amino-terminal region also has very important role on membrane binding [87] [88]. While these abilities were impaired with the removal of the amino-terminus, there was still some function present. This previous work utilized SP-B fragments as recombinant expression was not yet possible and native SP-B was only available full length.

Because of these previous results, the recombinant amino-term deleted SP-B was not expected to be as functional as native SP-B. However, some SP-B activity was observed with the recombinant samples. This result supports the conclusion that the method of expressing recombinant SP-B presented in this thesis is a viable source of SP-B for experimental and clinical applications. As seen in the results of the functional studies (leakage assay, lipid mixing, and CBS), we can clearly see that, while impaired, the recombinant SP-B does retain some SP-B activity.

The leakage assay experiments produced an interesting result. With the native SP-B samples, a steady increase of leakage was observed over a period of five minutes (Figure 22). This indicates that the native SP-B is causing an open pore to form in the membrane which allows the interior environment to continuously leak out. This increasing leakage is not seen with the recombinant SP-B samples (Figure 23) suggesting that in this case, pore formation does not occur. One of the main differences in the samples is the aforementioned lack of the seven amino terminal residues in the recombinant SP-B. It can be concluded from this that these residues are important in

pore formation in lipid films. This conclusion is supported by molecular dynamics simulations [88]. However, it is important to mention that this difference could also be caused by misfolding in the recombinant SP-B or impurities present in the recombinant sample.

The lipid mixing results were less promising than the leakage. While some small level of activity was observed with the recombinant SP-B, it was nowhere near as effective as the native SP-B sample (Figures 24 and 25). Similar results were found in experiments with SP-B fragments [48]. Ryan *et al*. found that with the leakage assay, the fragment without the amino-terminus retained some activity however, in the lipid mixing experiments it did not. They concluded that the amino-terminus was more important to lipid mixing than leakage which seems to be replicated in the experiments presented in this thesis. Once again, the loss of activity in the recombinant SP-B sample could also be due to misfolding and the presence of impurities.

In the CBS experiments, we also see SP-B activity with the recombinant samples. However, once again there was only partial activity when compared with native SP-B (Figures 26-38). This comes as no surprise because of the reasons listed above, though there were interesting observations. First of all, the recombinant samples were only effective when injected directly into the air-water interface. This could indicate that the recombinant SP-B has trouble allowing the surfactant to adhere to the interface and suggests this is another function of the amino-terminus. Another interesting observation was that during dynamic simulation experiments, hysteresis did not disappear after the first cycle in recombinant SP-B (Figure 38) as is usually the case with native SP-B samples (Figure 32). As mentioned in the results, the hysteresis is a

result of the multi-layered structures being organized underneath the air-water interface. This process is normally facilitated by SP-B (Figure 3) and once this is accomplished in the first compression-expansion cycle, it occurs much easier in subsequent cycles resulting in the disappearance of hysteresis (ie. the space between the compression and expansion lines in Figures 32 and 38). The fact that hysteresis is always present with the recombinant sample demonstrates an inability of the recombinant SP-B to properly form the multi-layered structures. This represents another possible function of the amino-terminus of SP-B. However, it must be emphasized that this assumption is not conclusive as this impairment could also be due to misfolding and the presence of impurities in the recombinant SP-B sample.

In this thesis, I have described a novel method for the expression and partial enrichment of a recombinant SP-B. I have also demonstrated that this recombinant SP-B retains some portion of native SP-B activity. Therefore, this technique shows promise that it can be developed into a viable source of SP-B for various experimental as well as clinical applications. Furthermore, the data emphasizes the importance of the amino-terminus to SP-B function. While the results of this thesis are very encouraging, more work is needed for this work to progress further. First of all, the conclusion that the impairment of the recombinant SP-B function is due to the amino-terminal deletion remains questionable because of the presence of impurities and the possibility of misfolding. To remove this doubt, a new plasmid could be designed that leaves the amino-terminus intact. Expression and enrichment of this full length SP-B can be done using the same conditions and procedures described here. Therefore, the sample of recombinant SP-B should fold the same way and contain the same impurities as the

sample used in these functional experiments except in this case, the SP-B would have its amino-terminus. Any difference observed in the activity between this SP-B and the amino-terminal deleted SP-B should be entirely due to the amino-terminus and remove the possible effects of misfolding and impurities out.

To solve the problem with purification, one solution could be to try to reduce the number of lyophilization steps which is likely resulting in much of the aggregation that is making the recombinant SP-B very difficult to work with. It is probably necessary to revisit the plasmid and design one better suited for enrichment.

One of the main sources of impurities are the SN fragments and incomplete digests that result from the cyanogen bromide cleavage. Some of these impurities are similar in size to SP-B which can make separation difficult. To work around this, a plasmid can be designed in which the methionine residues in SN are mutated. A possible design is shown in Figure 40 in which the four internal methionine residues of SN are mutated to alanine as seen in [89]. When the resulting gene is cleaved, the resulting products should include SP-B (~8 kDa), SN (~18 kDa), and if the reaction does not go to completion, undigested SN-SP-B (~26 kDa). With only three products of very different sizes, the separation should be much easier to achieve.

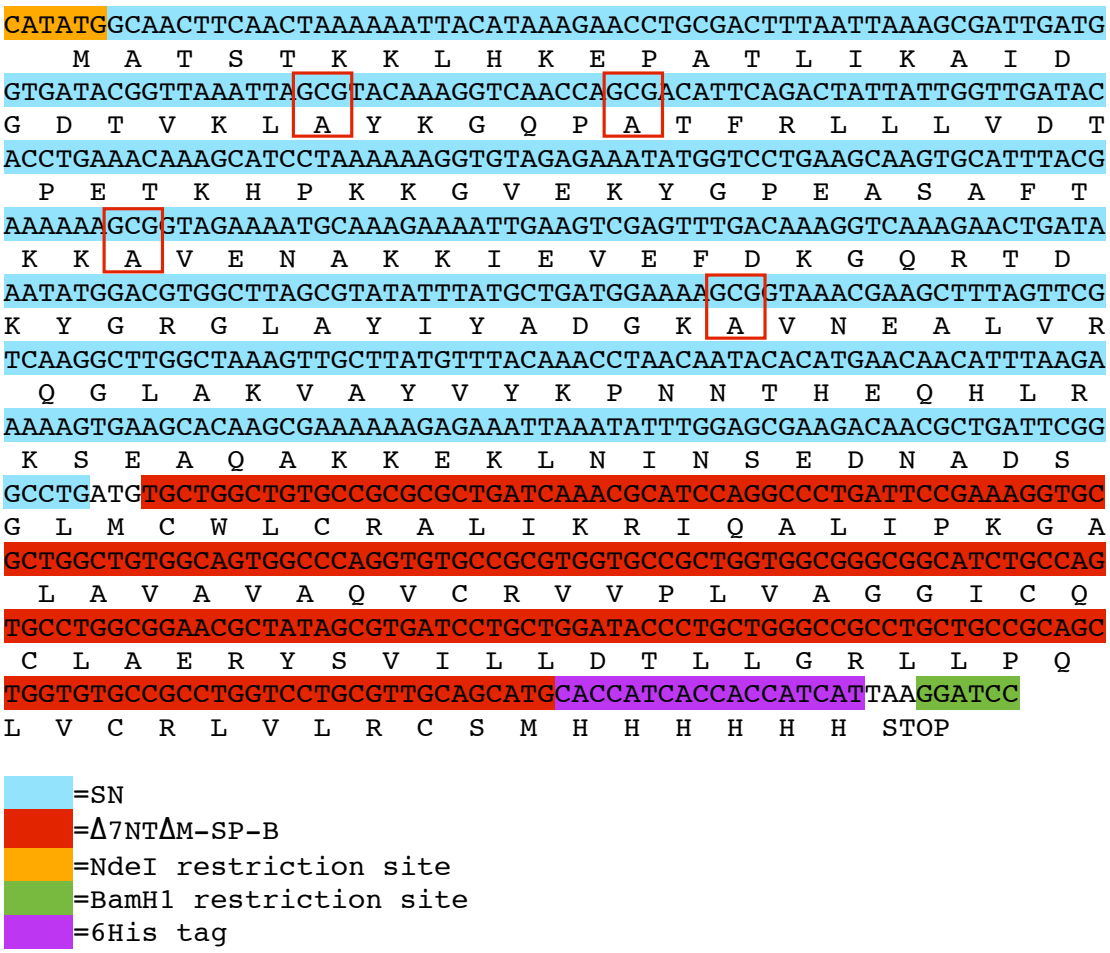

Figure 40: Possible future plasmid construct with methionine mutation in SN. Similar to SN-Δ7NTΔM-SP-B-6His (Figure 4) however the interior methionine residues have been mutated to alanine. Mutated residues are highlighted in red boxes.

The expression of SP-B alone could provide another possibility. It was thought that SP-B could not be expressed without a fusion protein due to its very hydrophobic nature however its expression alone here proves otherwise. The SP-B expressed in this way only occurs in small quantities and is always contaminated with the SN-SP-B fusion. It is possible that if a plasmid is designed containing just SP-B with a histidine tag, it could result in the expression of an easily enriched recombinant SP-B (Figure 41). If the presence of a ribosome binding site fragment is enough to express a small amount of SP-B, then perhaps the full length ribosome binding site in the correct location 3' of the start of the SP-B gene would produce enough recombinant SP-B to work with.

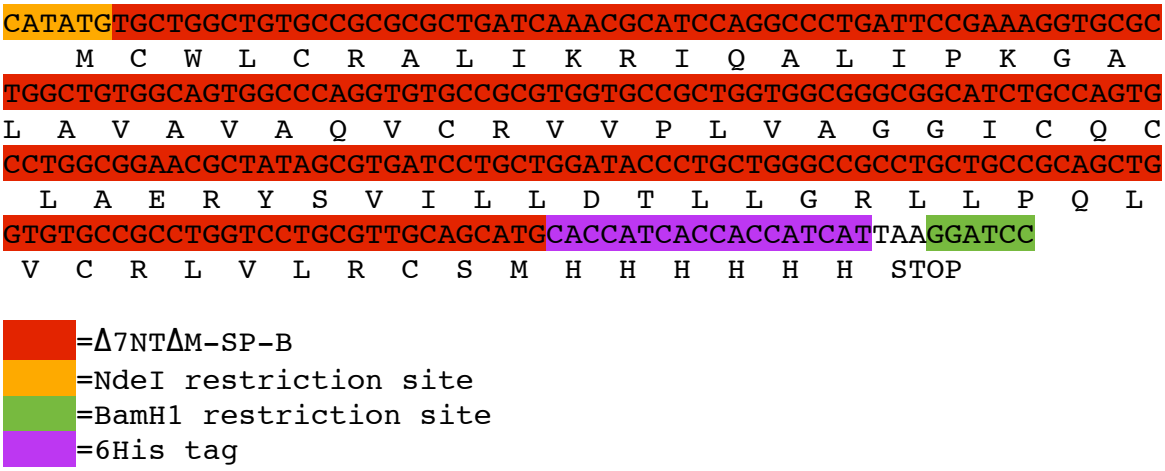

Figure 41: Possible future plasmid construct containing just the SP-B gene with a carboxy-terminal histidine tag.

Using the methods described above, producing an enriched recombinant SP-B sample is a distinct possibility. Once this has been achieved, SP-B can be expressed in the presence of ^{15}N and ^{13}C isotopes which would allow for three dimensional NMR and solving the tertiary structure of SP-B. This would greatly help our understanding of SP-B function as well as our understanding of surfactant as a whole.

Other methods that could be used to assess the structure of the recombinant SP-B would be circular dichromism (CD) and Fourier resonance infrared spectroscopy (FTIR). Both methods can give information related to the secondary structure of proteins. Previous experiments using native SP-B dissolved in an acetonitrile solution have indicated that SP-B has a largely alpha helical confirmation [90]. These experiments could be repeated using recombinant SP-B in the same conditions. By comparing the results to the native SP-B experiments, we can determine if the recombinant SP-B is structurally similar.

Finally, the ability to produce large quantities of enriched recombinant SP-B will have possible clinical applications. The recombinant SP-B could be used in future treatments for diseases such as RDS and ARDS.

References

1. Bastacky, J. et al. Alveolar lining layer is thin and continuous: low-temperature scanning electron microscopy of rat lung. *J. Appl. Physiol.* **79**, 1615-1628 (1995).

2. Possmayer, F. Physicochemical aspects of pulmonary surfactant. *Fetal and neonatal physiology* **2**, 1014-1034 (1997).

3. Johansson, J. & Curstedt, T. Molecular structures and interactions of pulmonary surfactant components. *Eur. J. Biochem.* **244**, 675-693 (1997).

4. Postle, A. D., Heeley, E. L. & Wilton, D. C. A comparison of the molecular species compositions of mammalian lung surfactant phospholipids. *Comparative Biochemistry and Physiology Part A: Molecular & Integrative Physiology* **129**, 65-73 (2001).

5. Veldhuizen, R., Nag, K., Orgeig, S. & Possmayer, F. The role of lipids in pulmonary surfactant. *Biochim. Biophys. Acta, Mol. Basis Dis.* 1408, 90-108 (1998).

6. Hawco, M. W., Coolbear, K. P., Davis, P. J. & Keough, K. M. W. Exclusion of fluid lipid during compression of monolayers of mixtures of dipalmitoylphosphatidylcholine with some other phosphatidylcholines. *Biochim. Biophys. Acta, Biomembr.* **646**, 185-187 (1981).

7. Goerke, J. Pulmonary surfactant: functions and molecular composition. *Biochim. Biophys. Acta, Mol. Basis Dis*. **1408**, 79-89 (1998).

8. Pérez-Gil, J. & Keough, K. M. Interfacial properties of surfactant proteins. *Biochim. Biophys. Acta.* **1408**, 203 (1998).

9. Whitsett, J. A. & Weaver, T. E. Hydrophobic surfactant proteins in lung function and disease. *N. Engl. J. Med.* **347**, 2141-2148 (2002).

10. Kishore, U. et al. Surfactant proteins SP-A and SP-D: structure, function and receptors. *Mol. Immunol.* **43**, 1293-1315 (2006).

11. Wright, J. R. & Clements, J. A. Lung surfactant turnovers and factors that affect turnover. *Lung cell biology. Marcel Dekker, New York* 655-699 (1989).

12. Lumb, R. H. Phospholipid transfer proteins in mammalian lung. *Am. J. Physiol-Lung C.* **257**, L190-L194 (1989).

13. Magoon, M. W. et al. Subfractionation of lung surfactant implications for metabolism and surface activity. *Biochim. Biophys. Acta, Lipids Lipid Metab.* **750**, 18-31 (1983).

14. Sullivan, L. C., Orgeig, S. & Daniels, C. B. Regulation of pulmonary surfactant secretion in the developing lizard, Pogona vitticeps. *Comp. Biochem. Physiol. A. Mol. Integr. Physiol.* **133**, 539-546 (2002).

15. Schurch, S., Qanbar, R., Bachofen, H. & Possmayer, F. The surface-associated surfactant reservoir in the alveolar lining. *Biol. Neonate.* **67 Suppl 1**, 61-76 (1995).

16. Perez-Gil, J. & Weaver, T. E. Pulmonary surfactant pathophysiology: current models and open questions. *Physiology (Bethesda)* **25**, 132-141 (2010).

17. Serrano, A. G. & Perez-Gil, J. Protein-lipid interactions and surface activity in the pulmonary surfactant system. *Chem. Phys. Lipids* **141**, 105-118 (2006).

18. Possmayer, F. A proposed nomenclature for pulmonary surfactant-associated proteins. *Am. J. Resp. Crit. Care* **138**, 990-998 (1988).

19. Kuroki, Y., Takahashi, M. & Nishitani, C. Pulmonary collectins in innate immunity of the lung. *Cellular Microbiol.* **9**, 1871-1879 (2007).

20. Wright, J. R. Pulmonary surfactant: a front line of lung host defense. *J. Clin. Invest.* **111**, 1453-1455 (2003).

21. Wright, J. R. Immunoregulatory functions of surfactant proteins. *Nat. Rev. Immunol.* **5**, 58-68 (2005).

22. Hawgood, S. & Poulain, F. R. The pulmonary collectins and surfactant metabolism. *Annu. Rev. Physiol.* **63**, 495-519 (2001).

23. Haagsman, H. P. Structural and functional aspects of the collectin SP-A. *Immunobiology* **205**, 476-489 (2002).

24. Casals, C. Role of surfactant protein A (SP-A)/lipid interactions for SP-A functions in the lung. *Fetal Pediatr. Pathol.* **20**, 249-268 (2001).

25. Sarker, M., Jackman, D. & Booth, V. Lung surfactant protein A (SP-A) interactions with model lung surfactant lipids and an SP-B fragment. *Biochemistry* **50**, 4867-4876 (2011).

26. Kingma, P. S. & Whitsett, J. A. In defense of the lung: surfactant protein A and surfactant protein D. *Curr. Opin. Pharmacol.* **6**, 277 (2006).

27. Sano, H. et al. Regulation of inflammation and bacterial clearance by lung collectins. *Respirology* **11**, S46-S50 (2006).

28. Korfhagen, T. R. et al. Altered surfactant function and structure in SP-A gene targeted mice. *Proc Natl Acad Sci U S A*, 93(18), 9594-9599 (1996).

29. Capote, K. R., McCormack, F. X. & Possmayer, F. Pulmonary surfactant protein-A (SP-A) restores the surface properties of surfactant after oxidation by a mechanism that requires the Cys6 interchain disulfide bond and the phospholipid binding domain. *J. Biol. Chem.* **278**, 20461-20474 (2003).

30. Schurch, S., Possmayer, F., Cheng, S. & Cockshutt, A. M. Pulmonary SP-A enhances adsorption and appears to induce surface sorting of lipid extract surfactant. *Am. J. Physiol.-Lung C.* **263**, L210-L218 (1992).

31. Head, J. F., Mealy, T. R., McCormack, F. X. & Seaton, B. A. Crystal structure of trimeric carbohydrate recognition and neck domains of surfactant protein A. *J. Biol. Chem.* **278**, 43254-43260 (2003).

32. Hakansson, K., Lim, N. K., Hoppe, H. J. & Reid, K. B. Crystal structure of the trimeric alpha-helical coiled-coil and the three lectin domains of human lung surfactant protein D. *Structure* **7**, 255-264 (1999).

33. Ikegami, M. et al. Surfactant metabolism in SP-D gene-targeted mice. *Am. J. Physiol.-Lung C.* **279**, L468-L476 (2000).

34. Gustafsson, M., Griffiths, W. J., Furusjo, E. & Johansson, J. The palmitoyl groups of lung surfactant protein C reduce unfolding into a fibrillogenic intermediate. *J. Mol. Biol.* **310**, 937-950 (2001).

35. Kramer, A. et al. Distribution of the surfactant-associated protein C within a lung surfactant model film investigated by near-field optical microscopy. *Biophys. J* **78**, 458-465 (2000).

36. Glasser, S. W. et al. Altered stability of pulmonary surfactant in SP-C-deficient mice. *Proc Natl Acad Sci U S A* **98**, 6366-6371 (2001).

37. Glasser, S. W. et al. Pneumonitis and emphysema in sp-C gene targeted mice. *J. Biol. Chem.* **278**, 14291-14298 (2003).

38. Amin, R. S. et al. Surfactant protein deficiency in familial interstitial lung disease. *J. Pediatr.* **139**, 85-92 (2001).

39. Johansson, J., Szyperski, T., Curstedt, T. & Wuethrich, K. The NMR structure of the pulmonary surfactant-associated polypeptide SP-C in an apolar solvent contains a valyl-rich alpha-helix. *Biochemistry* **33**, 6015-6023 (1994).

40. Clark, J. C. et al. Targeted disruption of the surfactant protein B gene disrupts surfactant homeostasis, causing respiratory failure in newborn mice. *Proc. Natl. Acad. Sci.* **92**, 7794-7798 (1995).

41. Nogee, L. M. Alterations in SP-B and SP-C expression in neonatal lung disease. *Annu. Rev. Physiol.* **66**, 601-623 (2004).

42. Brasch, F. et al. Involvement of napsin A in the C-and N-terminal processing of surfactant protein B in type-II pneumocytes of the human lung. *J. Biol. Chem.* **278**, 49006-49014 (2003).

43. Foster, C., Aktar, A., Kopf, D., Zhang, P. & Guttentag, S. Pepsinogen C: a type 2 cell-specific protease. *Am. J. Physiol.-Lung C.* **286**, L382-L387 (2004).

44. Guttentag, S. et al. Cysteine protease activity is required for surfactant protein B processing and lamellar body genesis. *Am. J. Res. Cell Mol.* **28**, 69 (2003).

45. Ueno, T. et al. Processing of pulmonary surfactant protein B by napsin and cathepsin H. *J. Biol. Chem.* **279**, 16178-16184 (2004).

46. Perez-Gil, J., Casals, C. & Marsh, D. Interactions of hydrophobic lung surfactant proteins SP-B and SP-C with dipalmitoylphosphatidylcholine and dipalmitoylphosphatidylglycerol bilayers studied by electron spin resonance spectroscopy. *Biochemistry* **34**, 3964-3971 (1995).

47. Hawgood, S., Derrick, M. & Poulain, F. Structure and properties of surfactant protein B. *Biochim. Biophys. Acta*.**1408**, 150-160 (1998).

48. Ryan, M. A. et al. Mapping and analysis of the lytic and fusogenic domains of surfactant protein B. *Biochemistry* **44**, 861-872 (2005).

49. Oosterlaken-Dijksterhuis, M. A., van Eijk, M., van Golde, L. M. G. & Haagsman, H. P. Lipid mixing is mediated by the hydrophobic surfactant protein SP-B but not by SP-C. *Biochim. Biophys. Acta*, *Biomembr.* **1110**, 45-50 (1992).

50. Cruz, A., Casals, C., Plasencia, I., Marsh, D. & Perez-Gil, J. Depth profiles of pulmonary surfactant protein B in phosphatidylcholine bilayers, studied by fluorescence and electron spin resonance spectroscopy. *Biochemistry* **37**, 9488-9496 (1998).

51. Ross, M., Krol, S., Janshoff, A. & Galla, H. J. Kinetics of phospholipid insertion into monolayers containing the lung surfactant proteins SP-B or SP-C. *Eur. Biophys. J.* **31**, 52-61 (2002).

52. Lipp, M. M., Lee, K. Y., Zasadzinski, J. A. & Waring, A. J. Phase and morphology changes in lipid monolayers induced by SP-B protein and its amino-terminal peptide. *Science* **273**, 1196-1199 (1996).

53. Ding, J. et al. Nanostructure changes in lung surfactant monolayers induced by interactions between palmitoyloleoylphosphatidylglycerol and surfactant protein B. *Langmuir* **19**, 1539-1550 (2003).

54. Taneva, S. G. & Keough, K. M. W. Dynamic surface properties of pulmonary surfactant proteins SP-B and SP-C and their mixtures with dipalmitoylphosphatidylcholine. *Biochemistry* **33**, 14660-14670 (1994).

55. Zaltash, S., Palmblad, M., Curstedt, T., Johansson, J. & Persson, B. Pulmonary surfactant protein B: a structural model and a functional analogue. *Biochim. Biophys. Acta.* **1466**, 179-186 (2000).

56. Olmeda, B., García-Álvarez, B., & Pérez-Gil, J. Structure–function correlations of pulmonary surfactant protein SP-B and the saposin-like family of proteins. *Eur Biophys J*, 42(2-3), 209-222 (2013).

57. Power, J. H., Doyle, I. R., Davidson, K. & Nicholas, T. E. Ultrastructural and protein analysis of surfactant in the Australian lungfish Neoceratodus forsteri: evidence for conservation of composition for 300 million years. *J Exp Biol* **202**, 2543-2550 (1999).

58. Griese, M. Pulmonary surfactant in health and human lung diseases: state of the art. *Eur. Respir. J.* **13**, 1455-1476 (1999).

59. Hallman, M., Glumoff, V. & Ramet, M. Surfactant in respiratory distress syndrome and lung injury. *Comp. Biochem. Physiol. A. Mol. Integr. Physiol.* **129**, 287-294 (2001).

60. Lam, B. C. C., Ng, Y. K. & Wong, K. Y. Randomized trial comparing two natural surfactants (Survanta vs. bLES) for treatment of neonatal respiratory distress syndrome. *Pediatr. Pulm.* **39**, 64-69 (2005).

61. Notter, R. H. *Lung Surfactants: Basic Science and Clinical Applications* (2000).

62. Ware, L. B. & Matthay, M. A. The acute respiratory distress syndrome. *N. Engl. J. Med.* **342**, 1334-1349 (2000).

63. Robertson, B. & Halliday, H. L. Principles of surfactant replacement. *Biochim. Biophys. Acta.* **1408**, 346-361 (1998).

64. Lewis, J. F. & Veldhuizen, R. A. The future of surfactant therapy during ALI/ARDS. *Semin. Respir. Crit. Care Med.* **27**, 377-388 (2006).

65. Gunther, A. et al. Surfactant alteration and replacement in acute respiratory distress syndrome. *Respir. Res.* **2**, 353-364 (2001).

66. Seeger, W., Grube, C., Gunther, A. & Schmidt, R. Surfactant inhibition by plasma proteins: differential sensitivity of various surfactant preparations. *Eur. Respir. J.* **6**, 971-977 (1993).

67. Gong, X. M., Franzin, C. M., Thai, K., Yu, J. & Marassi, F. M. Nuclear magnetic resonance structural studies of membrane proteins in micelles and bilayers. *Methods Mol. Biol.* **400**, 515-529 (2007).

68. Fan, J. et al. An efficient strategy for high throughput screening of recombinant integral membrane protein expression and stability. *Protein Expr. Purif.* **78**, 6-13 (2011).

69. Wüthrich, K. *NMR of Proteins and Nucleic Acids* (John Wiley & Sons, New York, 1986).

70. Pochapsky, T. C. & Pochapsky, S. S. *NMR for Physical and Biological Scientists* (Taylor & Francis, New York and London, 2007).

71. Williams, S. G. et al. Repressor titration: a novel system for selection and stable maintenance of recombinant plasmids. *Nucleic Acids Res.* **26**, 2120-2124 (1998).

72. Hashemzadeh-Bonehi, L. et al. Importance of using lac rather than ara promoter vectors for modulating the levels of toxic gene products in Escherichia coli. *Mol. Microbiol.* **30(3)**, 676-678 (1998).

73. Buck, B. et al. Over-expression, purification, and characterization of recombinant Ca-ATPase regulators for high-resolution solution and solid-state NMR studies. *Protein Expr. Purif.* **30**, 253-261 (2003).

74. Senthil, K. & Gautam, P. Expression and single-step purification of mercury transporter (merT) from Cupriavidus metallidurans in E. coli. *Biotechnol. Lett.* **32**, 1663-1666 (2010).

75. Moon, J. Y., Henzler-Wildman, K. A. & Ramamoorthy, A. Expression and purification of a recombinant LL-37 from Escherichia coli. *Biochim. Biophys. Acta*, *Biomembr.* **1758**, 1351-1358 (2006).

76. Lukovic, D. et al. Production and characterisation of recombinant forms of human pulmonary surfactant protein C (SP-C): Structure and surface activity. *Biochim. Biophys. Acta.* **1758**, 509-518 (2006).

77. Pryor, K. D. & Leiting, B. High-level expression of soluble protein in Escherichia coli using a His6-tag and maltose-binding-protein double-affinity fusion system. *Protein Expr. Purif.* **10**, 309-319 (1997).

78. Li, Y., Li, X., Li, H., Lockridge, O. & Wang, G. A novel method for purifying recombinant human host defense cathelicidin LL-37 by utilizing its inherent property of aggregation. *Protein Expr. Purif.* **54**, 157-165 (2007).

79. Bar, M., Bar-Ziv, R., Scherf, T. & Fass, D. Efficient production of a folded and functional, highly disulfide-bonded β-helix antifreeze protein in bacteria. *Protein Expr. Purif.* **48**, 243-252 (2006).

80. Lev, N. et al. Conformational stability and membrane interaction of the full-length ectodomain of HIV-1 gp41: implication for mode of action. *Biochemistry* **48**, 3166-3175 (2009).

81. Sharifahmadian, M. Production and Structural Studies of Lung Surfactant Protein B (SP-B) Peptides. *MSc. Thesis: Department of Biochemistry, Memorial University of Newfoundland* (2011).

82. Laemmli, U. K. Cleavage of structural proteins during the assembly of the head of bacteriophage T4. *Nature*, 227(5259), 680-685 (1970).

83. Burnette, W. N. “Western blotting”: electrophoretic transfer of proteins from sodium dodecyl sulfate-polyacrylamide gels to unmodified nitrocellulose and radiographic detection with antibody and radioiodinated protein A. *Anal. Biochem.*, 112(2), 195-203 (1981).

84. Gross, E. The cyanogen bromide reaction. *Meth. Enzymol.*, 11, 238-255 (1967).

85. Pérez-Gil, J., Cruz, A., & Casals, C. Solubility of hydrophobic surfactant proteins in organic solvent/water mixtures. Structural studies on SP-B and SP-C in aqueous organic solvents and lipids. *BBA - Lipid Lipid Met.*, 1168(3), 261-270 (1993).

86. Mawn, M. V., Fournier, M. J., Tirrell, D. A. & Mason, T. L. Depletion of free 30S ribosomal subunits in Escherichia coli by expression of RNA containing Shine-Dalgarno-like sequences. *J. Bacteriol.* **184**, 494-502 (2002).

87. Walther, F. J. et al. Critical structural and functional roles for the N-terminal insertion sequence in surfactant protein B analogs. *PLoS One* **5**, e8672 (2010).

88. Agnew, N. Unpublished Data. (2013).

89. Assadi-Porter, F. M., Aceti, D. J., Cheng, H. & Markley, J. L. Efficient production of recombinant brazzein, a small, heat-stable, sweet-tasting protein of plant origin. *Arch. Biochem. Biophys.* **376**, 252-258 (2000).

90. Cruz, A., Casals, C., & Perez-Gil, J. Conformational flexibility of pulmonary surfactant proteins SP-B and SP-C, studied in aqueous organic solvents. *BBA - Lipid Lipid Met.*, 1255(1), 68-76 (1995).